DEVELOPMENT OF IN-VITRO MOUTH METHODS FOR STUDYING ORAL PHENOMENA

by

THOMAS BENJAMIN MILLS

A thesis submitted to

The University of Birmingham

for the degree of

DOCTOR OF PHILOSOPHY

School of Chemical Engineering

College of Engineering and Physical Sciences

The University of Birmingham

Sept 2011

ABSTRACT

Manufacturers are under pressure to reformulate products to make healthier foods, without changing desirability or flavour. A better understanding of product breakdown under oral conditions is essential to structure novel products which are healthier without consumers noticing. In-vitro methods were developed to explore product behaviour when subject to a range of phenomena relevant to those in the mouth, with particular emphasis on lubrication behaviour. Polysaccharides common in food products were mainly used as model systems and salt release was studied in some systems.

Three in-vitro systems were developed and used in this study. Firstly, a stirred vessel was developed to gather data of salt release from gelatin, gellan and alginate systems, under quiescent conditions. This was a reliable method of tracking diffusion of sodium ions through the gel structures into a surrounding liquid, showing that diffusion was unaffected by the differing structure of the gels. The second system introduced the effect of compression. Only when pressures are sufficient to rupture the gel samples did compressions affect salt release over that observed in the stirred vessel study. Samples released the majority of their contained salt up to nine times faster, as a result of greater surface areas being exposed.

Finally, tribology equipment was developed, which explores the thin film, high shear behaviour of materials. An exploration of available equipment, processing parameters and configurations was carried out to determine optimum surfaces, normal forces and speed ranges which could be related to phenomena occurring in the mouth. The lubricating properties of inhomogeneous polysaccharides with different physical properties were studied. The mixing behaviour of the polysaccharide greatly affected the lubrication response; some

mixed quickly so lubricated more efficiently and vice versa. Finally, the developed tribology equipment was used to study the ordering process of a series of fluid gel samples, indicating that lubrication tracks the ordering process, with a decrease in lubrication when structure forms. The pattern of this response is a result of polysaccharide and salt content of the materials, with increasing content enhancing the change in lubrication experienced as more rigid gel particles are produced. The work presented in this thesis shows that the use of in-vitro methods can provide repeatable information on structure behaviour under conditions relevant to the mouth. This information could then be used to develop and assess future food products for their expected performance when consumed.

ACKNOWLEDGEMENTS

Firstly I would like to thank my supervisors Dr Serafim Bakalis and Prof. Ian Norton for their help and guidance throughout this project. I would also like to acknowledge the EPSRC for funding which has enabled this work to be completed.

My gratitude also goes to friends and family for their support and patience, especially during the writing stages of this project, and to colleagues and support staff within chemical engineering who have helped me with various obstacles during my time here.

TABLE OF CONTENTS

LIST OF FIGURES

LIST OF TABLES

NOMENCLATURE

c	Concentration (mol/m^3)
c*	Coil overlap concentration (w/w %)
D	Diffusivity (m^2/s)
E	Young's modulus for tribology ball (Pa)
E'	Young's modulus for tribology disc (Pa)
F	Friction force (N)
m_1	Concentration of sample in tribometer cell (% w/w)
m_2	Concentration of sample in external tank (% w/w)
P	Normal force (N)
q	Flow rate through recirculation tribology rig (%/s w/w)
r	Droplet radius (m)
R	Tribology ball radius (m)
t	Time (s)
$t_{1/2}$	Time to release 50% contained material (s)
V	External tribology tank volume (m^3)
W	Normal force (N)
κ	Contact pressure correction factor
μ	Friction/traction coefficient
ν	Poisson's ratio of tribology ball
ν'	Poisson's ratio of tribology disc
σ_{max}	Maximum contact pressure (Pa)

D_H High molecular weight dextran

D_L Low molecular weight dextran

DSC Differential scanning calorimetry

HFCS High fructose corn syrup

LBG Locust bean gum

MCR Modular compact rheometer

MTM Mini Traction machine (PCS instruments London)

PDMS Polydimethylsiloxane

SRR Slide/roll ratio (%)

CHAPTER 1. INTRODUCTION

1.1. MOTIVATION AND BACKGROUND

Intake of sodium (mainly in the form of common salt) is a nutritional requirement for the body. Sodium controls cell water content, facilitates nerve impulses and muscle movements, and influences blood pressure. Sodium distribution in an average male consists of 92g, with 50% in extra cellular fluids, 40% in bone and 10% in cells (BNF, 1981). Despite the crucial role of salt in the diet, excessive consumption has been linked to negative effects of hypertension and stroke, especially in those with a genetic predisposition (Cook *et al.*, 2007, Law *et al.*, 1991). The actual value required can vary vastly, based on individual weights, age and lifestyle with values from as little as 0.5g per day of salt for adults (NRC, 1999).

Historically, salt has been added to foods both to enhance flavour and as a preservative (Sleator and Hill, 2007). Before the advent of refrigeration, salt enabled food to be stored and transported long distances, enabling long sea voyages and large sustained armies. These obvious advantages made salt a valuable commodity (Collings and Spangenberg, 1980). The two main sources of salt used in production are from salt water and rock salt deposits.

Modern food production has changed dramatically in recent years, with large amounts of processed foods becoming more common and affordable. Foods such as soups, sauces, cereals and processed meats can account for around three quarters of a consumer's daily salt intake. Thus, the salt in these foods lead to many people exceeding their recommended daily allowance (RDA), often without their knowledge (Bull and Buss, 1980). Salt in food

products has multiple roles. For processed foods, shelf life is a major consideration, and as in historic use, salt is used to reduce water activity within the food, thus preventing bacterial growth and extending life. Other major roles of salt are for flavour (discussed in section 2.2.2) and structuring of products. An example of this is for processed meat products, where salt is needed to increase water retention maintaining an acceptable juicy structure during cooking (Desmond, 2006). Achieving the consumption target set by the Food Standards Agency (6g/day) is not possible without the food industry making significant efforts to reduce salt in foods. The value set is considered to be an achievable target, but still in excess of the actual daily requirements. Processed foods, while requiring less effort to digest and often containing higher levels of fat/salt and sugar, are structurally complex, the implication being that reformulation can have effects on other product attributes. In many cases, the removal of salt in excess of around 30% is not possible without adversely affecting the sensory characteristics of the product (Desmond, 2006). As such, a drive towards better understanding of both oral processing and our perception of tastants such as salt, and of salt behaviour and release from food structures, is underway.

The study of oral processing has been ongoing for many years as better understanding of the complex and variable process can lead to a host of beneficial discoveries, from helping to manage problems faced by people with swallowing disabilities (Hiiemae and Palmer, 1999) to providing indulgent foods with fewer health impacts (de Wijk and Prinz, 2007). Often the use of live subjects is a slow and variable process which has lead many studies (including the work presented in this thesis) to develop in-vitro systems to provide a repeatable platform to test structures under oral conditions (Salles *et al.*, 2007). Section 2.4 details a series of different approaches aiming for better understanding of oral processing. This is divided into a

series of different sections; a number of physical models exist which often focus on chewing and breakdown of structures. This approach is often supplemented by analysis of volatile release from these structures. However, a number of studies focus purely on these volatile compounds rather than on the process to release them. With this understanding a number of salt reduction techniques already employed are detailed, some of which are increasingly complex. This work looks at developing in-vitro models to represent phenomena occurring during oral processing, with particular emphasis on exploring the use of tribology as a new technique. With these systems, hydrocolloids as model systems commonly found in food products are studied.

1.2. OBJECTIVES

The aim of the work presented in this thesis was to develop in-vitro methods of the mouth with a focus on salt release from food based structures. This involves:

- Development of diffusion study methods:
    - Stirred tank environment
    - Compression effects (e.g. chewing and tongue palate interactions)
- Development of tribology equipment:
    - Configuration of equipment to relate to oral processing
- Introducing time dependant studies:
    - Investigate mixing and inhomogeneous samples and the relationship with the measurements made
- Dynamic studies in tribology:
    - Gelation induced by temperature variations
    - Factors affecting experienced lubrication change

1.3. LAYOUT OF THE THESIS

Chapter 2 consists of a critical literature review of work in the areas of oral processing, in-vitro mouth models and testing and categorising common food ingredients to gain a better understanding in order to develop new and better food products;

Chapter 3 contains a collected account of materials and methods used in this work, including descriptions of analytical equipment used during tests;

Chapter 4 concerns the initial stage in the development of an in-vitro mouth model focusing on the initial stages of processing and presents data of salt release from biopolymers;

Chapter 5 introduces the first stage of the use of tribology equipment for this application and explores configurations and comparisons with previous work carried out in the area;

Chapter 6 presents data on the developed tribology equipment looking at mixing within the tribology measurement cell, measurements of inhomogeneous samples and their importance for comparisons with the oral environment;

Chapter 7 looks at using tribology for dynamic measurements. Here data is presented on lubrication and viscosity change during ordering of biopolymers with viscosity measurements carried out for comparison of the produced sample;

Finally, **Chapter 8** contains all the major conclusions from this work and highlights further work to improve and further utilise the developed methods.

CHAPTER 2. LITERATURE REVIEW

2.1. INTRODUCTION

As was established in Chapter 1, the need for better understanding of the way we eat, the behaviour of food materials in the mouth, and the need to formulate new functional foods that taste good to the consumer whilst being nutritionally beneficial is important for academics and researchers in the food industry. The driving force behind the work carried out and presented in this thesis was the need to reduce salt in formulated food products. To achieve this, a better understanding of food material behaviour under oral conditions, with emphasis on salt, is crucial. This chapter presents a critical literature review of work in the area of oral processing, to identify which processes food structures are subjected to, and in-vitro mouth modelling, to identify what is being done to predict product behaviour in consumers. Finally, a review of work on tribology in the area of food and consumer product testing has been undertaken. This method has been recently identified as a potential tool to predict consumer response and provide structural behaviour of food products under conditions not experienced in the majority of in-vitro testing.

2.2. ORAL PROCESSING AND HUMAN PERCEPTION

In this next section, the areas of oral processing, the perception of flavour and the methods used to reduce salt in food, and their impact on taste perception are discussed.

2.2.1. Oral processing

Oral processing covers the intake of food into the mouth, the evaluation of food by the tongue, and the preparation for, and the act of, swallowing. In order to produce working methods that can relate to oral processing of food products, the conditions that are

experienced in the mouth need to be identified. For most people the shape and physical makeup of the oral cavity is similar, although differences exist across age, gender and health. A diagram of the oral cavity is presented in Figure 2.1 (Chen, 2009). A normal liquid mouthful is 30 ± 10.1 g for men and 25.2 ± 8.1 g for women (Hiiemae *et al.*, 1996). For solid foods this value decreases depending on the food in question; the size of the mouthful can be loosely correlated with hardness (Arai and Yamada, 1993). The mouth itself is an important and complex system with regards to oral processing. The mouth is the first contact of a food product, which then undergoes a number of serial and parallel processes: physical manipulation by movement of the oral surfaces, chemical change by saliva, and assessment by the tongue and oral surfaces.

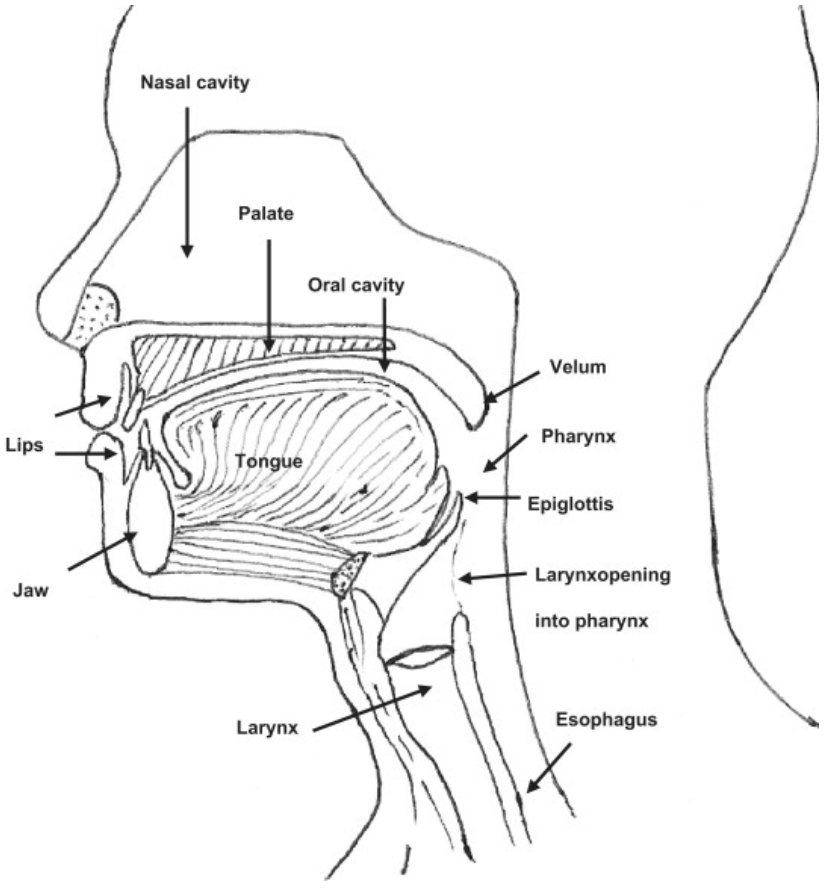

Figure 2.1. Diagram of the oral cavity reproduced from (Chen, 2009)

The process occurring in the mouth can be approximated by partitioning it into three main sections (Heath, 1991, Malone *et al.*, 2003). Firstly, the *oral processing* stage. For liquid products this is a relatively short stage lasting approximately two seconds, and involves taking in the product to the mouth and mixing it with saliva (Ertekin and Aydogdu, 2003). The product will experience low shear rates and a limited amount of mixing at this time. Initial processing for a solid product takes longer, and introduces a parallel mechanical process: the product is broken down into smaller pieces by chewing, while mixing with saliva to allow the formation of a soft bolus.

The second stage is *oral propulsion*. This is thought to be the level which has the most influence on the breakup of complex liquid structures, such as emulsions (Malone *et al.*, 2003). This stage involves the movement of the tongue towards the top palate, squeezing and inducing flow towards the back of the mouth, ready for swallowing. Here the fluid will experience high shears and forces, along with further mixing, before finally being swallowed (van Vliet, 2002). For solid products the bolus will be deformed and similarly forced backwards and down into the oesophagus. The final stage is *swallowing*, where the mouth is cleared, a small amount of material is retained by the oral surfaces which can then go on to play a further role in perception, as volatiles and tastants are released (Prinz *et al.*, 2006).

While this general description of oral processing applies to the majority of people, and appears quite simple, there are differences within this framework between individuals. This is as a result of variations in tolerances and preferences for food products. Work carried out into examining oral processing tends to originate from medical applications that look at swallowing defects, or similar related issues. As such, the focus of work is often not to

categorise the whole process, but to focus on where a small problem is present (Silva *et al.*, 2008). Furthermore, limited techniques can be applied, as any addition of equipment to the mouth can alter the processes occurring, leading to results which may not be accurate.

Videofluorography has been used in Hiiemae and Palmer (1999) to observe bolus formation and swallowing in patients with swallowing disorders, such as dysphasia, where some swallowed material is sometimes directed the into the lungs, rather than to the stomach. Patients eat a barium rich sample, which shows up on x-ray imaging, allowing the path of the food to be followed. The disadvantage is that exposure to radiation limits the technology to medical research, such as assessing dysphasia, where the radiation exposure is outweighed by the risk of remaining undiagnosed. Thus, studies in the normal population are rare. However, some progress has been made in relating textural properties of food to chewing patterns using this method. Mioche *et al.* (2002) show for meat samples that chewing cycles are affected by the readiness of material to be broken down in addition to shape and size. They also show how these samples affect movement around the mouth and positioning of the sample, an example image is shown in Figure 2.2. Current work considers the development of functional magnetic resonance imaging (fMRI) as a safe alternative to videofluorography (Barkhausen *et al.*, 2002). The radiation risk is removed, allowing people with normal oral processing to be studied. However, the imaging still relies on a suitable contrast material to be added to the product under study, and current technology can often lack the high resolution required for robust imaging. The contrast material itself can also affect the products structure and behaviour in the mouth, which prevents robust conclusions being made. Another approach looks at ultrasound images of tongue movements during oral processing. The need for a contrast material is removed, although the resolution of such images are quite low, and so

only crude differences between the movement and mastication of foods can be obtained (de Wijk *et al.*, 2006).

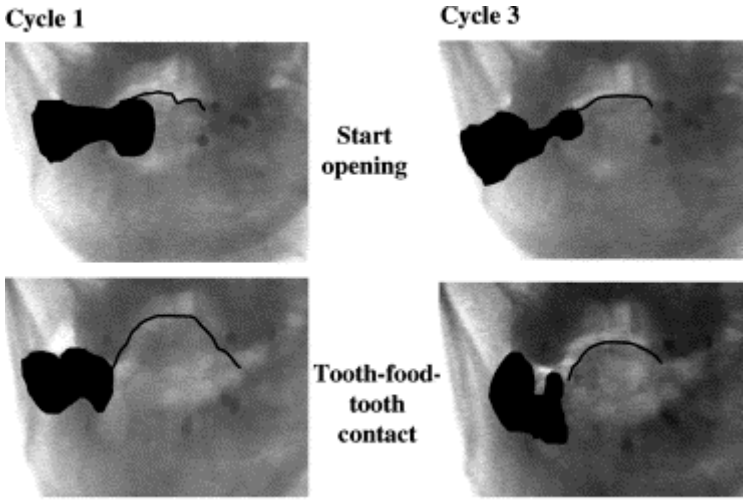

Figure 2.2. Front view videofluorography images of chewing barium coated tender meat (Mioche *et al.*, 2002)

A further area of interest considers the deposition behaviour of foods i.e. what is left behind on the tongue and oral cavity after swallowing. This method is more flexible as the mouth can be opened after swallowing, so the natural processes are not affected by the method of analysis. Video rate endoscopy has been developed for this purpose, which uses a small camera mounted on a flexible tube to allow the camera to be positioned in the mouth and moved to observe the entire cavity. Typically, this technology is used to look inside the body in cases like keyhole surgery, but can be used to look at material left behind on the tongue. The influence of factors such as viscosity or composition of the food on the deposition amounts and the time taken to clear the material after the first swallow can be studied in a quantifiable manor (Adams *et al.*, 2007, Pivk *et al.*, 2008).

Aside from mechanical manipulation, which occurs during oral processing, saliva interactions produce material and environmental changes. Saliva quantity and composition also depends on the material being processed in the mouth. Physically, saliva is secreted into the mouth to provide protection to the oral surfaces and to lubricate and dilute food as it enters the mouth during processing. Saliva contains a number of components such as enzymes and proteins which interact with the food structure, and break it down (Humphrey and Williamson, 2001). Work categorising saliva has been reviewed and extended recently in work by Schipper *et al.* (2007), where the composition and physical properties, such as rheology and lubrication, are presented. Saliva is shown to be a very complex fluid with a large number of components, despite consisting of over 99% water.

To conclude, although differences in oral processes exist between individuals a general picture of the processes occurring in the mouth can be gained from the current studies. However, the methods used do not allow for a large number of product specific studies to be carried out, as methods often lack definition and can be very time consuming.

2.2.2. Flavour perception

The perception of flavour within a food product is a result of a combination of factors, including the experience of gustatory (detected by the tongue) and olfactory (detected by the nose) sensations (Verhagen and Engelen, 2006). The experience of odour occurs when volatile substances, are carried from the mouth up into the nasal cavity, where they bind and interact with a series of specialised receptor cells (primary olfactory neurons) triggering a response which is sent and interpreted by the brain, in conjunction with all of the other odours and tastes (detailed below) experienced simultaneously (Coren *et al.*, 2004).

Epithial cells are responsible for taste perception, and are within the taste buds located in the fusiform papillae, these can be found on the tongue and oral cavity (Lindemann, 2001). Five distinct sensations are detected by the tongue: sour, sweet, bitter, salt and umami. The taste of salt itself relies mainly on the sodium ion component of sodium chloride. Within the body salt is responsible for controlling blood pressure, cell water content and facilitating nerve impulse transition. The scarcity of salt in natural products, combined with the vital role played by salt in the human body is thought to be the explanation for the selective, dedicated ability to taste it. However, salt is not just desirable because of its own taste, but also because of its ability to mask other, often unpleasant, tastes such as bitter, and for enhancing desirable flavours. This effect is seen even at levels that are sub threshold i.e. in foods that do not taste salty to the consumer. This has been observed in bread products, for example by Beauchamp and Stein (2008). The complexity of the system, combined with the diversity of an individual's experience and preferences, makes it challenging to critically assess products in-vivo. Currently, the only way to decrease this variability is by using large sample groups or trained sensory panels. These panels can be taught a repeatable and comparable vocabulary of descriptive words and intensity of flavour scales, which can then be used to rate products against. This allows for better comparison between individuals. However, with both approaches a great deal of time and associated cost is required, which limits the use of in-vivo testing (Carpenter *et al.*, 2000).

The condition in which salt is released affects how it is perceived. For example, the viscosity of the food product may affect how salty the product is thought to be. An example of this is seen where high viscosity fluids containing the same salt as a low viscosity version are perceived as less salty. This is due to differences in mixing: a higher viscosity fluid takes

longer to mix with saliva and as a result less material comes into contact with the oral surfaces containing the taste buds (Ferry *et al.*, 2006). Similarly, a comparison made between liquid and gelled model cheese structures revealed liquid products were perceived as more salty than gelled versions, despite containing the same level of salt. This was as a result of increased product mixing and contact with the tongue in the liquid version (Panouillé *et al.*, 2011).

Salt perception is also affected by how homogenous salt is within a product. A study by Noort *et al.* (2010) investigated the effect of an inhomogeneous distribution of salt within bread on perceived salt intensity. Findings show that having alternating layers of high and low salt within the food sample allows a reduction in overall salt levels to be achieved, without reducing perceived intensity. A similar approach has been investigated using gelatin as a model food product when considering sugar distribution. Layered gel samples with differences in concentration were used, maintaining the sample structure whilst reducing overall content. Samples with the same concentration, but a different distribution, were deemed to have more sugar than the homogeneous samples by a sensory panel (Holm *et al.*, 2009).

Not only does the distribution of tastant within the product affect perception, but the release profile can have an effect also. Altering the release of tastant whilst keeping the overall salt content the same has been explored using continuous liquid flow equipment where the concentration over time can be programmed. One such study on salt shows release profiles affect overall perception: an initial high burst of flavour results in an overall higher perception of salt than a sustained delivery of the same concentration (Busch *et al.*, 2009). For sugar, Burseg *et al.* (2010) showed that up to a 14% enhancement on perceived flavour can be

achieved by introducing an early pulse of higher concentration followed by a lower level, maintaining the same overall concentration.

It is agreed then that flavour perception is a complex phenomena and is different for each person and each product (Boland *et al.*, 2004, Etiévant, 2006). Consumer acceptance of new products and formulations is important for all manufactures of food products, but is difficult to predict without performing time consuming and expensive sensory trials. Our perception of flavour relies not only on the individual taste and odour chemicals in a product, but also their interaction between one another and their temporal behaviour during eating. For the perception of salt (and other tastes), pure quantity in a product does not necessarily dictate experienced intensity. This is promising for efforts to reformulate food products to contain reduced quantities of salt without affecting product flavour.

2.2.3. Salt reduction techniques

The desirable salt level in foods from a flavour perspective varies between individuals, and has been shown to be a function of an individual's regular intake of salt (Bertino *et al.*, 1982). The authors controlled salt intake at a lower than normal value in a group of subjects for a five month period. Subjects initially rejected the samples as tasteless and bland, but eventually became acclimatised to the lower sodium intake. As a result, a radical reduction in salt levels for processed foods would likely cause rejection by the regular consumer who would then move to alternative brands. Despite this, the first stage in efforts to reduce salt in the diet is often a simplistic reduction or reformulation approach, which has been used in a variety of products such as breads and processed meats. However, a gradual change is often used to prevent rejection, but the levels of salt are still higher than ideal from a health perspective (Desmond, 2006). This approach can often achieve a reasonable reduction in

ingredients such as salt and fat without adverse effects on flavour and consumer acceptance (Dubow and Childs, 1998, Girgis *et al.*, 2003). The main barrier for greater levels of reduction by this method comes from the potential for rejection. Manufacturers are reluctant to reduce salt within food products below the consumer's ideal level, as it would result in rejection and loss of revenue.

Salt substitution is possible by replacing salt with either a flavour enhancer or a non-sodium salt. In theory this approach maintains flavour while being lower in salt, and therefore 'healthier'. Potassium chloride (KCl) is commonly used as a salt replacement, although complete replacement results in excessive bitterness and the actual achievable level depends on product type (Morris *et al.*, 2010) but in some products such as feta can be up to a 50% replacement (Katsiari *et al.*, 1997). However, some limited success was achieved with mixtures in cured ham, but no progress with alternative salts was reported (Armenteros *et al.*, 2011). Another common example is the use of glutamates, such as monosodium glutamate and calcium glutamate (MSG and CDG, respectively), both of which have a strong umami taste and some saltiness and have been shown to retain consumer's liking of the product (Ball *et al.*, 2002). In respect to MSG, the disadvantage to this is that the harmful sodium component still remains, and the strong flavour introduced is limited in its application to certain foods. These replacements are not enough to maintain product flavour with reduced sodium levels.

Overall, efforts are being made to reduce the levels of salt in processed foods, however they are often slow and simplistic. Government legislation to force manufacturers to reduce salt

levels in food make it increasingly difficult to rely on these approaches, so more complex solutions are needed.

2.3. FOOD PRODUCT FORMULATION AND STRUCTURE

Hydrocolloids are commonly used as ingredients in a wide range of food products, and provide a wide range of structural properties for food formulations. As such, they are often used as model food products. A series of hydrocolloid systems were identified in this work, from their precedence in current literature, and within food products, to provide a range of food material behaviours for further study. The following section identifies these ingredients in more detail, and reviews publications which have previously studied them. Aside from this, a specific review on the use and study of some of these materials as 'fluid gels' is presented, which supports work carried out in Chapter 7. Finally, a short introduction to the study of food emulsions is presented as a model food for use in Chapter 5.

2.3.1. Hydrocolloid use in foods

Hydrocolloids cover a wide range of materials, including a variety of polysaccharides and gums, and are widely used in food formulations (Varela and Fiszman, 2011). The main application is as thickeners, rheology modifiers and gelling agents which impart structure to the product (Dickinson, 2003). Increasingly, the inclusion of hydrocolloids to replace fat or to modify texture after fat reduction has been seen in products such as mayonnaise or milk based drinks (Liu *et al.*, 2007, Yanes *et al.*, 2002). This is popular since healthy foods are becoming increasingly desirable, but also because fat is often more expensive so any reductions made can save money. However, whilst maintaining simple physical properties, this substitution still affects consumer acceptance as differences in mouthfeel and flavour are detected.

A further application studied for these materials in food products is their use as emulsifiers. Some surface active materials such as gum Arabic and modified starches have been shown to provide this functionality. Their main benefit over protein emulsifiers is that they can maintain stability during undesirable conditions such as under thermal shock. However, overall they are less efficient, requiring higher concentrations than protein in order to stabilise emulsions, which can have an effect on overall product characteristics (Chanamai and McClements, 2002, Dickinson, 2003, 2007, 2009).

A number of polysaccharides were used in this study, which were selected for study in this thesis because of their use in food products and related research projects. The following provides some details and uses for these materials. Alginate is a polysaccharide commonly used either as a sodium or calcium salt version, which is obtained from alginic acid from brown seaweed. Alginic acid consists of D-mannuronic acid and l-guluronic acid in varying ratios due to the natural variability of the seaweeds it is extracted from. Alginate is used in food products to provide structure as it gels with the addition of calcium ions. Wider applications include wound-dressing, tissue engineering and most relevant for this study, slow release drug delivery, which will have applications for flavour and tastant delivery (Rehm, 2009).

Gellan gum is a polysaccharide produced from fermentation of *Spingomonas elodea*, and exists in a number of functional forms. Gellan consist of straight chains of glucose, guluronic acid and rhamnose with acetate and glycerate present in the initial “high acyl” product. Different products are created by clarifying and/or removing acyl groups, the latter of which

creates what is referred to as a “low acyl” gellan. The addition of ions, such as sodium and calcium, promote gelation in all configurations, to varying degrees of sensitivity. Common uses in the food industry include bakery mixes and frostings, and as a stabiliser in liquid or low viscosity products with suspended ingredients (Imeson, 2009).

Gelatin is produced in a number of forms, and is a product of partial hydrolysis of collagen. The different products available stem from the source of collagen used to produce the gelatin. Common sources are pigskin, bovine skin and fish, which produce materials of varying characteristics, arguably most importantly in the strengths and gelation temperatures (Imeson, 1997). For most food applications the use of porcine or bovine gelatin is of most interest due to the melting temperatures being closer to that of the body leading to a melt in the mouth experience. Melting temperatures for fish gelatin tend to be around 14°C compared with approximately 29°C for porcine and 26°C for bovine (Koli *et al.*, 2011).

Agar is a hydrocolloid extracted from red algae composed of D-galactose and 3-6-anhydrogalactose. Commercial agar is made up of two polysaccharides, agarose and agaropectin, it is the agarose component that causes the gelation of the sample. These two components can be separated and agarose alone used as a gelling agent. Powdered agar is used commercially and unlike most other gelling agents, agar has a much higher melting point than its gelling point. Gelation temperature varies with increasing agar concentration, but is commonly below approximately 40°C, while temperatures of approximately 90°C are needed to re-melt the structures. Agar is often used in food products to create gelled structures such as fruit jellies (Nussinovitch, 1997).

Carrageenan is similar to agar in that it is extracted from red seaweed, but is distinguished by the quantity and positioning of the 3-6-anhydrogalactose joined to galactose. Commercial carrageenan exists in a number of forms depending on the specific seaweed used for manufacture. Commonly used samples consist of kappa, iota and lambda varieties which vary in their properties and strengths as gels. Added sodium promotes gelation, increasing gel hardness. Typically carrageenan is found in a number of dairy products such as whipped products and thickened milk drinks (Phillips and Williams, 2000).

Dextran is produced by bacteria fermentation and is a polysaccharide composed of α-1-6 linked D-glucose with different branches arising from the production method and bacteria. Dextran has a number of uses including replacing blood loss and as an anticoagulant (Klemm and Heinze, 2006). For food applications its use is limited, however a number of possibilities for ice cream and other frozen dairy products have been highlighted by McCurdy *et al.* (1994), which can increase the stability of the final product without adversely affecting its viscosity or rheological profile.

Guar gum is extracted from seeds of the guar bean or *Cyamposis tetragonolobus*. It consists of a series of mannose units, with a number of galactose side chains. Guar gum is widely used as a thickener in food products, and is used in ice cream to modify mouthfeel to leave a smooth texture (Clarke, 2004).

Xanthan gum is a polysaccharide created by fermentation of bacteria. Xanthan gum's structure consists of a linear chain of β-D-glucose with trisaccharide side groups. Common uses for xanthan gum exist in the food industry mainly for bakery products where it helps

retain structure during processing, in addition to helping to maintain moisture and retard staling. In solution, xanthan is shear thinning at low concentrations which is useful in many low fat products, such as dressings and sauces, where thickness is lost by oil removal (Phillips and Williams, 2000).

Pectin is a polysaccharide extracted from citrus fruit peel by a variety of techniques. Pectin is generally available in two forms high and low methoxy pectin (Williams *et al.*, 2000). Pectin is able to stabilise emulsion products but is most commonly used as a gelling agent in jams and preserves (Phillips and Williams, 2000).

Corn syrup is obtained by partial hydrolysis of starch using acid or enzymes and is categorised by the extent of hydrolysis carried out (Clarke, 2004). Corn syrup mainly consists of glucose but in commercial use is often further enzymatically modified to convert a portion of its glucose into fructose forming high fructose corn syrup (HFCS) which provides a much sweeter taste at a lower cost than sucrose. This enhancement makes HFCS common in a number of soft drink products (Ramanathan, 2006).

The wide range of polysaccharides studied in this work represents good model food systems as they are present in a number of products and also provide data for a number of different structures and behaviours.

Currently, the main application for controlled release from gels seems to be in drug release. Mangione *et al.* (2007) use an in-vitro approach to consider the effect of carrageenan structure on drug release in a Franz cell. The equipment consists of a small scale vessel with

a permeable membrane between the introduced sample and the recording section, which can be used to represent diffusion into biological tissues. This work, and others (Murata *et al.*, 2004), show that gels can be used to control release, in this case the in the form of the drug keptoprofen, and that manipulating the gel structure can alter the release profiles of the drug over time. For polysaccharides used herein, gelation mechanism varies slightly depending on structure, but generally they form reversible gels, by cooling below their gelation temperature. They exist initially in disordered states of chains, which upon cooling change to a helical state, which join together creating a structured network. This behaviour can be promoted with the addition of ions. The molecules in question tend to be of a greater size, slowing their release. Also, with drug release there is often no concern over the textural and flavour properties of the delivery system, which limits the relevance in food applications. Some research has been carried out in the area of flavour release from hydrocolloids, showing that gel structure can affect the release of volatile components of foods (Boland *et al.*, 2004, Koliandris *et al.*, 2008). However, the molecular sizes of the flavour compounds are likely to be greater than that of sodium ions (approximately 0.1nm) which are of interest in this study. This could indicate that similar patterns would not be seen for salt containing structures.

A number of different hydrocolloids are available for use in food products, with a variety of functional properties. The range of structures available could allow for complex release profiles of tastants in newly formulated foods, which have been seen in other applications. For example, as previously discussed in Busch *et al.*, (2009), a structure which bursts initially delivering a high concentration of salt combined with a mucoadhesive biopolymer which then delivers a longer and lower concentration of salt would result in a release profile that would

enhance the level of overall perception. Using these structures as model foods is a natural first step when considering salt release behaviour under oral conditions.

2.3.2. Fluid gels

For a variety of biopolymers the normal gelation process results in a solid quiescent gel. However, this can be altered in some cases with the application of shear during the gelation process. This results in the formation of a number of discrete particles in suspension, giving the final material a mixture of properties as both a solid gel and a liquid system. Two similar systems exist in this form which are referred to by different terms in literature. The first, which for the purposes of this work is termed a "sheared gel", is formed when a solid gel is broken up into small particles creating a suspension. The second is termed a "fluid gel", where the small individual gel particles are formed during the ordering process by the application of shear, and is of interest in this work. The main advantage of this method is that smaller more uniform particles are created which are spherical as emulsion droplets would be.

Previous work has shown that a number of materials can be processed in this manner to create fluid gels, such as agar and gellan (Altmann *et al.*, 2004, Norton *et al.*, 1999, Sworn *et al.*, 1995). Final properties of the material is dependent on a number of factors: the concentration of polysaccharide used; the addition of materials to promote gelation; the temperature profile used during gelation and; extent and uniformity of shear experienced (Gabriele *et al.*, 2009). Previous work on agar shows that as the initial gel nuclei form they reach an equilibrium point determined by the shear experienced. With increasing shear smaller particles are formed. The gels can be designed to form a variety of structures and are valuable to fat replacement applications.

It is clear then that fluid gels are interesting structures which are likely to be included in many processed formulations for the future, to give structure to liquid products and replace fats. As such, their behaviour in the mouth will be important to how they are received by the consumer. Further study of this material, with respect to lubrication behaviour, would provide fundamental information to add to the knowledge of the behaviour of these structures, and also give information on how they may perform in the mouth.

2.3.3. Emulsion use in foods

Emulsion use in food is widespread, both in processed foods and also some natural food products, such as milk. For processed foods a wide variety of emulsion based products exist, from soups to salad dressings and ice cream, all with their own independent textures and characteristics. The basic structure of an emulsion generally contains two liquids which are immiscible, often an oil and water, where one is dispersed as droplets within the other (O/W or W/O). This dispersion can be achieved using a number of techniques. The most basic of which involves simply mixing the two liquids together under very high shear, where the resulting dispersion depends upon the energy put into the system, and the liquid used. Usually in this case the emulsion produced has a very limited lifespan as the liquids are naturally immiscible, so will start to separate, as droplets of the dispersed phase collide and aggregate into clusters of droplets, or coalesce forming a discrete layer. To prevent this, a stabiliser is added, either in the form of an emulsifier or texture modifier, or in some cases a mixture of the two. The former works by locating at the droplet/continuous phase interface forming a layer. This is possible due to the structure of the molecules in question: one part is soluble in the dispersed phase while the other is soluble in the continuous phase. This forms a layer around the droplets and lowers interfacial tension, which increases stability and prevents droplets from coalescing (Hasenhuettl and Hartel, 2008). Texture modifiers work by

preventing movement of the droplets in the dispersion, and so prevent droplets from contacting. This can be achieved by a variety of additions, either by using thickeners to increase the viscosity of the continuous phase or by using gelling agents to solidify it. The choice often is determined by the intended use of the emulsion and the desired attributes.

From the basic emulsion structure, food products are often far more complex, either in the range of ingredients which interact with the emulsion, or even in the emulsion structure itself. For example phases can be gelled or frozen, or multiple layers of droplets can be present, as in a multiple emulsion containing further dispersed droplets within the dispersed phase (W/O/W or O/W/O). Traditionally, the use of emulsions in processed food products has been a function of structure and the enhancement of sensory attributes of a product. However, recently the use of emulsions for fat reduction has been implemented. This has given rise to products which not only contain less fat than competitors, without overtly affecting quality, but which can also be cheaper as the fat removed is often replaced with a cheaper material (in the case of low fat spread this is water). A further extension of this concept has started to consider introducing air droplets, which are ultimately cheaper still.

Emulsion use is widespread in food products in more forms than is described here, and in more applications and designs than the scope of this project. It is unsurprising then that emulsions are used as a common food analogue in sensory and experimental trials (see more in section 2.5.2 and 2.5.3), and should be considered when developing in-vitro mouth models.

2.4. IN-VITRO MOUTH MODELS

In order to reduce salt levels in processed foods, the behaviour of salt in food structures needs to be well understood (Durack *et al.*, 2008). The development of an in-vitro mouth system for this purpose is a relatively novel idea. Some in-vivo salt release work has been previously carried out, however they present difficulties. Jack *et al.*, (1995) investigated salt content in the mouth by way of conductivity sensors placed in the mouth during chewing. Authors found that for the participant studied a relationship between product texture and breakdown, and conductivity was evident. However, the use of in-mouth probes can affect the natural mastication process, and so may not be representative of normal consumption. Similar work has provided insight using this method, however this limitation remains (Davidson *et al.*, 1998, Neyraud *et al.*, 2003). In order not to disturb the natural behaviour of the participant some research looks at post mastication samples using techniques like video rate endoscopy, as previously discussed in section 2.2.

2.4.1. Developed in-vitro systems

Many studies have been undertaken attempting to link sensory perception with product properties and formulation. Malone *et al.* (2003) studied the link between lubrication properties of hydrocolloids and emulsions, and perceived smoothness and fattiness. The study of lubrication is better discussed in context and is detailed in section 2.5. van Vliet (2002) also reviews work in a similar area, commenting on links between texture perception and mechanical properties of products. These studies suggested that links can be made between sensory attributes and physical measurements, but that the relationship is complex.

The models that have been developed thus far tend to involve mechanical chewing of solid foods and volatile flavour release (Etiévant, 2006). Work by Xu *et al.* (2005) investigated the development of a mechanical jaw using actuators. The authors attempted to mimic the chewing cycles of a person, focusing on the motion of the jaw during mastication. Work by Prinz *et al.* (2007) focused more on the use of equipment to mimic conditions produced by tongue movement: an electric motor rotated a sample holder with a fixed mixing vane, and a video camera recorded images with mixing time. This apparatus allows changes to the material to be observed as a result of this mixing. Salles *et al.* (2007) develops this further still by producing a replica for physical chewing from in-vivo trials, also with the ability to look at flavour release by sampling volatiles and also collecting off-line samples. Future work would include swallowing and throat movements as a continuation of processing, in addition to more on and offline flavour testing.

For liquid products the focus has been on flavour release. Both Boland *et al.* (2006) and Juteau *et al.* (2004) studied the release of volatile components from gels. These studies indicated that the measurement of volatile release in a static environment does not compare to actual perception, suggesting that more dynamic in-vitro systems or in-vivo methods are needed. Similarly, Elmore and Langley (1996) have attempted to develop a dynamic measurement using a sealed vessel, where volatiles released from material can be analysed over time. Volatile release curves obtained in experiments for some compounds matched curves seen for sensory trials, where individuals rate intensity of volatiles as they are fed over time. However, the timescales in the experiment are longer than in sensory trials because of the increased size of the experimental apparatus compared with the oral cavity. Secondly, some volatiles which were detected during sensory testing were present in concentrations too

low for the mass spectrometer to detect. More recently, a very flexible system for volatile release was used by Rabe *et al.* (2002), where headspace analysis of a stirred tank was analysed. This consists of a similar system described in Elmore and Langley (1996), where volatiles are released from structures in a sealed vessel, which are then taken and analysed. The improvements of this system are in the automation of the introduction of materials to the vessel and the physical conditions experienced in terms of mixing and temperatures. This setup allows a more 'mouth like' experience for samples to be tested. The computer controlled vessel allowed for a variety of parameters to be altered such as flowrate, temperature, mixing and saliva flow, which produced good data. However, authors acknowledged that the individual's experience can still differ. Koliandris *et al.* (2008) investigated release rates of salt and ethyl burate (used as an artificial fruit favour, mainly orange) from gels into water. Liquid gels of bovine gelatin and locust bean gum (LBG) were made at varying concentrations. The release from the material injected into a beaker of water was recorded after twenty seconds using a sodium ion probe. For gelatin increasing concentration did not affect the measured level of sodium, but for LBG a statistically significant reduction in concentration of sodium in the bulk was recorded with increasing concentration from 0.2 to 1 % by weight. Researchers also investigated salt release from solid gellan and kappa-carrageenan/locust bean gum mixes. Water was added following two large strain compressions and sodium concentrations after twenty seconds was recorded. Again some differences were seen between samples with low acyl gellan and high concentrations of κ-carrageenan providing the highest level of sodium in the bulk. Differences in these levels were related to strain at rupture and to the extent of fracture in the compression experiments, with increasingly brittle gels releasing greater amounts of salt after the 20 seconds.

A number of different systems exist to quantify odour and taste molecule release from food, or food like structures. An emphasis on odour volatiles is present in the literature and many comparisons with actual sensory data are not conclusive. For salt very limited study on release is available and what is available looks at relatively simple release conditions and structures.

2.5. TRIBOLOGY

In this section the fundamentals of tribology, the study of lubrication and wear are detailed. Tribology has been relatively recently identified as a tool to look at food structure behaviour under the thin film behaviour occurring in the mouth. Development of this technique to look at a wider range of material behaviours which can be potentially linked to sensory experiences would provide further information to predict consumer response to future formulations.

2.5.1. Tribology theory

Tribology as a research tool has been used for many years dating back as long as mechanical equipment has been implemented on a large scale. The primary application for knowledge gained in this area is in the field of mechanical engineering and related fields such as combustion engine components and train wheel traction (Barwell, 1974, Nakada, 1994). These applications are concerned with lubrication and friction effects, related to rubbing and rotating surfaces in machinery that is susceptible to wear. As such a lubricant is used to reduce the friction experienced, and thus improve the efficiency and lifetime of equipment. Research into specific applications, in addition to the exploration of novel lubricants have been carried out and are fairly well documented. Several reviews have dealt with developments and categorisation of tribology and lubricants. Initially from development of bearings and large scale machinery problems to modern zero gravity tribology problems,

where loading by weight is essential for component operation, but this is not provided in zero gravity conditions, in addition to small scale components such as magnetic discs (Archbutt and Deeley, 1900, Bartz, 1978, Nakada, 1994, Roberts, 1986, Spikes, 2001, Talke, 2000, Zaretsky, 1990).

Friction is a force that is present in everyday life, wherever there is movement of one surface over another. The term tribology deals with friction, lubrication and wear effects in these systems. Friction force is defined as:

$$F = \mu W \ldots \text{Eqn 2.1}$$

Where F is friction force (N), μ is the friction coefficient (or traction coefficient) and W is the normal force applied perpendicular to the direction of friction. Friction coefficient is often used to represent the characteristic friction of a system for comparison.

Friction for a given system is usually dependant on a number of factors including temperature, surface roughness, relative speeds and the lubricant present. To categorise lubricants, friction coefficient across a range of speeds is often assessed. The resulting data is often presented as a Stribeck curve, which consists of traction coefficient at low, moving to high average speeds between surfaces (Czichos, 1978, Stribeck, 1902). A sample schematic is presented in Figure 2.3. A lubricant's effect will differ depending on the extent of entrainment (the volume present) between the two surfaces. This gives rise to three main regimes in the Stribeck curve across the speed range studied. Initially at low speeds the lubricant is not entrained, or only in very small volumes, and does not have sufficient pressure to move the surfaces apart. As such boundary lubrication is present, where both surfaces contact causing high friction. With increasing speed, fluid is forced between the surfaces beginning to separate them causing

partial contact from larger asperities, but reducing friction overall, this is termed the mixed regime. This behaviour continues with increasing speed, until surfaces become completely separated, entering the hydrodynamic regime (elastohydronamic regime when soft surfaces are investigated). At this point, friction between the surfaces is determined by the drag caused by the fluid, which is influenced by its viscosity and structure.

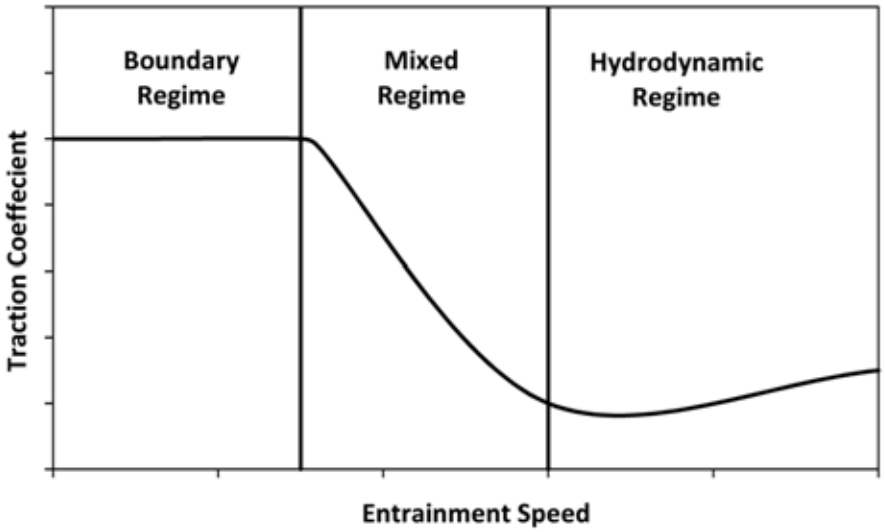

Figure 2.3. Characteristic Stribeck curve displaying the different lubrication regimes with increasing speed, from left to right the boundary, mixed and hydrodynamic regime

Within the scope of this research a number of different configurations of tribometer are in use. Firstly, commercially available systems which have been used consist of the mini traction machine (MTM), commonly used in this and other works. Two generations of the device exist currently which operate in a similar manner. The two measurement surfaces consist of a rotating disc mounted in a sample pot onto which a rotating ball on a shaft is lowered at a 45° angle creating a contact point between the two surfaces. The friction force is measured by way of a laterally placed force transducer attached to the ball arm. As the surfaces rotate a force is created perpendicular to the applied normal force, which is measured and displayed as a friction force from calibration loads. Friction coefficient is often presented with friction

force having been divided by normal force. A comparison is made with data in the literature generated with the first generation MTM later in this work, in Chapter 5.

Secondly, both Anton Paar and Thermo Scientific have produced rheometer attachments for tribology experiments. Both systems function in a similar fashion and consist of a mounted ball attached to the main rheometer shaft which is controlled to regulate rotational speed. This is paired with a sample holding cell attached to the bottom measurement plate of the rheometer and contains the sample. Within the cell are angled walls with three raised rectangles which act as the second contact. Normal forces are applied by the ball height and rotation speed is controlled. Torque in the ball shaft is measured by the rheometer as in rheology tests, and this resistance is converted to a friction force. Data from the Anton Paar system is presented later in this work (section 5.2.4), and compared with the developed MTM. In conjunction with this, a number of in house created equipment exists. One device, which is also a rheometer attachment, is created at Unilever Vlaardingen by Goh *et al.* (2010). The device presents an intermediate development between the two previously available configurations, opting for a flat disc as a secondary contact (similar to the MTM, but not driven). The controlled contact as in the previous rheology attachments is driven by the main rheometer shaft. However, instead of a single ball, two hemispheres are mounted equidistant from the centre. Data is produced from torque measurements on the shaft as before.

The MTM configuration allows friction and lubrication to be obtained for a variety of surfaces and samples. The information provided covers a range of different lubrication behaviour from boundary to hydrodynamic lubrication which is beneficial when looking for correlations with sensory studies. With further modification to include soft surfaces, relevant

contact pressures and model food systems the MTM shows good promise for use in mimicking thin film behaviour associated with oral processing.

2.5.2. Lubrication correlations with mouthfeel

Mouthfeel characteristics of food products are determined by a variety of factors (Verhagen and Engelen, 2006), as such it can be difficult to predict consumer responses to new or reformulated products without using sensory panels. Lubrication properties of materials have been shown to relate to how they are perceived by the mouth, when they are sheared between the tongue and the palate (de Wijk and Prinz, 2005, Malone *et al.*, 2003). As such, tribological behaviour of foods has become popular a topic in research.

Various types of tribology equipment for use in this field have been developed, either from modification of existing equipment or from original design. A common configuration used is that of a mini traction machine (MTM, PCS Instruments, London), which consists of an independently controlled rotating ball and disc which form the measurement contact (Bongaerts *et al.*, 2007, Chojnicka *et al.*, 2009, Malone *et al.*, 2003). In the majority of cases the mixing of material in the bulk of the sample, and its effect on what material is present at the contact point is not considered in detail.

Further to previous work on the development of methods for in-vitro measurements under oral conditions, the ability to add material for processing over time would extend the range of experiments that could be carried out. This situation would be similar to a food product being taken into the mouth, undergoing mixing and dilution with saliva. Using a tribometer in a similar way has been seen in previous work, which considers the saliva depletion by astringent compounds between contacts (Rossetti *et al.*, 2009). The method was shown to

distinguish the effects of different compounds, but was not sufficient to predict in-vivo results, and in addition methods involved using a pipette to introduce compounds in very small volumes.

In conclusion, tribology has been shown to provide lubrication data for food like products which in turn can be approximated to the movement of the tongue in the mouth against the palate, creating a region of squeeze flow between soft surfaces. The extent of comparisons made between tribology and the mouth is still fairly limited.

2.5.3. Sensory perception and tribology

Some efforts have been made to compare the friction of a product observed in the tribometer to the sensory perception of lubrication in the mouth, or to infer differences that should exist in the mouth. The common method is to use Stribeck curves to compare friction at different speeds. Malone *et al.* (2003) considered emulsions of varying fat content, and found trends in sensory scores for "fattiness" and differences in lubrication behaviour over different speed ranges. Similarly, work by Chojnicka (2009) investigated sensory and frictional differences in milk of varying fat contents, and showed correlations for a number of properties such as “creaminess” and “softness”. However, the experimental measurements did not consider the effect of mixing and transport to the recording surfaces which may be present in the mouth. It has been suggested previously that a reduction in flavour perception on increasing concentration of biopolymers is a result of mixing patterns in the mouth. Thus, this should be considered when drawing comparisons between in-vivo and in-vitro methods (Ferry *et al.*, 2006, Koliandris *et al.*, 2008).

It is clear that tribology does not offer a one-to-one comparison with sensory data since the processes occurring in the mouth are far more complex than represented by tribology equipment. However, sensory correlations can be drawn, and with further refinement and extension of testing conditions better correlations and predictions may be drawn.

2.6. CONCLUSIONS

There is a clear need to reduce salt for manufacturers. As such a number of studies are being carried out to reduce salt levels in foods without affecting flavour. Inevitably, with these innovations some changes in salt release and product structure will occur. To further improve these studies, knowledge of how food is broken down in the mouth and how salt is released and perceived by the consumer is needed. The use of an in-vitro mouth model for the purpose of salt release is not well studied in the literature, but has previously provided useful information, mainly for volatile release from food structures. In conjunction with this sensory testing of developed structures is very time consuming and expensive, which means it is only used in the later stages of product development, increasing the need for more in-vitro understanding. Specifically, tribology as a relatively new tool for in-vitro mouth correlations has the potential to provide a wide range of food material properties under the thin film, squeeze flow conditions found in the mouth.

CHAPTER 3. MATERIALS AND METHODS

3.1. MATERIALS

3.1.1. Gel samples used for salt release experiments (Chapter 4)

Salt release experiments were carried out using three commercially available food grade biopolymers: 250 bloom gelatin from porcine skin (Sigma, UK); low acyl gellan (Kelcogel, USA); and sodium alginate (Sigma UK). All were prepared as per manufacturer instructions, outlined below. The different formulations made for comparison are detailed in Table 3.1. All sample concentrations are percentage weight concentrations.

Table 3.1. Sample formulations used (%weight)

Polymer Type	Polymer Concentration (%)	NaCl Concentration (%)
Gelatin	6	3,1,0
	8	3,1,0
	10	3,1,0
Gellan	0.5	3,1,0
	1	3,1,0
	1.5	3,1,0
Alginate	3	3,0
	4	3,0

Gelatin samples were prepared by adding dry gelatin and NaCl to a beaker, then adding distilled water to make the total sample weight of 100g. The beaker was then covered, stirred and heated to approximately 60˚C and left for 30 minutes for the biopolymer to dissolve. The samples were then poured into plastic cylinders (76mm height, 22mm diameter), covered with Parafilm and chilled at 6˚C for 24 hours.

Gellan samples were prepared in a similar way at 90˚C, however the NaCl was added at the end of the 30 minutes stirring time, since the salt promotes gelation, so the sample must be at sufficiently high temperature to prevent it gelling too quickly. Samples were then set and stored as with gelatin. Alginate samples were set chemically with the addition of Ca^{2+} ions. Sodium alginate solutions with the desired alginate concentration were made up by heating a total sample weight of 100g to 80°C, and stirring until the alginate was fully dissolved. The liquid solution was then poured into a length of 12mm diameter dialysis tube, which was then sealed and immersed in a water bath containing 100ml of distilled water and 1% calcium chloride. Due to the dimension restrictions of the dialysis tube alginate samples had a reduced diameter and increased height compared with the other samples.

3.1.2. Tribology samples selected from literature (Chapter 5)

The samples used in this section were oil in water emulsions containing, 10, 20, 30 and 50% oil in addition to pure water and oil samples for control. Emulsions were prepared using required weight percentages of vegetable oil, 1% Tween 20 and making up to 200ml with distilled water. The samples were sheared for 3 minutes in a Silverson high shear mixer at 10,000 rpm. Samples were produced on the same day of testing. In Malone *et al.* (2003) simple guar solutions of 0.05, 0.2, 0.4 and 0.6% concentration were used to produce a series of Stribeck curves. In this work, Stribeck curves were produced for 0.2, 0.4 and 0.6% guar samples. These samples were prepared by adding to distilled water the desired weight percentage of guar gum (Sigma) and dispersing by stirring for 1 hour.

Samples of dextran and guar were produced by dissolving required concentrations in water. Guar gum samples used were Meyprodor®30 molecular weight of 420 kDa (G_L) and Meyprodor®400 (Danisco, Denmark) molecular weight 2660 kDa (G_H). Samples were

provided by the Division of Food Sciences, The University of Nottingham, Sutton Bonington Campus, Loughborough, Leicestershire LE12 5RD, UK. Coil overlap concentration (c*) values in aqueous solution were 0.55% w/w and 0.15% w/w. Two dextran samples of pharmaceutical grade (Pharmacos, Denmark) with molecular weight of 40 kDa (D_L) and 500 kDa (D_H), respectively, were used. c* values in aqueous solution were 15% w/w for D_L and 7.7% w/w for D_H (Koliandris *et al.*, 2010).

3.1.3. Tribology samples selected for studies of mixing (Chapter 6)

Three samples were selected that have some precedence in published soft tribology work, that differ in their rheological properties. Xanthan gum (non-Newtonian, Sigma Aldrich, UK), corn syrup (Newtonian, Cargill, USA) and pectin (non-Newtonian and mucoadhesive, Sigma Aldrich, UK from citrus) were used (de Vicente *et al.*, 2006, Sandford *et al.*, 1981). Viscosities were matched at high shear rate (1000 s^{-1}) materials used had concentrations of 2.5% w/w of pectin, 75% w/w of corn syrup and 1.5% w/w of xanthan. All samples were prepared by mixing the specified concentrations with distilled water at room temperature (~20˚C) until dispersed.

3.1.4. Tribology samples selected for ordering studies (Chapter 7)

Experiments were carried out using three commercially available biopolymers: k-carrageenan (Sigma, UK), agarose (Sigma, UK) and low acyl gellan (CP Kelco, USA). All were prepared as per manufacturer instructions, outlined below. The different formulations made for comparison are detailed in Table 3.2.

Table 3.2. Sample formulations (% weight)

Sample	Concentration (%)	KCl (%)
κ-carrageenan	0.25	0.1,0.2,0.3
κ-carrageenan	0.5,1	0.1
Gellan (Low Acyl)	0.5	0.1,0.2,0.3
Gellan (Low Acyl)	0.25,1	0.1
Agarose	0.5,1,2	0

Samples were produced by heating water to 80°C, to which the powdered polymer was added while stirring and covered. Samples were left for complete hydration and the appropriate quantity of salt (KCl in the case of gellan and k-carrageenan) was added and allowed to dissolve for 30 minutes before testing.

3.2. METHODS

3.2.1. DSC experiments on gelatin

Phase transitions of the prepared gelatin were investigated using differential scanning calorimetry (DSC) (Perkin-Elmer DSC7) to obtain melting temperatures. Gelatin samples were prepared in the same way as for release experiments and pans were prepared at approximately 20mg. Samples were heated at 10˚C /min from 5 to 45˚C to produce curves. All experiments were performed in triplicate.

3.2.2. Rotational viscometer

Viscosity measurements were carried out using a Bohlin Gemini HR nano rheometer (Malvern, UK) using a 60mm acrylic parallel plate, geometry. A small volume of fluid is placed in a stationary temperature controlled plate to which an upper plate is lowered leaving a controlled gap. Parallel plate systems allow for more complex systems with particulates,

which are found in systems used here; however, the shear experienced is less uniform than the cone and plate alternative.

3.2.3. Salt release experiments from gel systems (Chapter 4)

Salt release experiments were carried out using two configurations, one to study salt release under quiescent conditions and another under compression. A baffled jacketed vessel (75mm in diameter, 112mm in height) was used to study release of salt from a system under application of low shear. A square jacketed vessel (200mm by 100mm and 50mm in height), beneath a 40mm diameter texture analyser probe (Stable Micro Systems, TA XT2) to investigate the effect of cyclic compression during release was used. Both systems were fitted with a conductivity probe (Mettler Toledo, inlab 710 platinum 4-cell conductivity probe) and overhead stirrer (25mm diameter propeller type). Vessel specifications are shown in Figure 3.1.

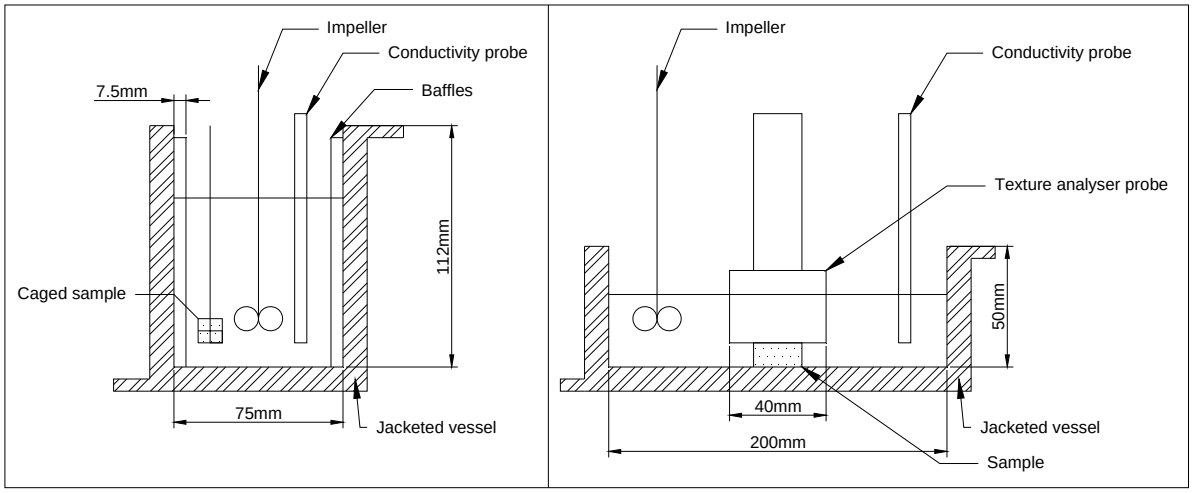

Figure 3.1. Vessel Designs of the two in-vitro rigs developed, left, the stirred tank diffusion rig, right, the compression rig with texture analyser overhead

Each of the formulations was tested to follow the release of NaCl from the gel structure to a surrounding volume of water. Samples of gel were cut into 3g (±0.1g) cylindrical segments

(22mm diameter, approximately 7.5mm height) from plastic preparation cylinders. These were then covered and replaced in the fridge at 6˚C and used within 6 hours. The vessel was set up and filled with 200ml of distilled water and allowed to equilibrate at 25˚C, for 15 minutes, while stirring at 100rpm to ensure a uniform concentration in the liquid. The conductivity probe was then placed into the vessel and set to record every 2 seconds. A single gel sample kept in place by a wire mesh was then added to the vessel 10 seconds after data logging was started. Experiments were carried out for 4 hours at both 25˚C and 37˚C, and performed in triplicate. Gelatin experiments at 37˚C reached a maximum significantly before this time and so were performed for 20 minute runs.

NaCl release from the structures was followed using a conductivity probe in the main body of water. Maximum expected conductivity was calculated from calibration curves that had been previously obtained (approximately 940 μS/cm). Actual maximum values differed slightly from the expected value (1-2% difference). This could be due to some sample variability and the probe calibration changing slightly over time. Because of this, results have been normalised and presented as a fraction of total release. Control experiments at 0% salt were carried out to confirm the stability of a long term conductivity reading and ensure no significant contribution is made to the value other than the addition of salt to the samples.

3.2.4. Mathematical modelling of the diffusion process (Chapter 4)

Effective diffusivities of each system can be obtained using the diffusion mode in COMSOL multiphysics (COMSOL Inc. Burlington, MA, USA), with comparison to the average experimental data for each concentration. The system was drawn in 3D using the transient diffusion model showing the gel sample within a volume of water (Figure 3.2). The diffusion equation (Eqn 3.1) was used. Physical properties (density and heat capacity) for both gel and water were set using COMSOL default values for water (998kg/m^3 and 4183 J/(kgK)

respectively at 25˚C). The approximation made for the gel is considered suitable since it consists of over 90% water.

$$\frac{\partial c}{\partial t} + \nabla(-D\nabla c) = 0 \text{...Eqn 3.1}$$

Equation 3.1 is taken from COMSOL Multiphysics, where c is concentration of salt, t is time and D is diffusivity. The diffusivity of the water was set to a high value (10 m^2/s) to simulate a fully mixed vessel. External boundaries of the water were set to insulated, and temperature was considered constant. The program was linked to MATLAB and run for a number of diffusivities within the sample and compared to average experimental data for each experiment. Values for diffusivity were estimated by minimising the sum of squares between average experimental and theoretically predicted data.

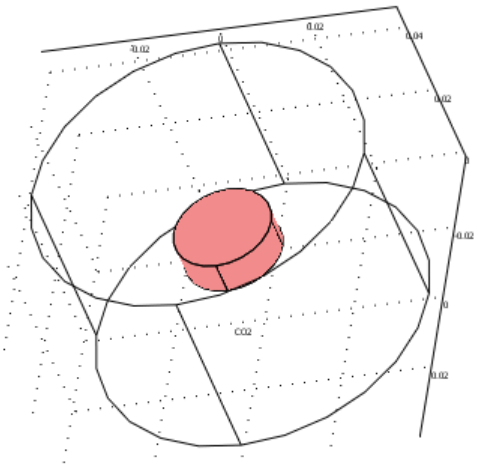

Figure 3.2. 3D model geometry used within COMSOL, dimensions represent actual experimental conditions, gel volume is equivalent to a 3g sample, water volume is 200ml

3.2.5. Salt release under compression (Chapter 4)

For the second stage of experiments, the effect on release of repeated compression of the gel samples was studied to mimic some oral processing. The tank geometry was changed to allow a flat bottom surface to be used with a texture analyser. Samples were fixed within the vessel by lowering the compression arm to contact point. 200ml of water was then added and

compressions were carried out every 3 minutes over a 20 minute period. Conductivity was recorded as per the initial experiments. Control tests with no compression were carried out as a baseline. Following this, tests using a low strain (30%) and high strain (75%) were conducted. Alginate samples were not tested in this section since the sample dimensions were different due to their production method in dialysis tubing. This difference means that compressions could not be carried out in a comparable manner to the other samples.

3.2.6. Tribometer initial design (Chapter 5)

A mini traction machine (MTM PCS Instruments, London) was used to perform experiments. The machine consists of a ball loaded onto a disc, which are independently driven to allow different relative motion. This produces a small contact point where material is assessed. The tribometer in its original configuration allows for the control of speed of both contacting surfaces, a fixed temperature, the normal force applied and the ratio of speeds of the contacts. With recent work the contact surfaces (previously which consisted of a steel ball on a steel disc for machine lubrication tests) have been extended to allow soft materials which it is believed will represent the soft tissues of the mouth and skin for these new applications.

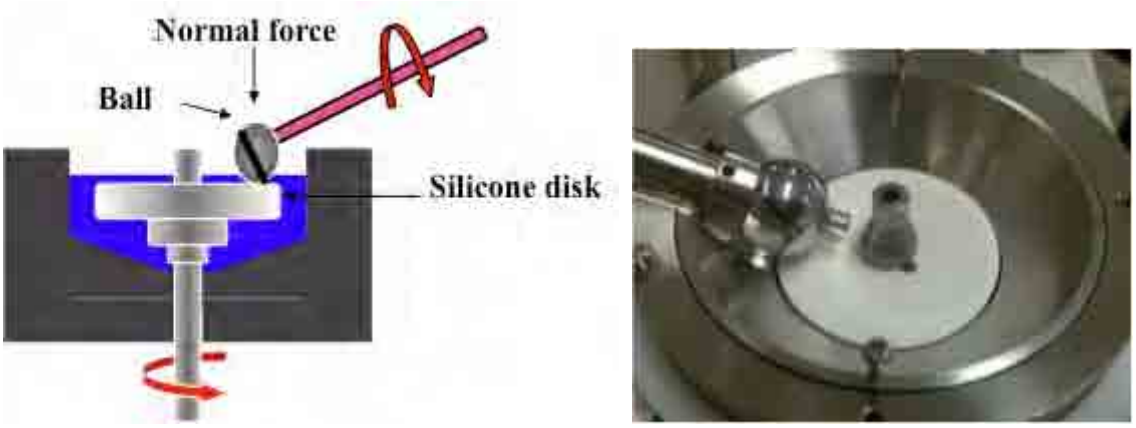

Figure 3.3. MTM Schematic, left, Side view schematic of MTM configuration right, image of MTM cell with volume reducing insert in place

For all tests the surfaces were sonically cleaned in ethanol for 5 minutes followed by 10 minutes in distilled water, they were then air dried and fitted into the tribometer cell. Sample sizes used were 40ml in all cases while temperature, normal force and slide/roll ratio (SRR) were set for each individual experiment. Where Stribeck curves were carried out 6 sweeps were made alternating between ascending and descending runs, without unloading for each step (see section 2.5.1 for details of Stribeck curves). A series of measurements at 16 average speeds logarithmically set between 1 and 750mm/s in Table 3.3 were taken. In some cases values at very low speeds proved unrepeatable due to a difficulty in the motors achieving the correct speeds, and so were omitted.

Table 3.3. Calculated ball/disc speeds for a standard Stribeck curve

Average speed	Ball speed	Disc speed
1	0.75	1.25
1.2	0.9	1.5
2	1.5	2.5
3	2.25	3.75
4	3	5
7	5.25	8.75
11	8.25	13.75
17	12.75	21.25
27	20.25	33.75
44	33	55
71	53.25	88.75
113	84.75	141.25
182	136.5	227.5
291	218.25	363.75
467	350.25	583.75
750	562.5	937.5

The speed range selected is based on previous work carried out to cover the different lubrication regimes. At the lower speeds (below approximately 10mm/s) boundary lubrication is expected, at the intermediate speeds (approximately 10-100) mixed lubrication is present, above this speed full separation of the surfaces and hydrodynamic lubrication dominates. SRR was kept at 50% again because of previous work in this area which allows

for easier comparison of results, but also to give a more complex mixture of sliding and rolling friction which would be expected in the mouth (Bongaerts *et al.*, 2007, Malone *et al.*, 2003).

3.2.7. Tribology surface comparisons (Chapter 5)

Typically in a tribometer, a steel ball and steel disc are used as contacts, however for oral applications these surfaces are of little use. Previous work in the area has allowed a range of surfaces to be used, including more recently soft materials (Bongaerts *et al.*, 2007, Dresselhuis *et al.*, 2008a). In this work the use of either a steel ball or in-lab made Polydimethylsiloxane (PDMS) ball on commercially available silicone elastomer and in-lab made PDMS discs was investigated. Further to this a brief comparison replacing the soft PDMS ball with a silicone o-ring mounted around a barrel was made. Experiments were carried out at 37 °C using vegetable oil, Stribeck curves were obtained using a normal force of 1N with a SRR of 50%.

3.2.8. PCS Instruments tribometer literature (Chapter 5)

Firstly, oil in water emulsions containing 10, 20, 30 and 50% oil, in addition to samples of pure water and oil run as controls were studied using the tribometer. Stribeck cures were carried out for each of the emulsion samples. Secondly, the effect of different droplet sizes on these results was investigated, using emulsions produced at 50% oil, 1% tween 20 concentrations using a cross flow membrane emulsification process which allows accurate droplet size control. These samples were produced to give a small and large droplet size, categorised in a mastersizer before and after running Stribeck curves. A comparison between the data produced here and that in work from Malone *et al.* (2003) was carried out. The emulsions in this case differed from the literature as the emulsifier used by Malone *et al.*

(2003) (Triodan 55) was not available, Tween 20 was use as a substitute, furthermore the oil and water samples were pure samples containing no emulsifier.

Guar samples at 0.2, 0.4 and 0.6% concentrations were compared. Stribeck curves of the previous speed ranges at 3N load and SRR of 50% were carried out. Once again a comparison of data from Malone *et al.* (2003) is made of the two sources.

3.2.9. Anton Paar MCR tribology attachment (Chapter 5)

The second comparison is made from a tribology attachment for rheometers, produced by Anton Parr. Initially two emulsions and a pure oil sample were compared made by the same method as above. Samples of dextran and guar were also used. All Modular compact rheometer (MCR) measurements were produced and carried out by the University of Nottingham (Koliandris *et al.*, 2009). In all cases the Stribeck curves were run for comparison, given the volume and geometry differences the speeds used by the MCR were lower to provide the range of lubrication behaviours. Normal force in both cases was 1N, SRR was 50% for the MTM and 200% for the MCR as only the ball is a moving surface in this case. PDMS was used for the MTM surfaces and the MCR plates, steel was used for the MCR ball since soft materials cannot be used.

3.2.10.Timed tribology configuration (Chapter 6)

The MTM previously discussed in section 3.2.6 was used to carry out this section of experiments. Surfaces were produced in house from PDMS, to allow soft surface contacts and a low contact pressure, usually associated with an oral environment. A load of 2N was applied with a SRR of 50% to give both sliding and rolling friction. Modifications were made to the cell chamber lid allowing a pump attached to an external tank to circulate material

between cell and external tank. Timed experiments at a fixed speed of 100mm/s, which lies in the mixed lubrication regime, were carried out. The tribometer chamber initially contains 50ml of water, to which samples were then added.

This setup allows flowrate into the chamber to be controlled as well as a fixed entry point and constant cell volume. With this configuration the effect of concentration on traction over time can be seen. Because of the controlled flow rate a mass balance can determine the concentration of material present in the cell at any time. This information can be compared with discrete experiments performed by running Stribeck curves on individual concentrations.

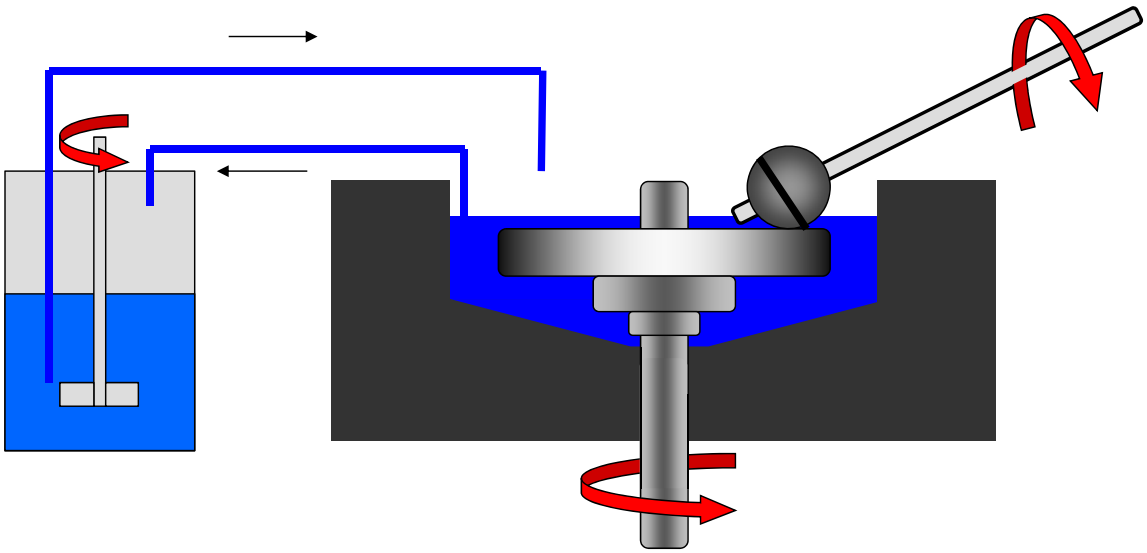

Figure 3.4. Circulation tribometer configuration for continuous tribology experiments

3.2.11.Mixing measurements with tribology (Chapter 6)

For these experiments individual dyed droplets of material were added by hand while traction was recorded. Food colourings (Dr Oatker natural food colourings, Germany), dissolved in distilled water were used for all studies. 1ml of colour in 100ml of distilled water was used for the base sample, with a single droplet imaged for each experiment. A video was taken at 60 frames per second and was used to track the path of the droplets and breakup patterns to

estimate a timescale for mixing within the chamber, determined by eye when the droplet colour was sufficiently diffuse and could not be identified.

3.2.12.Tribology measurements during ordering (Chapter 7)

The standard tribometer discussed earlier was used with steel ball and elastomer disc contact surfaces. A volume reducing insert was used to reduce the necessary sample size to 20ml. This works by filling the space between the wall and the edge of the disc, creating a sample volume directly above the disc. This insert was used in order to eliminate dead zones around the disc allowing a more homogeneous sample to be produced. A computer controlled water bath was attached to the tribometer pot jacket to implement the temperature profiles, in this case a 1.5°C/min cycle from 40°C to 20°C for carrageenan, 45°C to 20°C for Gellan and 40°C to 10°C for Agarose to sufficiently cover the ordering process. Timed experiments at 500mm/s over the length required to achieve the desired 1.5°C/min cooling rate for each sample. Ideally a speed in the mixed lubrication regime would be used to allow better comparison with effects in the oral environment. However, preliminary experiments at lower speeds than 500mm/s for some samples were too slow, allowing large solid gel section to form in the tribometer cell, producing inhomogeneous samples. 500mm/s would lie on the very edge of the mixed regime, offering a compromise. Similarly, reverting back to the use of a steel ball and elastomer disc allowed more repeatable results, as at high speed vibrations caused by slightly uneven surfaces of PDMS made recording difficult. Further modification of the tribometer chamber to increase mixing efficiency may offer a solution to this problem, allowing a lower speed assessment, without allowing large sections of the sample to experience low shears. With the use of the volume reducing insert the sample temperature probe is no longer in contact with the sample. Initial experiments show a lag of 3.5°C ± 0.5°C between sample temperature at the ball and the temperature probe. This lag is present

because the temperature probe is located in the metal volume reducing insert and not the sample bulk, although the lag in measurements should be consistent across the temperature range studied. Traction coefficient against temperature data is presented uncorrected for this lag, however subsequent data comparing gelation temperature between tribology and rheology have been altered to include a +3.5°C correction.

3.2.13. Viscosity measurements during ordering (Chapter 7)

The rheometer used was a Bohlin Gemini HR nano Rheometer (Figure 3.5), with a 60mm acrylic parallel plate system with a 1mm gap. The parallel plate geometry was used as a particulate system was present. Testing carried out also used the same geometry because of the particulates formed, to provide a large enough sample to be representative, and to prevent having to excessively move samples to allow different geometries to be fitted between runs. Samples were produced at a rate of 1.5 °C /min at $200s^{-1}$ and tested by measuring viscosity between 0.1-200 s^{-1} at 10°C. All experiments were carried out in triplicate, samples were loaded hot into both tribometer and rheometer where production took place. Immediately after production gels were tested in the rheometer.

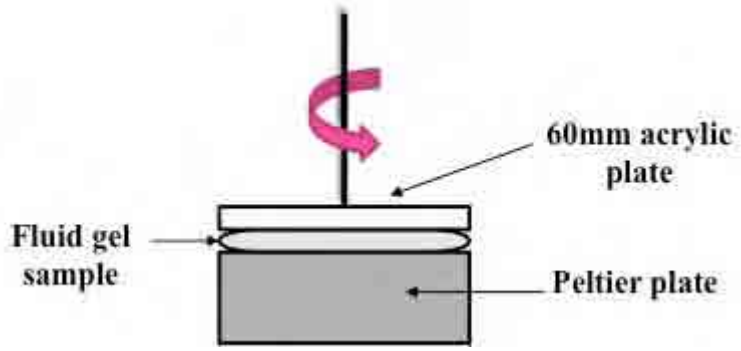

Figure 3.5. Bohlin Gemini rheometer geometry schematic, 60mm acrylic parallel plate configuration with temperature controlling peltier plate

CHAPTER 4. IN-VITRO MODEL FOR SALT RELEASE FROM GEL STRUCTURES

4.1. INTRODUCTION

Currently effort has been devoted to developing in-vitro methods to investigate food structure in the mouth, which is discussed in some detail in section 2.4, with work focussing on solids processing in the mouth (Mielle *et al.*, 2010, Xu *et al.*, 2005). Relatively little focus has been given to the release of sodium chloride in-vitro. Koliandris *et al.* (2008) does begin to explore this, although the release of salt is not the main focus of the work. Overall, the aim of the work presented in this chapter is to develop an in-vitro system for following the release of salt from food structures, which can be related to oral processing.

This chapter initially covers the development of two in-vitro rigs (see Figure 3.1) to encompass the food intake environments at the beginning of oral processing, with the introduction of mechanical stress. The release of NaCl from three common food grade gels (gellan, alginate and gelatin) into water was investigated. The phenomena which govern the release were investigated, and related to polymer type and concentration, salt concentration and temperature. Modelling work was then carried out to compare with experimental data, which can be used to determine diffusion coefficients of the systems. This model has then been extended to predict the release times for different sample geometries and sizes, which could form part of a food formulation.

4.2. RESULTS AND DISCUSSION

4.2.1. Salt release experiments

In this section diffusion of NaCl from gel structures under quiescent conditions using a stirred vessel is described (Figure 3.1 (a)). Preliminary experiments were carried out on the three gel samples (gellan, alginate and gelatin) to determine suitability for the study. Firstly, samples needed to be sufficiently concentrated to remain intact during testing. Secondly, sample concentrations needed to be below their solubility limits in water. Finally, the different concentrations of gelling agent were of different hardness to the touch. Gelatin was used in this work since it potentially offers different release behaviour above and below its melting point. It is also a common food additive and used in products such as desserts, dairy products, and processed meats (Rousselot, 2011). It is known from previous works that gelatin has a relatively low melting point compared with the other samples of approximately 30-32˚C which is below the 37˚C temperature used in experiments to mimic mouth temperature. This is dependent on bloom strength, concentration and the temperature profiles used to set and anneal the samples (Dranca and Vyazovkin, 2009, Gilsenan and Ross-Murphy, 2000).

DSC curves for gelatin samples were obtained to confirm and characterise the melting behaviour of the samples. Figure 4.1 shows the data collected for 6, 8 and 10% gelatin. Samples of approximately 20mg were heated at 10˚C/min from 5 to 50˚C. Results are normalised for 20mg samples, the peak melting point for all three concentrations of gelatin was approximately 32˚C ±1˚C. An increase in energy required to melt the samples was proportional to increasing gelatin concentration. Melting enthalpies were 0.48 mJ/g for 6% gelatin, 1.03 mJ/g for 8% and 1.49 mJ/g for 10%.

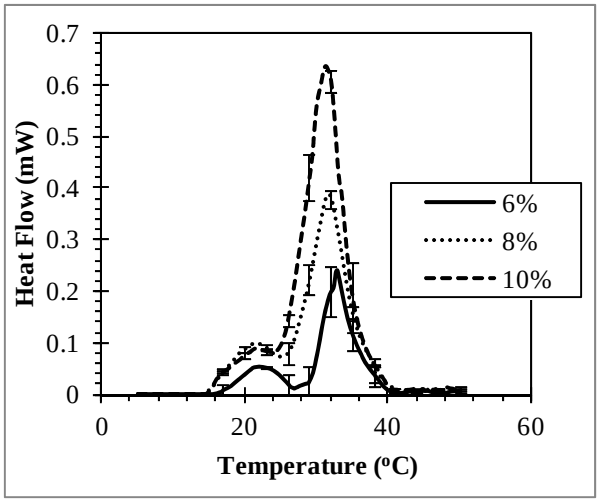

Figure 4.1. DSC data for gelatin, curves show data for 6, 8 and 10% gelatin being heated at 10˚C/min. Results are normalised for 20mg samples.

The first stage of testing used the stirred tank environment given in the materials and methods section and in Figure 3.1 (a). Gelatin, gellan and alginate samples, at varying concentrations, were added to the vessel of distilled water while conductivity was recorded to track salt release, as detailed in Section 3.2.3. Initially, control experiments with no added salt were carried out for a single concentration of each sample. This was performed to ensure that any rise in conductivity seen over the course of the experiment was as a result of the added salt and not any impurities in the gel sample. An example of results is shown in Figure 4.2. An increase in conductivity was recorded over time, however the value achieved is only approximately 1% of the measured conductivity observed when 3% salt is added to the samples. For the 8% gelatin case a maximum conductivity of 10µS/cm was recorded over a 3 hour period in comparison to about 950µS/cm when 3% NaCl was present. This increase observed, and presented in Figure 4.2, is due to slight impurities in the gel material, which are released to equilibrium within the surrounding distilled water. The same level of conductivity was found for all three biopolymer samples used, at a value of 12 ± 5 µS/cm. These values

are considered insignificant compared with the maximum expected in release experiments (950µS/cm).

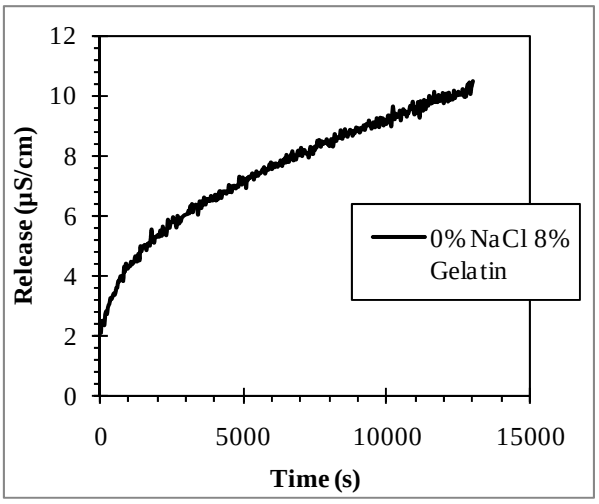

Figure 4.2. Example 0% NaCl run for gelatin, conductivity recording over time of 0% NaCl, 8% Gelatin sample for control purposes. Release was recorded over a 3 and a half hour period at 25˚C in a body of 200ml of distilled water.

Having shown that conductivity could be used to measure changes in salt release in a stirred tank environment without being added to by the gel samples themselves, samples of different hydrocolloids with added salt were investigated. Figure 4.3 shows the release of ions from all three gel samples over time at a temperature of 25˚C. For each sample a comparison is made between the different polymer concentrations used at a constant sodium chloride level of either 1 or 3% by weight. Increasing polymer concentration did show a slight reduction in release rate of the average values, however the differences fall within the error bars of one standard deviation from the mean of three repeats. On comparison of a single concentration curve for each of the three materials tested, the pattern of release is the same, with values for each of the samples overlapping (see Figure 4.4). Initially, there was a fast release which slowed as the system neared equilibrium. Experiments at 25˚C resulted in relatively slow release rates, with 90% release of salt taking approximately 2 hours. This is expected for a diffusion controlled release: the characteristic diffusion length for this timescale, taken to be a

simplified one dimensional approximation of $2\sqrt{Dt}$, is 0.4cm (Crank, 1975), which is of the order in the studied system. Decreasing the salt concentration in all samples did not change the actual release rate. Curves for 1 and 3% NaCl for both gellan and gelatin are shown in Figure 4.5 a and b, respectively. As would be expected a lower maximum conductivity value was recorded in line with the decreased quantity of salt present, with values averaging at 320µS/cm for 1% down from 950µS/cm at 3% NaCl.

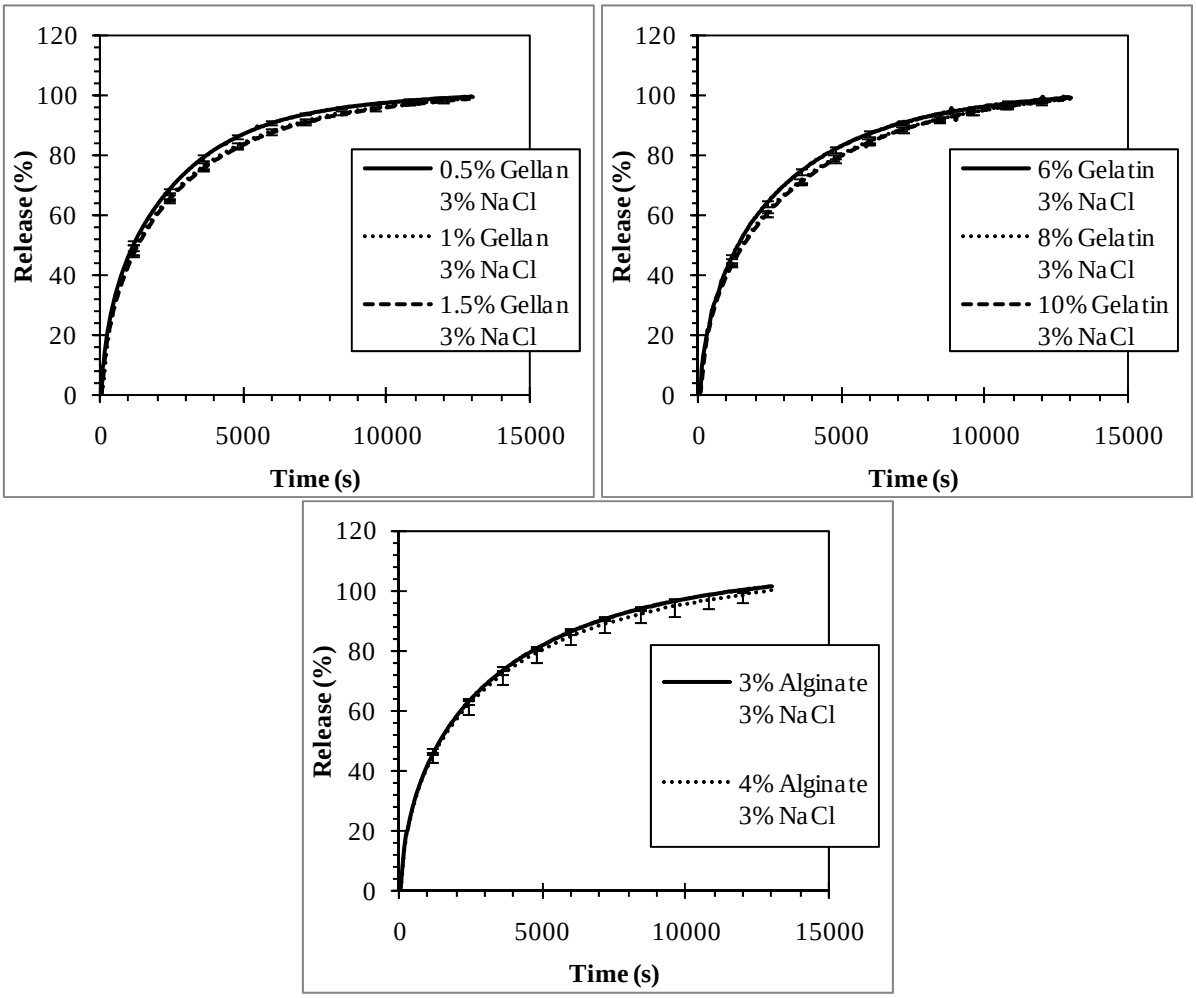

Figure 4.3. Release comparison between concentrations at 25˚C, graphs show NaCl release as a percentage of total release over time for samples of Gellan, Gelatin and Alginate. Experiments were carried out at 25˚C in all cases with 3g samples at 3% NaCl concentration in a body of 200ml of distilled water. Conductivity was recorded to track release, and averaged over 4 independent runs. Error bars represent 1 standard deviation of the mean.

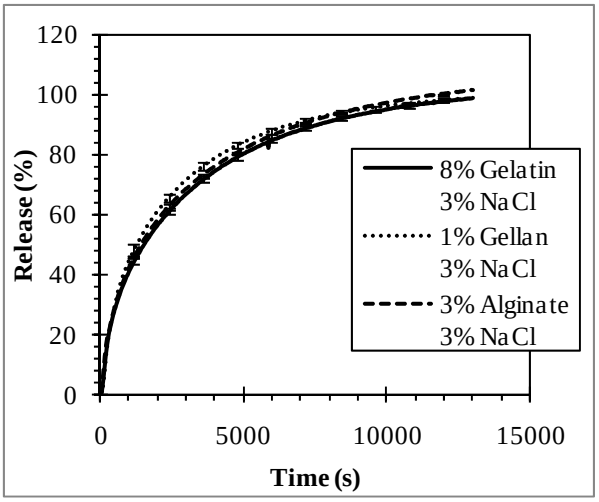

Figure 4.4. Release comparison between materials at 25˚C as a percentage of total release over time. Experiments were carried out with 3g samples at 3% NaCl concentration in a body of 200ml of distilled water. Conductivity was recorded to track release and averaged over 4 independent runs. Error bars represent 1 standard deviation of the mean.

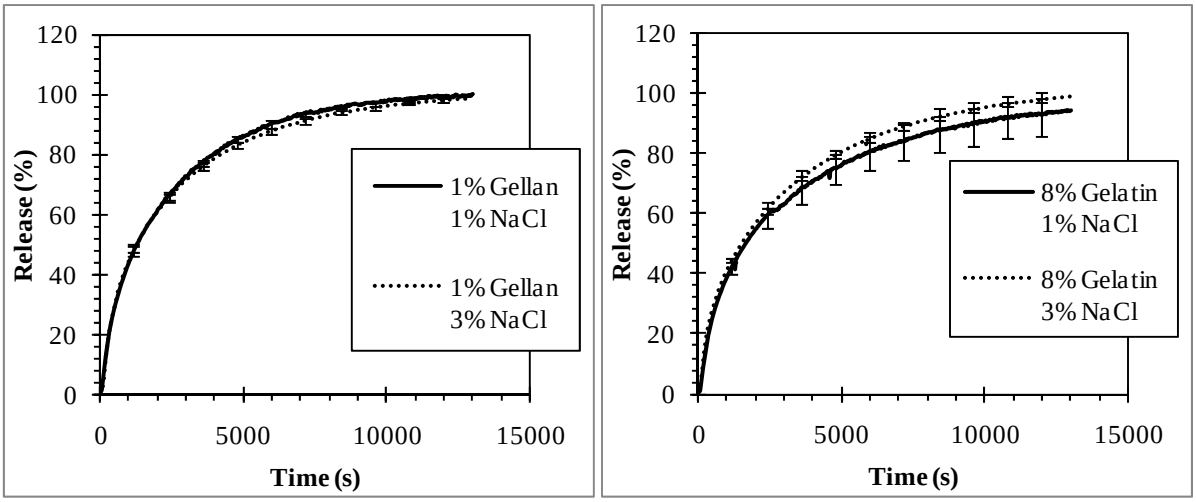

Figure 4.5. Release comparison between NaCl Concentrations as a percentage of total release over time for samples of Gellan and Gelatin at 1% and 3% NaCl concentrations. Experiments were carried out at 25˚C in all cases with 3g samples in a body of 200ml of distilled water. Conductivity was recorded to track release and averaged over 4 independent runs. Error bars represent 1 standard deviation of the mean.

Samples were then tested at 37˚C to simulate temperatures in the mouth. At 37˚C the release profiles for gellan and sodium alginate were similar to those obtained at 25˚C but a faster release is observed. A small decrease in release rate with increasing polymer concentration was observed. However, as previously described, the differences fall mostly within 1 standard deviation of the mean values (see Figure 4.6). A slightly faster overall release rate was observed at 37˚C than at 25˚C, with 90% release after around 75 minutes compared with 112 minutes at 25˚C. Again, this is expected for diffusion at the higher temperature, a comparison is made in Figure 4.7. The increase in temperature for water would lead to an expected increase in the diffusion coefficient by approximation from the Stokes-Einstein equation below (Einstein, 1905). Figure 4.8 shows the results for gelatin with varying polymer and NaCl concentrations.

$$D = \frac{RT}{N} . \frac{1}{6\pi kP} \dots Eqn\ 4.1$$

Where, D is diffusion coefficient, R is the gas constant, N is Avogadro's number, T is the absolute temperature of the system, k is viscosity and P is radius of the diffusing particle.

For gelatin, release does not occur on the same time scale at 37˚C as for gellan and alginate. It can be seen from the graph that a sigmoidal pattern is present with a much faster release. Initially a lag phase occurred followed by an increase in concentration, which slows as the final equilibrium concentration was achieved. When added to the water, the gelatin sample begins to melt (since 37˚C is above the melting temperature of 32˚C found in DSC experiments). Thus, the curve shows the slower release at first as the gelatin starts to melt. This is then followed by a rapid increase, with the final conductivity being reached after approximately 10 minutes, as compared to the 3 hours required at 25˚C. In this situation,

diffusion of the sodium ions through the gel no longer determines release rate; heat transfer to the gel sample and subsequent mixing into the bulk governs the rate.

The results obtained in this study show good repeatability, proving the method useful for gathering data on salt release from a variety of structures. Between each polymer concentration some difference was observed, suggesting that increasing polymer concentration slows release from the structures, due to greater physical interference from polymer chains within the structure. However, for the concentrations used here the results were not significantly different.

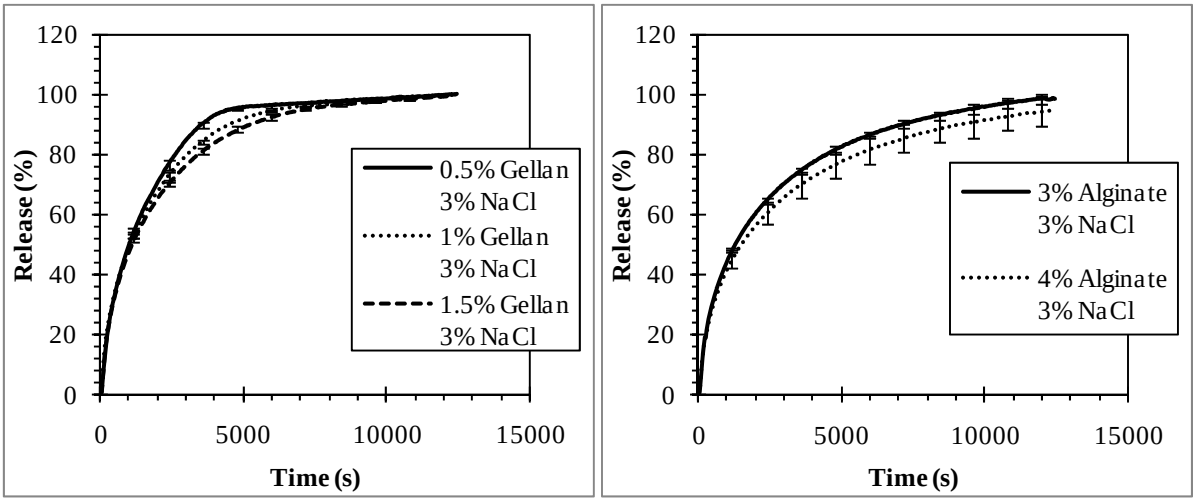

Figure 4.6. Release comparison between concentrations of polymer as a percentage of total release over time for samples of Gellan and Alginate at different polymer concentrations. Experiments were carried out at 37˚C in all cases with 3g samples at 3% NaCl concentration in a body of 200ml of distilled water. Conductivity was recorded to track release and averaged over 4 independent runs. Error bars represent 1 standard deviation of the mean.

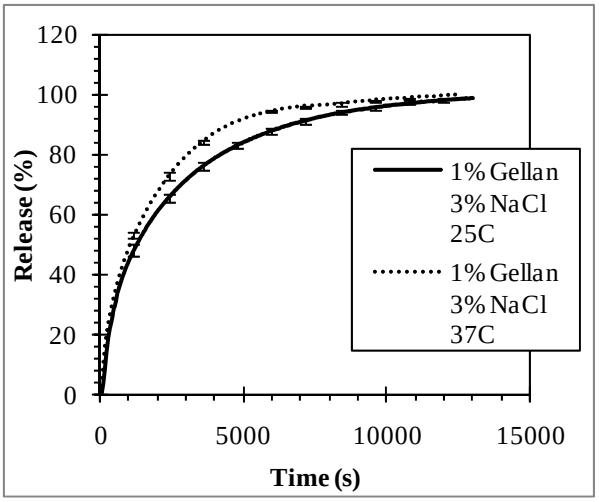

Figure 4.7. Sample comparison of gellan at 25 °C and 37 °C as a percentage of total release over time. Experiments were carried out with 3g samples in a body of 200ml of distilled water. Conductivity was recorded to track release and averaged over 4 independent runs. Error bars represent 1 standard deviation of the mean.

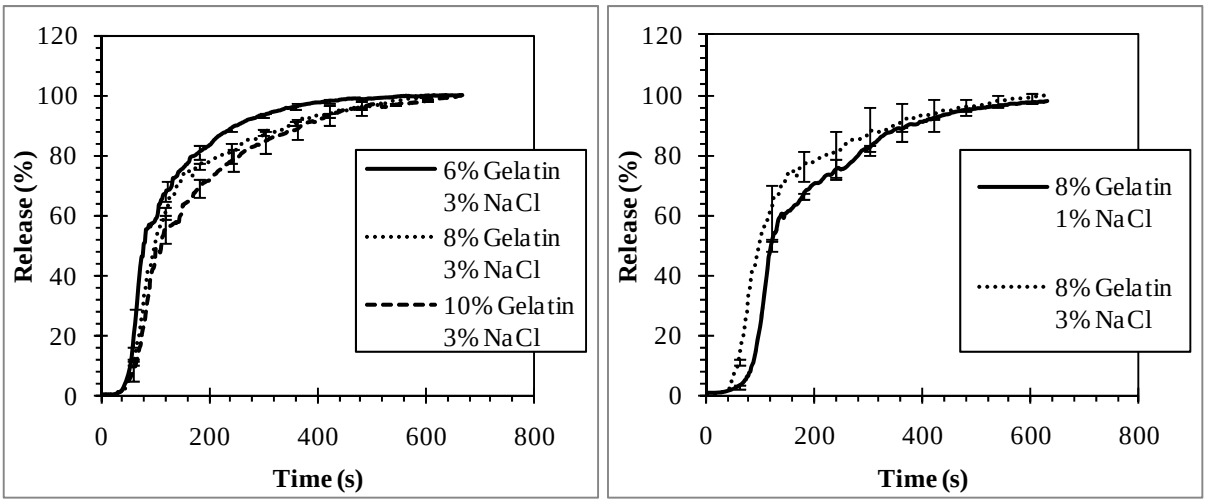

Figure 4.8. Release data for gelatin at 37 °C as a percentage of total release over time left, release for three gelatin concentrations at a fixed 3% NaCl level. Right, comparison of release between samples with a fixed gelatin concentration at 1 and 3% NaCl levels. Experiments were carried out with 3g samples in a body of 200ml of distilled water. Conductivity was recorded to track release and averaged over 4 independent runs. Error bars represent 1 standard deviation of the mean.

4.2.2. Mathematical modelling of salt release

Having obtained experimental evidence that the technique provides information on NaCl release from biopolymer structures, a model was developed using COMSOL, with a geometry to match the experimental conditions. The system was set up to assume pure Fickian diffusion within the gel samples, as described in section 3.2.4. The model can then be used to generate data for diffusion controlled release and compared with experimental data. The curve generated from the model using the free diffusion value of sodium ions in water (which assumes no gel sample and no mixing) follows the same shape and order as experimental data, with the exception of the case in which gelatin melted. Therefore, it can be assumed that release occurs by diffusion in these cases and the effective diffusivities of the samples can be calculated using the model.

The code was run as a script coupled with MATLAB, altering the effective diffusivity to minimise the sum of squares between actual and calculated values (see Appendix 2). A sample comparison of calculated and experimental data can be seen in Figure 4.9. Initially, over approximately 200s the predicted salt released was faster than the measured salt release, but overall there was close agreement between experimental method and model. The slight initial difference could be attributed to a lag in recording in the physical system, or to a delay caused by raising the gel temperature to match the water surround.

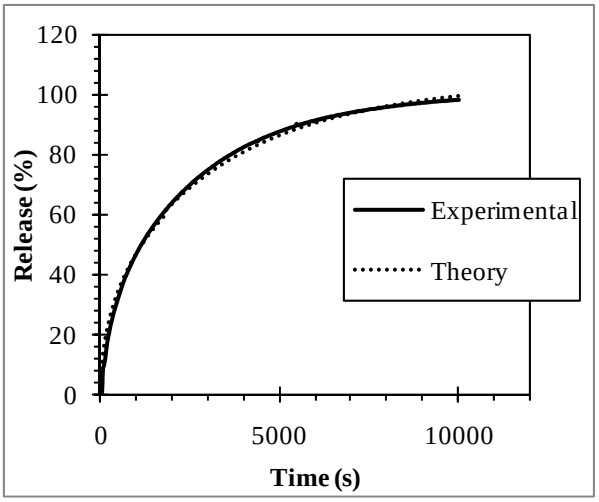

Figure 4.9. Comparison of experimental and model generated data for gellan, sample experimental data from 3% NaCl 1% Gellan in Figure 4.3 is compared with model generated release data using the closest fitting diffusivity of 1.12×10^{-9} m^2/s.

Table 4.1 and Table 4.2 show a list of estimated effective diffusivities gathered from the model at 25˚C and 37˚C respectively. Values varied slightly with concentration across samples. A standard deviation of 1.6×10^{-11} m^2/s was calculated from a characteristic set of individual experiments although values presented in tables 4.1 and 4.2 are obtained from comparison with averaged release data. The results were very close to the value of free diffusion of sodium ions in water given in the literature (1.334×10^{-9} m^2/s at 25˚C) (Lide, 2004). This indicates that the sodium ions move through the gel structure essentially unhindered. For gelatin similar experiments were previously carried out using silver ions, which have a similar effective ionic radius to sodium (115 and 102 pm respectively (Shannon, 1976)). The nature of the gelatin's open network structure means that diffusion of silver ions was unaffected, at least in the range of concentrations used in the literature (Yabuki, 1927). A similar situation must exist for gellan, whereby the structure generated during gelation was not sufficiently dense to prevent small ions diffusing through. Details from a recent review Miyoshi (2009), show that most of the water within the gellan structure remains as

clusters of free water which sodium ions would diffuse through at a normal rate. There are some studies in which diffusion through gel structures was shown to be slower than water (Stiles, 1920, Stiles, 1923). However, the methods involved investigated salt diffusion through a gel using a precipitating indicator, where silver nitrate dispersed in the gel, forms silver chloride as salt diffuses through the gel structure giving a visual change. The indicator used has been subsequently shown to influence diffusion rate, so the gel's effect is not certain. Furthermore, the magnitude of difference between the water and gel samples was very small: in the same order of magnitude as the differences seen in this work, and therefore not significant for applications to control salt release from structures.

Table 4.1. Effective Diffusivities (25˚C)

Polymer Type	Polymer Concentration (%)	Effective Diffusivity ($x10^{-9}$ m^2/s)
Gelatin	6	0.99
	8	0.93
	10	0.93
Gellan	0.5	1.15
	1	1.12
	1.5	1.01
Alginate	3	0.96
	4	0.93

Table 4.2. Effective Diffusivities (37˚C)

Polymer Type	Polymer Concentration (%)	Effective Diffusivity ($x10^{-9}$ m^2/s)
Gellan	0.5	1.52
	1	1.32
	1.5	1.20
Alginate	3	0.93
	4	0.99

4.2.3. Compression effects on salt release

In order to relate the release of salt from gels in-vitro to release in the mouth, the effect of compression of the gel on the salt release rate was investigated. This increases the complexity of the measurements, but more accurately mimics oral processing i.e. mastication. Materials were tested using the stirred tank environment described in the materials and methods section (Figure 3.1 (b)). A texture analyser was used to provide compressions. Samples of gellan at 0.5, 1 and 1.5%, and gelatin at 6, 8 and 10%, were tested at 0%, 30% and 75% strain, while salt release was measured and tracked using conductivity (further details are available in Section 3.2.5). Testing at 0% strain allowed a baseline for comparison of higher strain experiments, while 30 and 75% gave results below and above the strain required to fracture the gels. Figure 4.10 shows three repeat force/distance curves for a single gelatin sample collected during 30% strain (low stress) environment. The structure is elastic under the small strains where the curves overlap for each compression. These results can be correlated with a low force environment which is useful to highlight any release mechanisms caused by compressions in the mouth before fracture occurs. In order to investigate structure breakdown effects on salt release, repeat compressions at 75% strain were carried out. This could be likened to chewing of large particles or fracturing from squeeze flow during swallowing of smaller particles in the mouth. At the larger compressions (75% strain, Figure 4.11) the curves change with each compression. Initially, there is a large peak force (40N) where the gel begins to break. On subsequent compressions the force required for the compression is reduced to 2N as the gel is further broken up, and smaller sections were pushed out from under the probe. The force required for 30% compression is around 2.2N while 75% required 40N. Both values are still significantly lower than the average bite forces reported in the literature. Values vary depending on product being tested and the individual in question but

for soft rubber an average of 213N has been reported (Paphangkorakit and Osborn, 1998). This suggests the gel samples would be easily broken in the mouth.

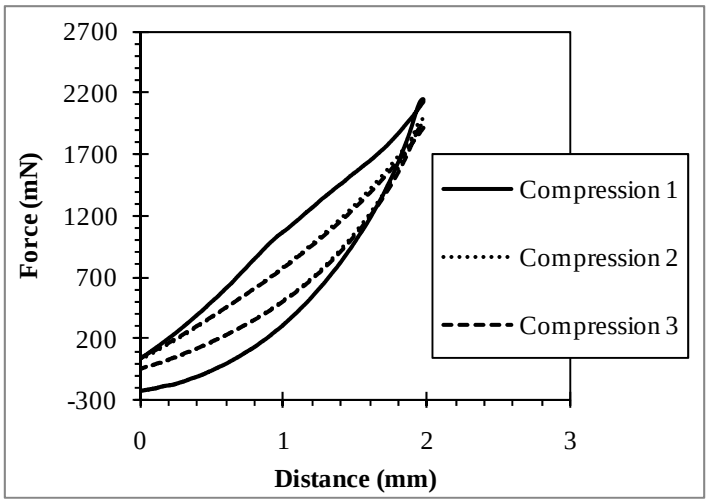

Figure 4.10. Force distance curves for gelatin at 30% strain, using a 6% gelatin 3% NaCl sample. 3g cylindrical segments were compressed at 1mm/s, 30% of the original height, 6 times with 3 minute intervals, compressions 1 to 3 only are presented for clarity.

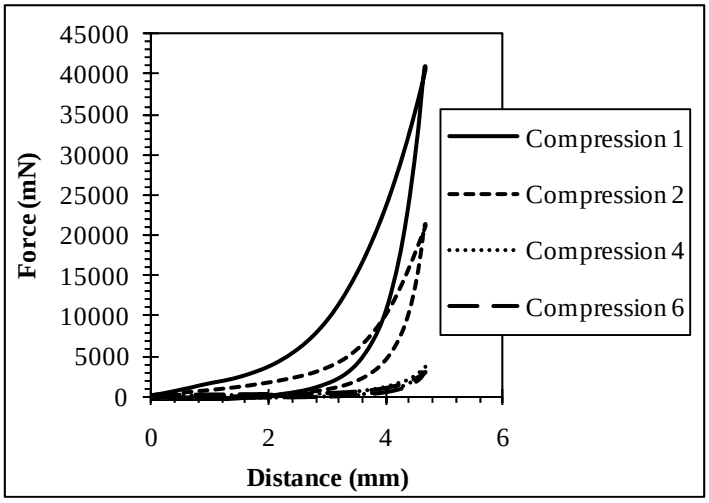

Figure 4.11. Force distance curves for gelatin at 75% strain, using a 6% gelatin 3% NaCl sample. 3g cylindrical segments were compressed at 1mm/s, 75% of the original height, 6 times with 3 minute intervals, compressions 3 and 5 are omitted for clarity.

Having obtained this information for each of the samples, salt release was studied under compression. Figure 4.12 shows release results for gelatin under three conditions. The 0% average curve represents a control test with the texture analyser probe in contact with the gel sample, but with no compressions performed. Here the results follow release experiments previously described with diffusion determining the release rate. However, the overall release rate is slower due to the reduction in surface area, caused by the probe head and vessel bottom covering part of the gel sample. At the low compression strain (30%) salt release was unaffected: the average curve for these runs follows the same pattern as the 0% compression, indicating no extra release. Bot *et al.* (1996) showed that compression up to the fracture point leaves gelatin relatively unchanged, and as compression experiments at 30% do not fracture the gels no increase in release of salt is expected.

At the higher strain of 75% a noticeable effect on release is observed. In these figures curves are presented as individual runs, as a large variation in results exist. Before the first compression takes place, release curves for 75% compression follow the 0 and 30% strain results as expected. After this point a distinct increase in release rate can be observed, which further increases with subsequent compressions. Observation of the gel samples, in conjunction with the force-distance data generated, showed fractures occurring after the first compression, with further breakup to differing degrees with subsequent compressions. The increase in release rate can be explained as a consequence of the increase in surface area generated when the gel is fractured.

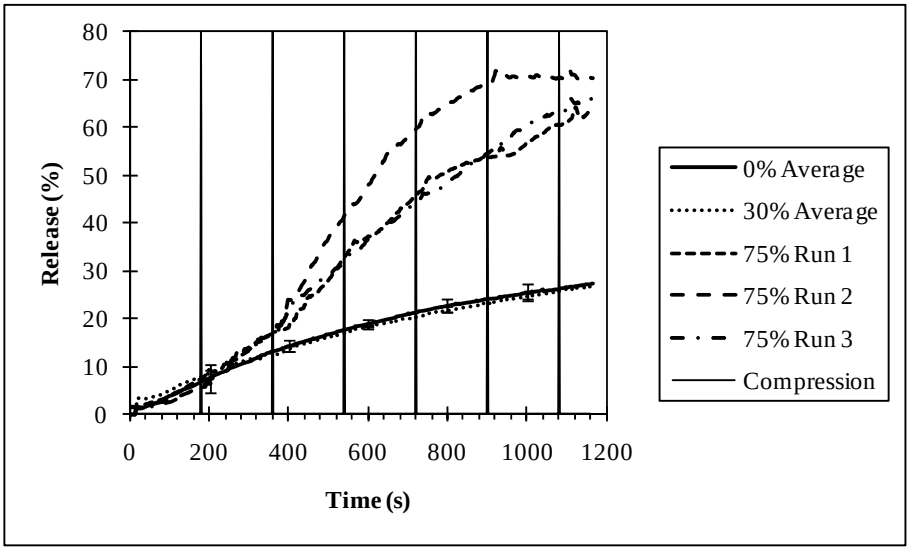

Figure 4.12. Release profiles for gelatin under different strains, from a 6% gelatin 3% NaCl sample at increasing strain rates. 0% and 30% strain are shown as an average of 4 runs with error bars at 1 standard deviation from the mean. Compressions at 75% strain are shown as individual runs due to diversity. Vertical lines at 3 minute intervals represent onset times for each compression. Experiments were carried out at 25˚C in all cases with 3g samples in a body of 200ml of distilled water. Conductivity was recorded to follow release and presented as a percentage of total release.

Having shown that the fracture of gelatin samples affects the release of salt, gellan samples were investigated. Results are presented in Figure 4.13. A similar pattern to that observed for gelatin is evident. At 75% compression a significant increase in salt release was recorded. However, the increases in release rate did not occur at the same point for all samples. As can be seen, samples 1 and 2 fractured after the first compression, giving rise to a large increase in release rate. Conversely, sample 3 did not fracture on the first compression, but did at the second compression. Thus, the salt release follows the 0% compression curve until the second compression. This difference in behaviour between samples is probably due to the presence of cracks or weak points in samples 1 and 2, which were not present in sample 3. Visual observations throughout the gellan experiments reinforced the hypothesis that the increases seen are caused by the increase in surface area. At 30% compression no fracture

was observed; at 75% compression large visible failures were present after the first and second compressions, in line with increases in conductivity recorded.

Figure 4.14 shows a comparison of the individual second run for both gelatin and gellan at 75% strain. Prior to the first compression (the first 180 seconds) the 2 gel samples show the same release profile, which corresponds with pure diffusion. However, gelatin reaches a higher maximum amount of release in the 20 minute period, which is a result of the difference in the extent of the gel fracture. Gelatin tended towards multiple failures, resulting in many small segments, which have a larger surface area. The gellan samples tended towards large fractures and deformation while remaining in a single block, or splitting into a small number of sections. This results in a smaller increase in surface area. Similar behaviour has been reported by Harris *et al.* (2008), where gellan with different cross linkers were subjected to similar strain experiments. The authors showed that the gels split diagonally through the middle of the sample, but remained in large parts. Similarly, it has been shown in previous studies that more rigid gels released less flavour volatiles as the forces applied to them caused less fractures, and therefore exposed less surface area (Boland *et al.*, 2004). For the gels studied in this work the gellan samples were the most rigid, which could have contributed to the reduced release.

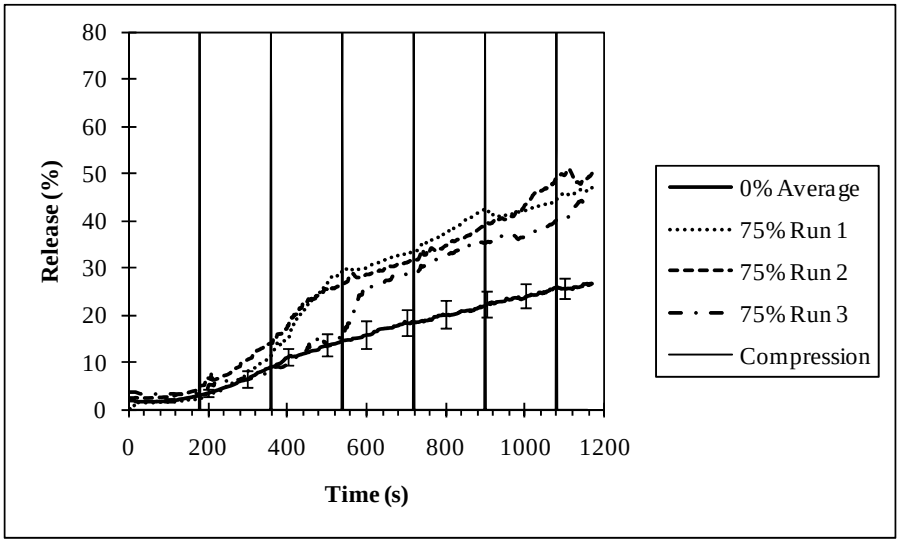

Figure 4.13. Release for gellan under 75% strain from 1% gellan 3% NaCl. Compressions at 75% strain are shown as individual runs due to diversity, 0% results are presented as an average of 4 runs with error bars at 1 standard deviation from the mean. Vertical lines at 3 minute intervals represent onset times for each compression. Experiments were carried out at 25˚C in all cases with 3g samples in a body of 200ml of distilled water. Conductivity was recorded to follow release and presented as a percentage of total release.

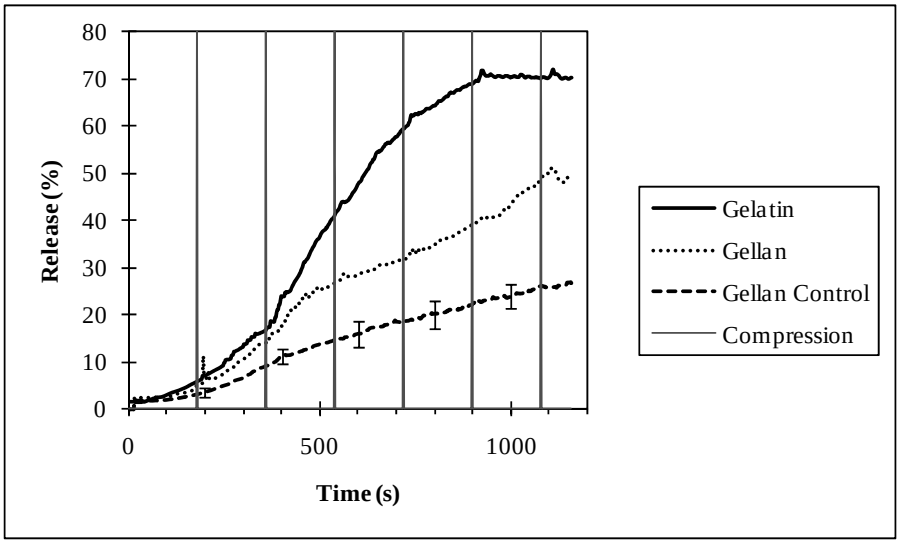

Figure 4.14. Release comparison at 75% strain, for 1% gellan 3% NaCl and 6% gelatin 3% NaCl. 0% strain results for gellan are presented as a baseline. Vertical lines at 3 minute intervals represent onset times for each compression. Experiments were carried out at 25˚C in all cases with 3g samples in a body of 200ml of distilled water. Conductivity was recorded to follow release and presented as a percentage of total release.

For gellan samples, Harris *et al.* (2008) also showed that in some cases water is expelled from the structure on compression, although this was not evident in this work. If water were expelled during the compressions carried out in this work it would be expected to release salt at a faster rate. No increase in release is observed in the 30% samples where the compressions do not break the structures and therefore it is assumed no water is expelled during the compressions. It is possible that the high levels of salt added to the samples affected the behaviour of the gel. Tang *et al.* (1996) showed that for gellan samples the mechanical properties of the gellan where greatly affected by the ion concentration present around an optimum concentration. Above this optimum, gels were more brittle, and had a reduced strength. This could explain the findings in this work where no water is expelled since the salt concentration was much higher to that of Harris *et al.* (2008).

The model that was developed for diffusion was also used to investigate how salt release is dependent on the size of the gel pieces, in order to determine whether it would fit to the observations made during compression experiments. The model was run with a reduced geometry size, which assumes multiple identical samples that have the same combined volume as the original i.e. to represent the increased surface area on fracture, modifications made to the MATLAB file are shown in Appendix 2. By comparing the release times under compression with the model generated times, an estimate of particle sizes present after compression can be calculated. As a further extension of this work, salt release times for a theoretical liquid product with micron sized gel droplets can be calculated. Currently, some low fat spread products use gel encapsulated oil droplets to control lipophilic volatile release, so a similar approach for salt may be relevant (Malone and Appelqvist, 2003). In order to use the developed COMSOL model with these systems, the cylinder geometry used originally

was altered to a sphere with equivalent volume (Figure 4.15). This made automation of the model simpler and quicker to run. The change is also a better representation of an emulsion type product with gelled droplets. However, allowance has to be made for the change in surface area of samples with the same volume.

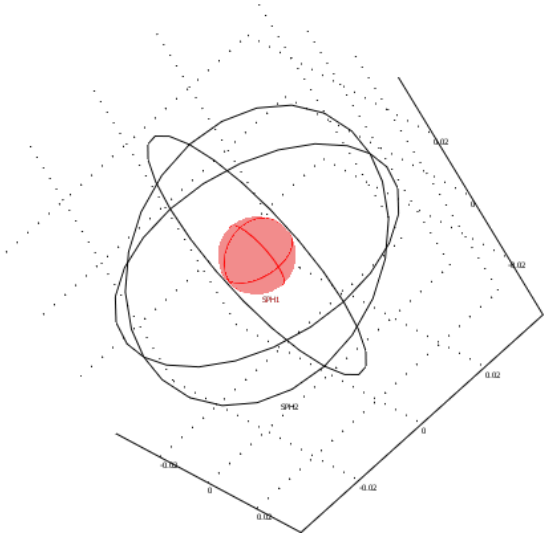

Figure 4.15. Altered COMSOL geometry used in calculations concerning compression experiments, assuming a spherical gel sample with the same volume as cylindrical samples used in experiments. A spherical geometry for the 200ml of distilled water is also used.

The time taken to release 70% of the contained salt for a range of sample sizes relevant to those used in this study is shown in Figure 4.16. The maximum point shows the time for release from a sphere, which is volume equivalent to cylinders used in previous experiments. This calculation maintains the sample mass and salt concentration within the sample. The time is then compared with the experimental data to determine what effect the change in geometry, and therefore the surface area, has on release profile. The time predicted for the sphere to release 70% of the contained salt is around 30% longer than actual data for the cylinder, this is due to the reduction in surface area (by about 25%) caused by the geometry change. The time taken to release 70% of the contained salt for experiments at 75% compression in gelatin correlates with model data for spheres with a radius of around 3.6 mm.

This 70% release value is taken since this is the level reached in the 20 minutes experimental time. Again, the time to release 50% salt in gellan is predicted to be around 30% slower than in the actual cylindrical data. Here the results taken from the 75% compression experiments would be expected for spheres with a radius of around 6 mm (Figure 4.16). Again the 50% release value is taken since this is the level of release observed in the compression experiments for gellan samples. This indicates that the increase in salt release rate observed is due to the increase in surface area caused by breakup under compression, and that gelatin breaks into smaller segments than gellan. In both cases the particle sizes would be smaller for cylinders, and in reality irregular shapes were formed. Studies into particle sizes created during mastication have shown that a range of particles sizes are created. These works try to better understand the processes occurring in the mouth by examining different foodstuffs taken from the mouth during chewing. Factors such as particle sizes, saliva contents and residence times can be related to physical properties to describe how the mouth deals with different products. Jalabert-Malbos *et al.* (2007) show that for a range of foods, sizes from 0.4-4mm, with a median size of approximated 2mm, were found when ready for swallowing. Mielle *et al.* (2010) observed particle sizes after 4 and 8 chews of peanuts, which vary over a similar range. This suggests that the sample sizes created during the compression experiments in this study are representative of food samples at the very beginning of mastication.

Figure 4.17 shows expected release times for small gelled emulsion droplets (20-60 microns). Release at this scale is very fast (less than 1 second), indicating that this alone would not form an effective method for controlling salt release, as the sodium ions still diffuse through the gel matrix. For all instances, increasing radius does not give a linear increase in time. An

analytical solution to this situation can be found in Crank (1975) as a sphere in a stirred media. This has been applied in the release of volatiles in emulsion droplets which are of comparable scale and time to release 50% of the contained volatiles is described by:

$$t_{1/2}=(0.162r^2)/D...Eqn\ 4.1$$

where $t_{1/2}$ is time to release 50% material, r is droplet radius and D is diffusivity. This means that time to release a set percentage of salt will increase proportionally with radius squared.

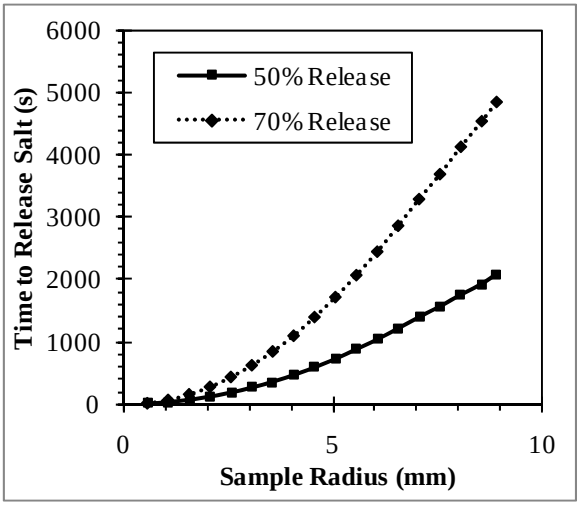

Figure 4.16. Model generated time to release salt from gellan, release of 50 and 70% of contained salt as a function of sample radius as generated by the spherical COMSOL model is presented. Example data is presented for 1% gellan 3% NaCl with an effective diffusivity of 1.12x10-9 at 25˚C.

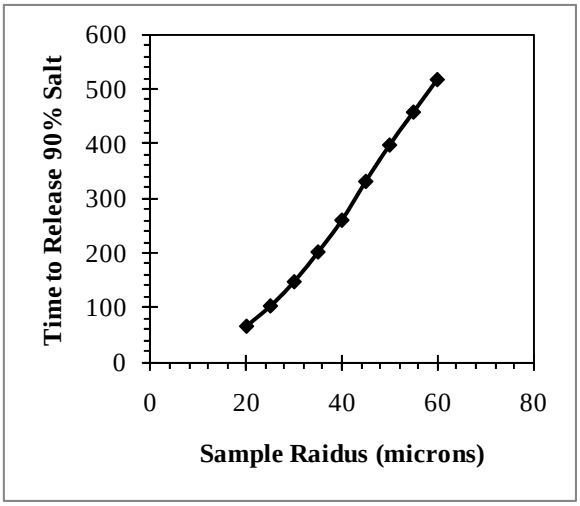

Figure 4.17. Model generated time to release 90% salt from emulsion sized gel droplets as a function of sample radius as generated by the spherical COMSOL model. Example data is presented for 1% gellan 3% NaCl with an effective diffusivity of $1.12x10^{-9}$ at 25˚C.

4.3. CONCLUSIONS

Two in-vitro methods were developed that can be used to follow release from model structures, in this case the release of salt from hydrocolloid gels. This can be extended to include different structures which can be compared with the gel experiments carried out in this study. Release curves gathered from the different hydrocolloids (gelatin, gellan and alginate) show that there is very little to impede the diffusion of sodium ions out of the structure into the surrounding media. Thus, these hydrocolloids alone cannot be used to control salt release. Compression effects on the release rate of salt are observed when forces are sufficient to cause gel fracture and increase surface area. The gel's structure determines the change in release: more brittle gels tend to release salt quicker as compressions cause greater breakup, a larger surface area and shorter diffusion paths. In the single phase structures tested there is no evidence of increased release rate with compressions, unless fracture occurs. When compressions are at a high enough strain to cause fractures within the samples (>75% in this study), the release increases depending on the extent of failure and

increased surface area. Gelatin, tending towards many discrete pieces when it fractures, released faster than gellan, which compressed forming fractures, but stayed in a single piece. It is clear that for semisolids at least, deformations during oral processing are important (Finney and Meullenet, 2005), and that the deformations themselves can affect the amount of breakage and flavour release. This study has shown that there is not much control for salt release using these gels. However, more complex structures may allow other release profiles to be designed.

Modelling the process has allowed effective diffusivities of each system to be obtained, and while they do not vary significantly to that of water, the values can be used to predict release rate from a variety of different geometries and conditions which match analytical solutions for similar systems in Crank (1975). This model can also be used to calculate release rate for different materials in future testing.

CHAPTER 5. TRIBOLOGY

5.1. INTRODUCTION

This chapter concerns the first steps in setup and modification of tribology equipment for use as part of an in-vitro mouth model. Tribology is the study of lubrication, friction and wear between surfaces. The technique allows information to be gathered on small scale thin film behaviour of materials, an area which current food research has not investigated in significant detail. Previous studies have shown tribology to be a promising instrumental method for correlations with oral behaviour, specifically squeeze flow between the tongue and palate. This information combined with other physical measurements such as rheology and texture analysis gives an increasingly encompassing understanding of oral processing (Koliandris *et al.*, 2010, Malone *et al.*, 2003, Mossaz *et al.*, 2010).

An investigation into parameters such as rotational speeds of the ball and disk and sample volumes, along with different measurement surfaces, which can be used with the developed tribology equipment, is presented. The use of steel or soft elastomer/PDMS surfaces is explored and their characteristics presented. Further to this, tribology work carried out by Malone *et al.* (2003) and Koliandris *et al.* (2009) was in part replicated and compared. Comparisons of tribology data with sample properties and with sensory correlations made in these studies are also made with data gathered here. Shortcomings of currently used methods are highlighted to support the need to develop more dynamic tribology measurements, presented in later chapters. A series of oil in water emulsions at different levels of oil are compared using tribology, in addition to guar and dextran samples. Full sample preparation is presented in sections 3.2.8 and 3.2.9.

5.2. RESULTS

5.2.1. Initial tribometer setup

Previous work in the area of tribology has identified a number of factors that affect lubrication. These factors include normal forces, rotational speeds of both the ball and disk surfaces, slide roll ratios (SRR) and measurement surface characteristics among others. This past exploration is further detailed in section 2.5 of the literature review. The design of tribology equipment in this work attempts to mimic oral conditions as closely as possible, while retaining a quick repeatable setup. Deformable surfaces, which are closer to oral surfaces than steel contacts, are preferable but the use of actual tissues as in work by Dresselhuis *et al.* (2008a) is impractical for regular testing. Additionally, contact pressures, as a function of normal force and surface deformability, should relate to those in the mouth. Speed ranges that correlate to sensory ratings need to be considered. This includes the mixed lubrication regime as in work by Malone *et al.* (2003). Finally, as an extension to current tribology work the ability to perform temperature controlled, timed experiments under constant conditions, with material added and cleared would improve the method in order to mimic eating.

The initial design of the equipment focused on exploring the contribution of some of the factors mentioned above to better plan future experiments. Factors were explored by carrying out a series of Stribeck curves, as detailed in section 2.5. The curves consist of friction measurements made between the two rotating surfaces, with a lubricant in place across a range of rotational speeds from 1mm/s up to either 1000 or 1500mm/s. Sample volume was briefly investigated in this study. As traction is measured by deflection of the rotating arm

perpendicular to the normal force, liquid flowing around the ball rather than between surfaces could influence the arm's position and therefore change the measured deflection. Results indicated that provided the added sample is able to cover the disk and provide material to the contact, results were unaffected by sample volume (in homogenous samples). In all cases 40ml allowed good coverage without overfilling the cell (Figure 5.1). Vegetable oil was used in this volume study as a model liquid food sample, however it is possible that a volume effect could be seen with highly viscous samples. However, a simple system was chosen since the lubrication properties of a more structured material such as a biopolymer solution would be more complex, and so differences might not be as a result of sample volume.

Normal force was investigated as it is expected that with increasing downward force an increase in friction and reduction in entrainment of sample in between the rotating surfaces would be observed. Normal force can be specified, and is kept constant by the equipment during experimentation. However, as this force determines the contact pressures, experienced (for a given set of surfaces) the selection is made based on the desired contact pressures and order of friction force which best relates to the mouth. As the equipment is designed to mimic the oral surfaces, relatively low pressures are more desirable. Thus a 1N force was chosen, since this is the lowest force available on the equipment and gives contact pressures in the order of those observed in the mouth (Hori *et al.*, 2009). Further details of contact pressures are presented later in Section 5.2.2.

As a result of the low pressures used, wear on the contact surfaces is not expected. This would allow for reuse of the surfaces, and long timed experiments. This assumption is tested and shown in Figure 5.2 by running 50 Stribeck curves on the same contacts. For these

conditions the friction recorded did not change; therefore, it is assumed that no wear occurs during these conditions. The only exception to this case is when using materials which interact with the surface and deposit material on the contact track. In this case, a gradual change over time can be observed. However, complying with the cleaning regime between tests eliminates this effect.

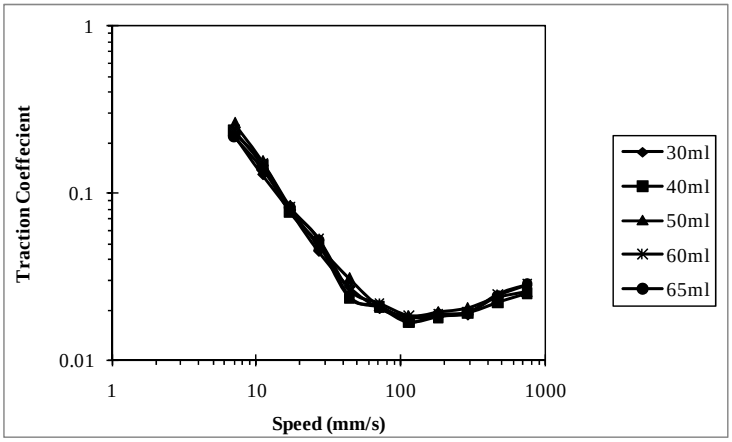

Figure 5.1. Effect of cell volume on Stribeck curves of sunflower oil. Experiments were run using a steel ball and elastomer disc tribopair with a normal force of 1N.

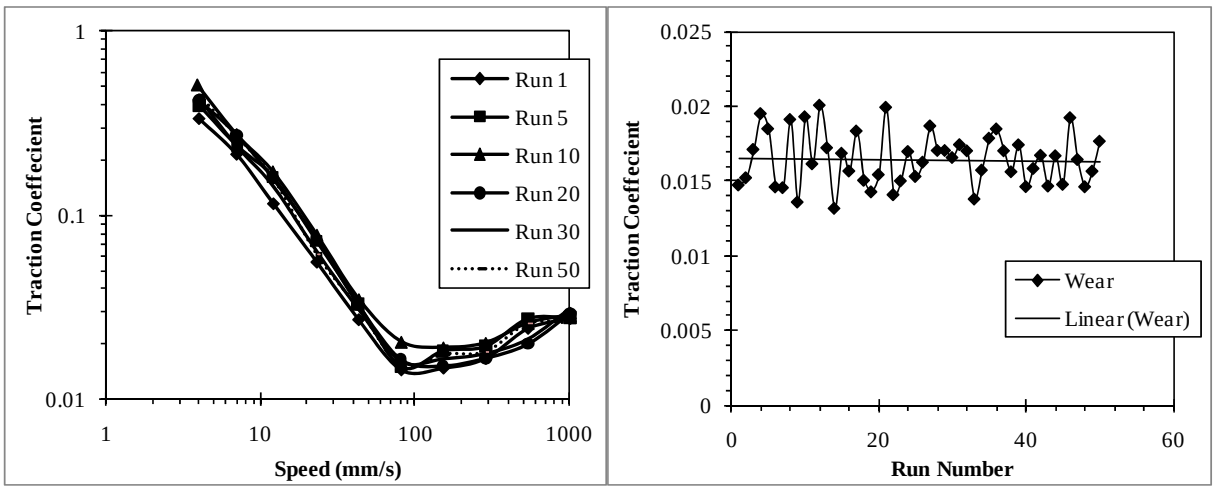

Figure 5.2. Surface wear testing, left, Stribeck curves of a sunflower oil sample run 50 times continuously to identify possible surface wear. Sample curves are presented for clarity. The sample is tested with a steel ball and elastomer tribopair with a 1N normal force, right, variation of traction coefficient at 150mm/s for each of the 50 runs.

Typically to gather information about the lubrication properties of a material a Stribeck curve is carried out. Stribeck curves are traction measurements taken across a range of speeds alternating between a low start speed and a high start speed to ensure there is no hysteresis in measurements. Between each run the ball can either be kept loaded at the desired force or reapplied. For simple materials there is no hysteresis provided the ball remains loaded between runs. Figure 5.3 shows a comparison of timed Stribeck curves, run with and without unloading between runs. When the ball is unloaded the subsequent run from low to high speed starts lower at around 0.2 for run 2 and 0.8 for run 3 compared with a range of 1-1.2 for the other runs. These two runs also finish at a much higher traction coefficients of 0.3 and 0.6 respectively compared with the previous runs of around 0.03. The following high to low run returns to the same as initial runs. It is unclear the exact cause of this effect, or whether it is a flaw in the operation of the equipment. However, the motion of the ball as it unloads and reloads may cause air bubbles or other surface coatings to become trapped. This may affect subsequent readings, and only when the run starts at high speed is the material between the contact properly replaced. This entrapment of air may reduce the level of lubricant in the gap between the surfaces, increasing the amount of friction experienced.

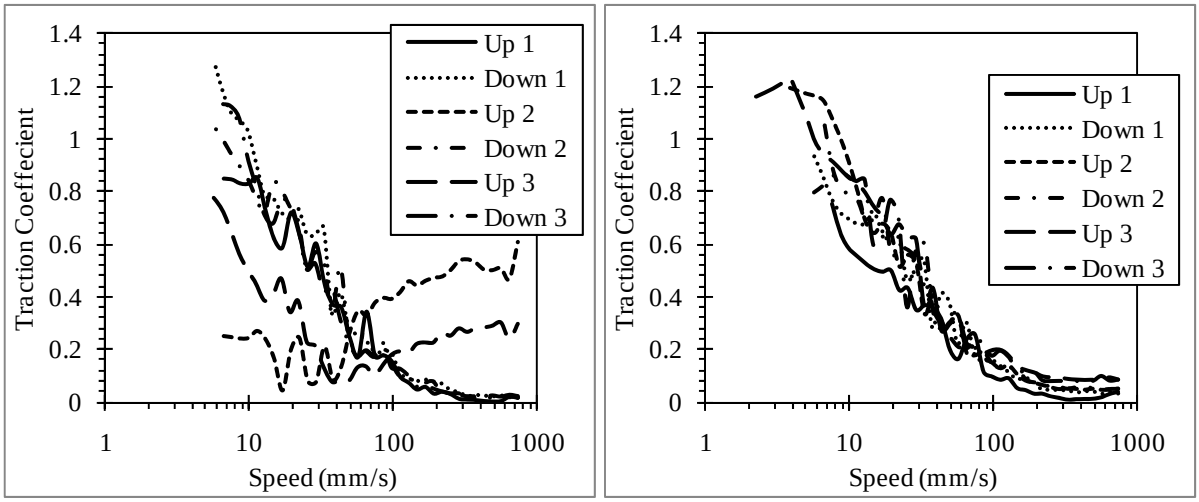

Figure 5.3. Effect of unloading between runs left, 6 Stribeck curves run on a sunflower oil sample, the ball is unloaded and reloaded between each run. Right, data without unloading between each step. Curves are run in alternating ascending and descending speed runs starting from low to high speed. All curves are run with a steel ball and elastomer tribopair and a normal force of 1N.

5.2.2. Surface comparisons

With the initial setup tested and validated, the next stage of the work investigated the effect of the available contacting surfaces. Table 5.1 details the values used for standard Stribeck testing used for surface comparison. Two different materials for each the ball and disk were tested in four combinations shown in Table 5.2. PDMS was used to make a ball and disk, which can be paired together or used with a commercially bought stainless steel ball, or disc cut from commercial elastomer sheets. Surface characteristics of these materials are detailed in the following discussion section.

Table 5.1. Tribometer settings

Variable	Value
Volume	40ml
Slide/roll ratio	50%
Speed range	1-1000mm/s (MAX 1500mm/s)
Normal force	1N (MAX 2/3N)

Figure 5.4 shows a comparison of Stribeck curves performed for different surface combinations. The Stribeck curve is usually split into sections which describe the type of lubrication occurring. Firstly, the boundary regime, which occurs at very low speeds, contact on contact friction dictates the friction recorded. At around 10mm/s the mixed regime is present, where a mix of contact and lubricating fluid determines friction. With further increasing speeds the hydrodynamic regime is reached, where surfaces are fully separated and friction is determined by fluid properties alone.

For the oil sample used here very little of the boundary regime is observed since the oil lubricates efficiently from a low speed. Boundary friction is a function of the roughness of surfaces (Table 5.4) and their deformability (Table 5.5). Rougher surfaces reduce effective contact area, as contact is made by the peaks in the surfaces, so friction is decreased. However, this effect can be balanced with deformable surfaces since more compliant materials will compress on contact and increase contact area (Myant *et al.*, 2010). When speed increases, liquid is entrained causing a mixed effect on friction. Part of the friction experienced is a result of surface/surface contact and part comes from the rheological properties of the lubricating fluid. From the start of the curves at the low speeds in Figure 5.4 it can be seen that there is a difference between specimens used. Table 5.2 contains a sample traction coefficient for each of the three regimes for each contact pair. It should be noted for the samples presented here no clearly defined boundary region is present, but as some change in gradient is experienced at the very start of three of the pairs the value of traction coefficient at the lowest speed is considered predominantly boundary friction. For this comparison the PDMS ball with both disc materials show the highest traction coefficient, followed by the steel ball and elastomer disc at approximately half the value of the PDMS ball configuration.

Finally, the steel ball and PDMS disc pair are at a much lower traction coefficient of 0.02 compared with 0.16 for PDMS ball tribopairs. However, further into the mixed regime, at approximately 8mm/s, the PDMS ball and disc pair reduce traction coefficient to follow the steel ball and elastomer disc curve. This change suggests that when the two configurations reach the same traction sufficient fluid entrainment has occurred in the PDMS ball and disc tribopairs to reduce the initial increased friction caused by having overall rougher surfaces. The final stage shows hydrodynamic lubrication where the friction is dominated by the entrained fluid, here all the curves overlap and roughness has no effect since surface contact is eliminated, although the speed this occurs at is higher with increasing roughness of both surfaces. This trend is similar to data in Bongaerts *et al.* (2007), where the effect of the roughness of PDMS in relation to the Stribeck curves shows the same pattern with increasing roughness. A direct comparison of these surfaces in the same system has not been previously carried out. Surface roughness seems to have a large influence over lubrication recorded, with material properties having less of an effect, although it can still influence the shapes of the curves.

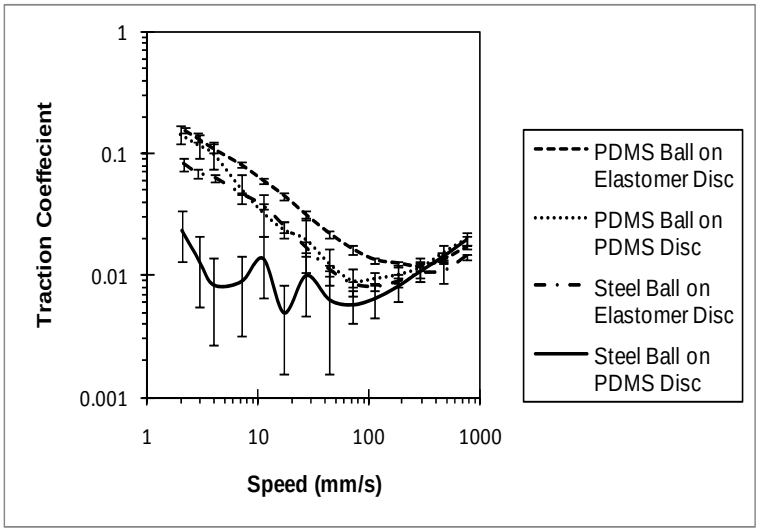

Figure 5.4. Ball/disc pairing comparisons, Stribeck curves run on sunflower oil with available surface combinations. Each curve represents an average of 6 runs alternating between ascending and descending speed sequences at a 1N normal force.

Table 5.2. Traction coefficient values for surfaces

Surfaces (ball/disc)	Boundary friction (2mm/s)	Standard deviation	Mixed friction (45mm/s)	Standard deviation	Hydrodynamic friction (750mm/s)	Standard deviation
PDMS/Elastomer	0.156	0.009	0.022	0.001	0.017	0.001
PDMS/PDMS	0.145	0.024	0.013	0.004	0.020	0.003
Steel/Elastomer	0.082	0.010	0.011	0.001	0.014	0.001
Steel/PDMS	0.023	0.010	0.006	0.005	0.019	0.002

Each of the configurations has its own characteristics, which are summarised in Table 5.3. The PDMS/Elastomer pair produces curves with good definition across the speed ranges, showing clear differences between the different regions as speed increases. However, it has quite high mixed friction coefficients, and can have larger deviations between elastomer samples, as roughness is not always uniform from commercially produced sheets. PDMS surfaces produced in the lab provided mid range friction values with good definition across the speed range, and reasonable repeatability since surface roughness is determined by the moulds used. The steel ball with elastomer disc pairing produced similar results to

PDMS/PDMS surfaces. However, once again there are issues associated with the variability of the elastomer sheets. The use of the steel ball is also not ideal since it does not offer a deformable surface desirable for in-mouth comparisons like the PDMS and elastomer specimens. The final pairing of the steel ball and PDMS disc pair produces very low friction values since these are the two smoothest surfaces. This results in poor definition of the different regimes, in addition to the aforementioned issues. The error bars recorded for this pairing are accentuated due to the logarithmic traction coefficient scale however in reality the absolute variation between samples are similar to PDMS/PDMS results.

Table 5.3. Summary of surface characteristics

Surfaces (ball/disc)	Curve definition	Overall friction values	Surface properties
PDMS/Elastomer	Good definition across regimes	High overall friction	Two deformable surfaces, but variability between elastomer discs
PDMS/PDMS	Good definition across regimes	Medium overall friction	Two deformable surfaces, consistent surface properties
Steel/Elastomer	Good definition across regimes	Medium overall friction	One deformable surface, variability between elastomer discs
Steel/PDMS	Poor definition across regimes	Low overall friction	One deformable surface

In addition to these configurations, the use of a silicone o-ring instead of a ball was investigated. Results presented in Figure 5.5 show a comparison between the PDMS ball and o-ring. The overall friction caused by the o-ring is distinctly higher across the regimes, and is shifted horizontally and vertically upwards from the PDMS results. The main cause of this is from the altered geometry creating a different contact area, and therefore a different pressure between surfaces. Hertzian contact pressure was calculated for each combination to give an indication of differences caused. Hertz equations used are as followed from Fischer-Cripps (2000):

$$\sigma_{max} = (1 - 2\nu)\frac{P}{2\pi a^2} \ldots Eqn\ 5.1$$

where $\sigma_{max}$is maximum contact pressure across the contact, a is the contact area, P is the normal load, ν represents the poisson's ratio of the ball (and disc for ν'). To calculate contact area further information relating to the contacts is required.

$$a^3 = \frac{4}{3}\frac{\kappa PR}{E} \ldots Eqn\ 5.2$$

where R is the radius of the ball in this environment, and E is ball Young's modulus. κ acts as a correction factor, the effective stiffness, for surfaces with different elastic properties given below (ν' and E' represent values for the disc material).

$$\kappa = \frac{9}{16}\left[(1 - \nu^2) + \frac{E}{E'}(1 - \nu'^2)\right] \ldots Eqn\ 5.3$$

Literature suggests the range of in mouth pressure contacts to be around 30kPa, rising to a possible maximum of 60kPa, during swallowing in some subjects. This makes the o-ring a questionable choice in this situation, as the pressure is much higher approximately 1300kPa compared to 100kPa for PDMS surfaces (Hori *et al.*, 2009, Shaker *et al.*, 1988). Reducing the normal load to 1N in equation 5.1 allows the PDMS/PDMS contact to reach 60kPa while maintaining two deformable contacts, making them a good choice for use in this study. This option is preferable to introducing complex surface modifications or the use of actual tissues to completely match the surfaces of the mouth, which could then introduce variability in individual surfaces. Furthermore, a reduction in the contact pressure could be obtained through lower normal forces or softer surfaces. However, this would require further equipment modification and introduce more variability to the data. The current load cell cannot control the normal force below 1N effectively and so would need replacing. This also

means the measurements would be more affected by disturbances. In conjunction with this the force sensor used to detect friction values may no longer be sensitive enough to record the friction generated in this situation.

Table 5.4. Specimen surface properties

Surface	Sa/ nm (average roughness)	Sq/ nm (root mean square roughness)
PDMS Disk	246	293
PDMS Ball	516	658
Elastomer Disk	516	699
Elastomer Disk repeat 2	783	1004
Stainless steel ball	8.84	43.2

Table 5.5. Specimen Young's modulus

Specimen	Young's Modulus (E, Pa)	Poisson ratio
PDMS	2.4×10^{6}	0.5
Steel	2.07×10^{11}	0.293
Elastomer	6.9×10^{6}	0.5

Young's modulus of samples available, values are taken from, Bongaerts *et al.* (2007) for PDMS, Samco silicone for elastomer and from PCS Instruments London for the steel.

Table 5.6. Hertzian contact pressures

"Ball"	Disc	Contact pressure at 3N (kPa)
Steel	PDMS	165
PDMS	PDMS	100
O-ring	PDMS	1300

Calculated Hertzian contact pressure using equations 5.1-5.3 for different configurations used in the present study

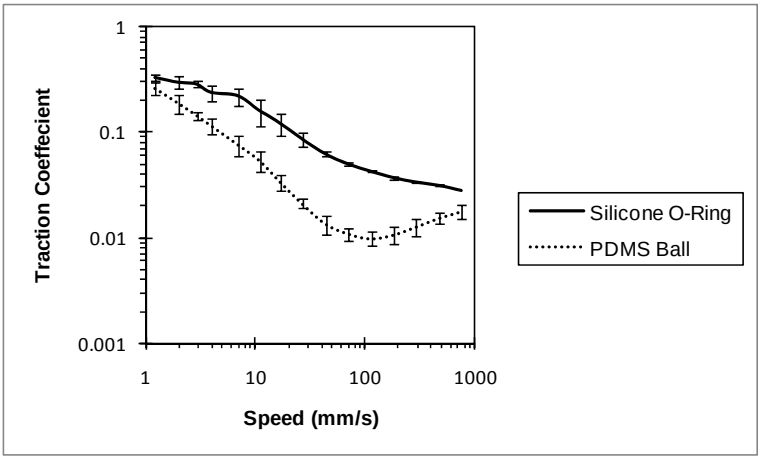

Figure 5.5. Ball/o-ring comparison, Stribeck curves for a sunflower oil sample, using either a silicone o-ring or PDMS ball against a PDMS disc. Each curve represents an average of 6 runs alternating between ascending and descending speed sequences at a 3N normal force.

5.2.3. PCS Instruments mini traction machine (MTM 1)

With a desirable experimental setup confirmed, a series of comparisons with applicable literature were carried out. In this section, measurements are validated using published work of Malone *et al.* (2003). Traction behaviour of oil in water emulsions is considered. In the literature the tribological behaviour of emulsions differing in their oil content was evaluated using tribology, in addition to being rated by a sensory panel. Figure 5.6 presents Stribeck curves of samples of differing oil contents from this study and the literature. Comparison of results for emulsion Stribeck curves gave slightly different patterns. Firstly, since the pure oil and water samples were run without emulsifier, this meant these samples were not comparable, as the literature suggests that the emulsifier affects their behaviour. Secondly, the overall positions of the curves differed. Values presented in the literature were lower than those produced here. This is possibly as a result of the surface roughness of the ball and disc which were reported as lower in Cassin *et al*, (2001). Furthermore, the emulsifier used was different: Tween 20 was used in this study, while Triodan 55 was used by Malone *et al.* (2003). A further contributing factor to the results presented in the literature is that samples

were made to be isoviscous at $50s^{-1}$ by addition of guar gum, and as guar gum itself is shown to affect lubrication this will affect any comparison made.

The curves presented by Malone *et al.* (2003) show two distinct patterns. Firstly, at 15% oil a greater initial traction is observed which is much closer to that of the water curve. This continues through the mixed regime. The second grouping consists of 20, 30, 55% oil emulsions which follows the oil Stribeck curve through the boundary and mixed regime. At approximately 100mm/s an overlap of all the curves takes place, after which two new groups of curves emerge. At the highest friction the 55% oil and pure oil samples have approximately the same progression, with the remaining samples grouping at lower levels of friction. This change in pattern can be explained by way of the different lubricating mechanisms at each stage. At high speed the bulk viscosity has a large effect on friction, and so samples containing 30% oil and below have a much lower viscosity than those containing 55% oil and pure oil giving rise to a divide. At the lower speeds friction of the 20% and above oil samples have sufficient oil associated with them to form a film between surfaces, sufficient to lower friction. However, in the 15% sample a predominantly water film is formed which is not as effective at lubricating. A comparison with data gained in this work is difficult since samples and conditions are slightly different. However, groupings are present for the curves in this work. Initially, at low speeds some differentiation is observed, at higher frictions pure oil and water grouped, which is likely due to the absence of any emulsifier present in these samples. Of the emulsions 20-50% oil are initially grouped at 0.4, slightly below the pure samples while 10% oil is lower still at 0.25. As speed increases this same grouping persists until water is seen to plateau at 0.1 while the 10% oil sample overlaps the rest of the emulsion samples. At these low speeds the oil component is expected to dominate friction, reducing friction to

the same level as seen in literature. The 10% oil sample is expected to have higher friction than in the literature as it does not have enough oil to maintain good lubrication, however this is not the case. It is possible that the extra emulsifier present in the emulsion acts to further reduce friction in this sample. At high speeds for the emulsion samples two groupings are observed. Firstly, at higher friction values the 10% oil sample is present, below this a grouping of the 20-50% oil samples are seen. It is expected here again that a thick film of material separates the contacts and so the traction coefficients are a function of the bulk rheological properties of the sample.

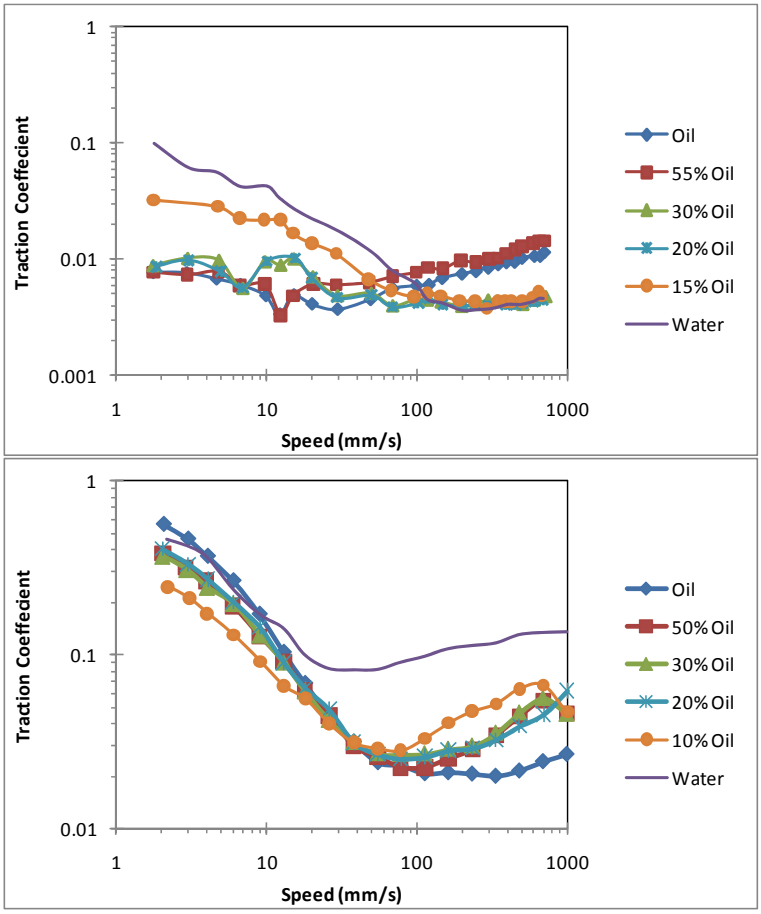

Figure 5.6. Stribeck curve emulsion comparison data for a series of oil in water emulsions with different oil percentages. Top, data from literature performed with a steel ball and elastomer disc tribopairs, bottom, data performed in-lab with a PDMS ball and disc tribopair. Both experiments were carried out at 35°C with a normal force of 3N.

On comparison of the published data, one possible limitation with data obtained from Stribeck curves run on emulsions is that the shearing undergone during the tribology experiment could affect the droplet size of the samples. The shearing could further emulsify the sample, or conversely the extensional flow between the gap could deform the droplets sufficiently to allow individual droplets to coalesce together. For our comparison this factor was investigated. Both before and after the tribology experiments samples of the emulsion were taken, and droplet size was measured using a mastersizer. Results are given in Figure 5.7 for 10% and 20% oil samples before and after running in the tribometer. The droplet distribution was virtually unchanged before and after processing for these samples. In addition, in Figure 5.8a the emulsions produced are compared indicating that while the range of droplet sizes does change slightly due to the changing oil content overall similar stable emulsions were produced, so average droplet sizes remain fairly constant (Figure 5.8 b)

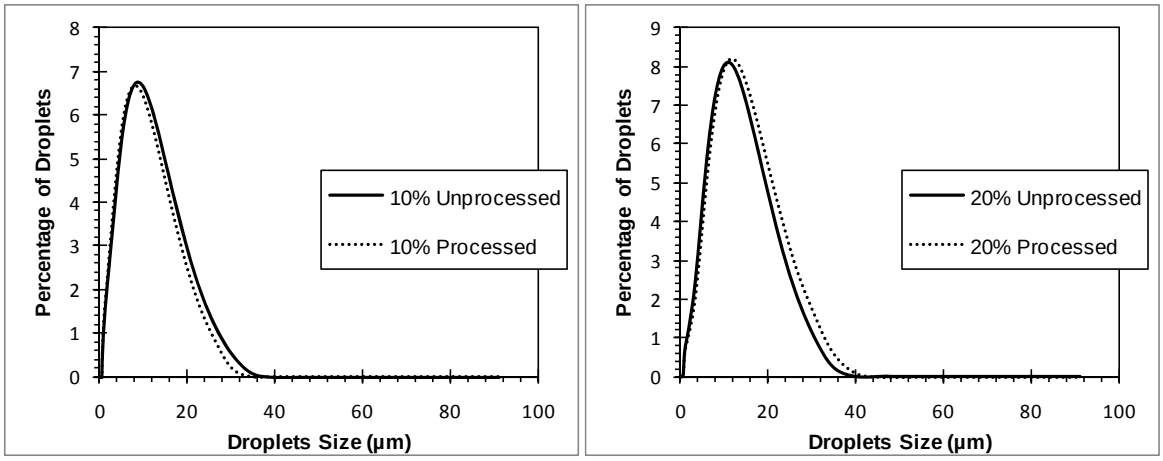

Figure 5.7. Droplet size comparison (Left, 10% oil Right, 20% oil) performed by mastersizer of emulsion samples before and after running a Stribeck curve. Data presented is an average of 3 samples measured.

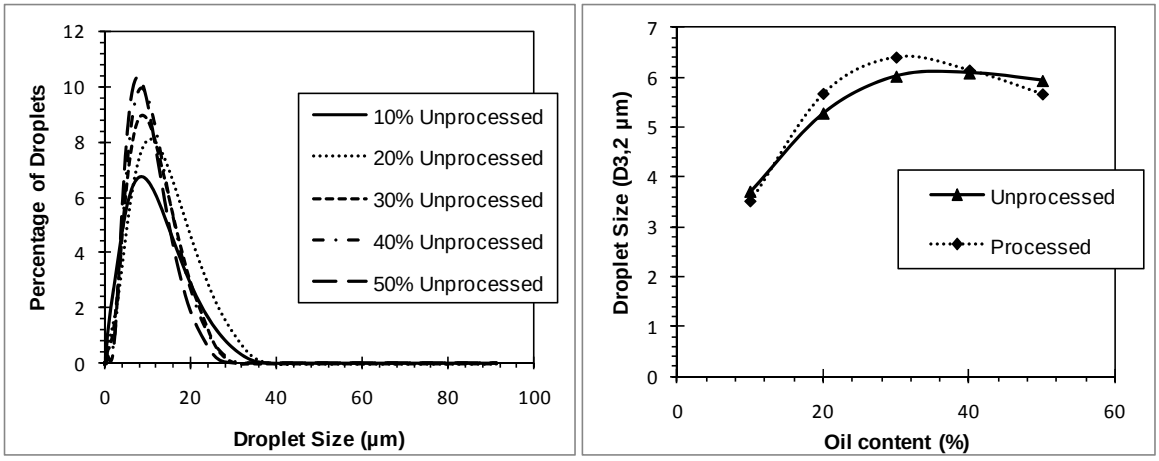

Figure 5.8. Droplet size comparison across concentrations performed by mastersizer, left data for oil in water emulsions of different oil content immediately after production. Right, comparison of the mean droplet size for all samples before and after processing in the tribometer *d32* is presented for comparison with Dresselhuis *et al* (2008b)

As an extension to this work, two new emulsions made with identical components, but with deliberately different droplet sizes were produced. One sample contained droplets with a *d32* of 6µm which are termed "small: and one sample contained droplets with a *d32* of 27µm which are termed "large" (distributions shown in Figure 5.10). Here, some difference was seen in droplet sizes, but not in Stribeck curves. Figure 5.10 a) shows that for the large droplet sample there was a shift in the droplet size distribution after processing. However, for the small droplets, as reported previously, there was virtually no change in droplet size. The observation could be a result of the sample with the larger droplet size being slightly unstable, which would make it prone to coalescence or breakup when exposed to disturbances. This should be a consideration when testing structures using tribology which are unstable under these flow conditions. Similar findings are highlighted in work by Dresselhuis *et al.*, (2008b) where a range of emulsion samples of different sizes and emulsifier content are tested. Samples of "small' (*d32* of 1-1.9 µm) and "large" (*d32* of 2-3 µm) were analysed before and after shearing in a tribometer configuration. It was found that in all cases increased average

droplet size after processing except for cases that were formulated to be stable to coalescence. The effect of "large" droplets was not shown to be different to "small" droplets although the range of droplet sizes was much smaller than the 27 µm droplets used in this work. Under shear, emulsions with a larger number of bigger droplets have been shown to have a greater tendency to coalescence and so a greater effect is expected for the droplet sizes studied here (Klink *et al.*, 2011).

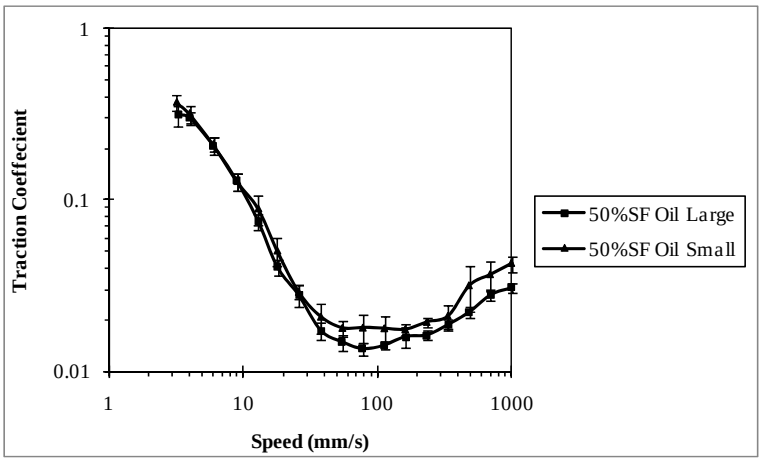

Figure 5.9. Stribeck curve of different droplet size emulsions, 'small' and 'large' (distributions shown in Figure 5.10)

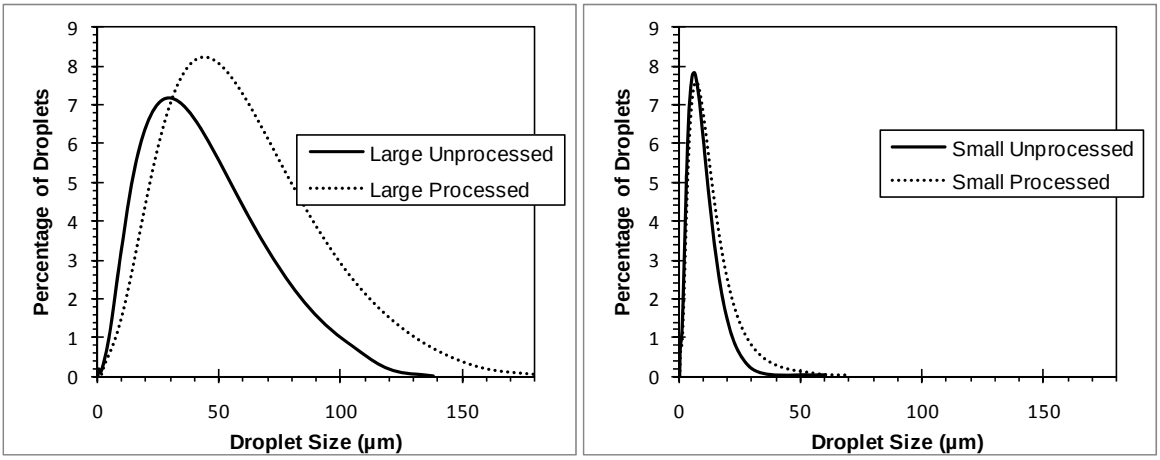

Figure 5.10. Large vs. small droplet comparison (left, large droplets right, small droplets), performed by mastersizer. Data shows distribution before and after processing in the tribometer of two emulsions produced with "large" and "small" droplets.

The second section of work presented in Malone *et al.* (2003) investigates the behaviour of guar solutions. Results from this study are compared in Figure 5.11. Both the results presented in the paper and work here show similar patterns. A water control run is presented in the literature. Results show it does not have good lubrication characteristics and has a high friction across the speed range usually considered. Increasing guar concentration leads to a reduction in the friction experienced after the initial boundary contact is overcome. At low speeds the polymer chains are too large to enter the gap and affect friction and so the curves tend to overlap. In the mixed regime the gap opens sufficiently to allow polymer to have an effect, which separates the results given by each concentration. Overall comparisons are reasonable given the time difference between work and the inability to obtain identical samples.

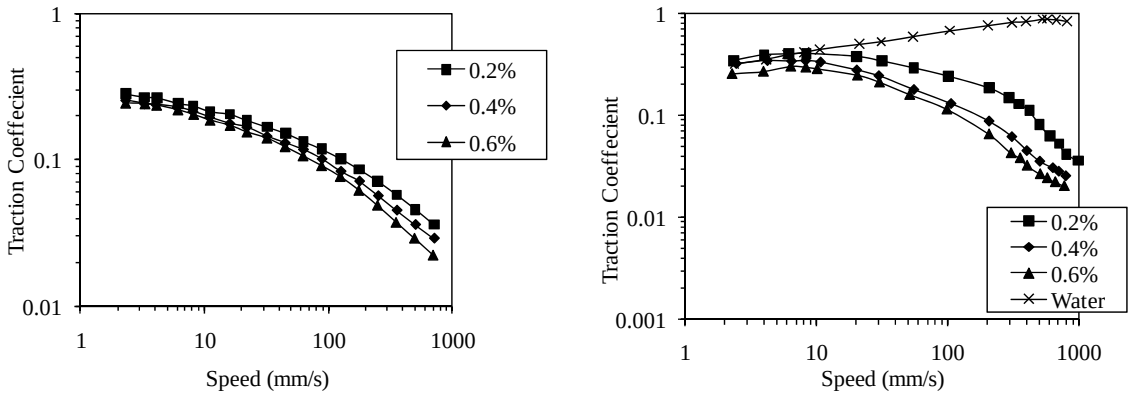

Figure 5.11. Stribeck curves of guar samples of different concentrations. Left, data produced in-lab, right, literature results for comparison, (Malone *et al.*, 2003). Each curve represents an average of 6 runs alternating between ascending and descending speed sequences at a 1N normal force.

5.2.4. Anton Paar MCR

As a result of the recent interest in tribology in fields other than the automotive, and as the full scale tribology equipment has quite a high associated cost (approximately £50,000 for the MTM), modification of existing equipment to measure tribological properties have recently been developed both for independent research (Goh *et al.*, 2010) and commercially for sale

(Anton Paar, Thermo Scientific). Work carried out by the University of Nottingham using an Anton Paar tribology attachment for the MCR is replicated using the MTM. Although not as complex the MCR was suggested to provide similar information to the MTM system but at a significantly reduced cost. A schematic diagram of the system is shown in Figure 5.12. The configuration is different to that of the MTM and so the pattern of entrainment is expected to be different. The first difference to note is that the plate surface is fixed giving pure sliding friction measurements, whereas for the MTM a mixture of sliding a rolling friction is usually used. Entrainment for the MCR relies on the mounting plate being repelled away from the rotating ball opening a gap to lubricate the plates whereas the MTM has a movable arm for the ball. The arrangement of the MCR ball means that a range of shears are present across the plate surface. This is a result of the small geometry of the sample holder, in addition to a stationary zone at the bottom of the mounting plate.

Initial experiments compare two simple oil in water emulsions, with a pure oil sample as a control in Figure 5.13. Results from the MCR for the speed range studied resulted in noisy data, but there are three sections of friction identified and the absolute values are similar to those of the MTM. However, the shape of the curve does not follow a typical Stribeck curve pattern. Overall quite a flat range of frictions are recorded, with oscillating values around the mixed regime. For the MCR data the mixed regime is only present over a very short speed range and the noise in the data may therefore be a result of operating at the boundary between surface contact and lubricated behaviour and alternating between the conditions. For the MTM the three regimes of a typical Stribeck curve are more distinct with a clear and smooth decrease in traction coefficient across the mixed regime. Distinction between the samples was similar in both cases, with the 100% oil samples showing a higher friction initially, while

30 and 55% oil samples had similar friction values. After the initial difference, values for all the samples are very similar.

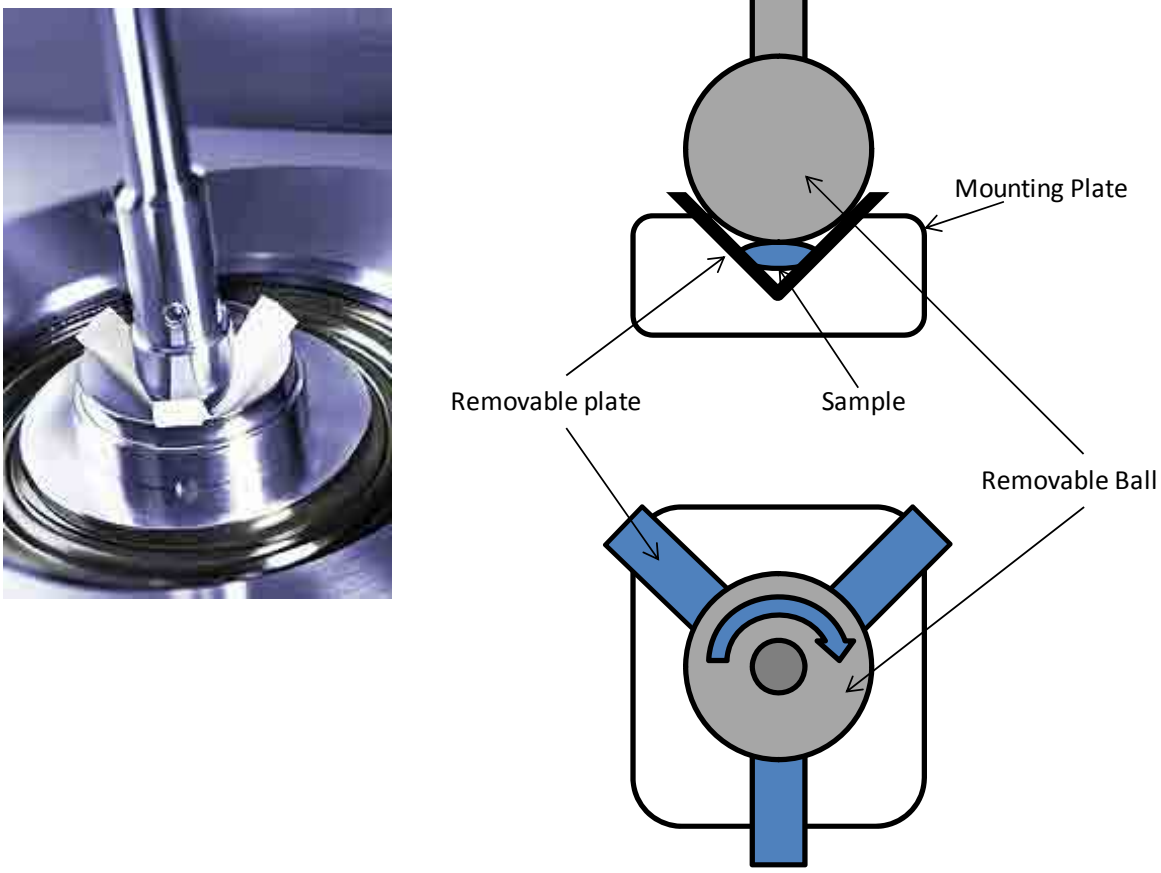

Figure 5.12. Anton Parr MCR tribology attachment, image and schematic diagram of Anton Parr tribology attachment for MCR (Anton_Parr, 2011)

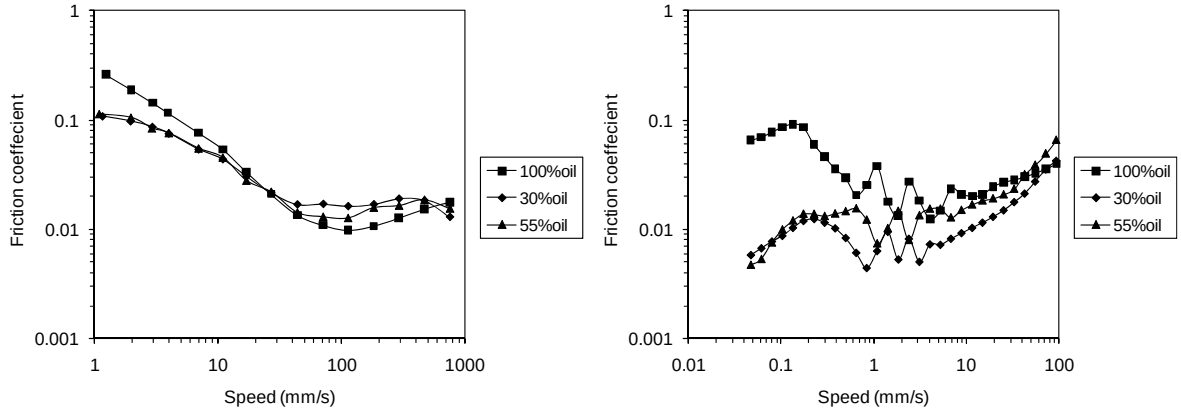

Figure 5.13. Emulsion comparison of MTM and MCR equipment, Stribeck curves for two emulsions at 30% and 55% oil with a pure oil control are presented. Left, data from the MTM at the standard speed range, right, data from the MCR (data provided by Dr Anne-Laure Koliandris, University of Nottingham) across a reduced speed range encompassing the equivalent lubrication regimes. Each curve represents an average of 6 runs alternating between ascending and descending speed sequences at a 1N normal force.

Hydrocolloids were also used for comparison. Data was generated for guar and dextran samples by running Stribeck curves with the MCR and MTM; details of these samples are described in section 3.1.2. Overall, these samples provided smoother data; less variation between each speed was experienced and with increasing speed the movement through the different lubrication regimes expected in a standard Stribeck curve were observed. This improvement in the data gathered is especially clear for the MCR data where a series of unexpected peaks and troughs were seen for the emulsion samples. Comparisons are presented in Figure 5.14, for guar samples of different concentrations and molecular weight. Results from the MTM show a smooth progression between regimes, although only a small section of the hydrodynamic regime is present. The MCR results are less variable than previously observed in emulsion samples, showing clear definition between the different samples. However, a very sharp decrease in friction is experienced through the mixed regime and only a small range of speeds are associated with this type of lubrication. This narrow range makes it difficult to perform further testing that operates in a specific regime. A similar

pattern is present in Figure 5.15 for dextran samples, while there are larger differences in behaviour of each sample. The same sharp decrease is seen when entering the mixed regime which offers only a small range of speeds covering this behaviour. In both systems the 20% high molecular weight dextran has a much lower traction coefficient than the other samples with no boundary lubrication being obvious.

For both systems the trends can be seen within the samples: increasing guar concentration increases the lubrication effect mainly in the mixed regime, with the lower molecular weight samples producing more of a lubrication effect. This is likely to be because of the smaller size of molecules allowing more entrainment of sample, and therefore more lubrication. For dextran, once again increasing concentration increases lubrication. However, in this instance the high molecular weight samples produce better lubrication for a given concentration.

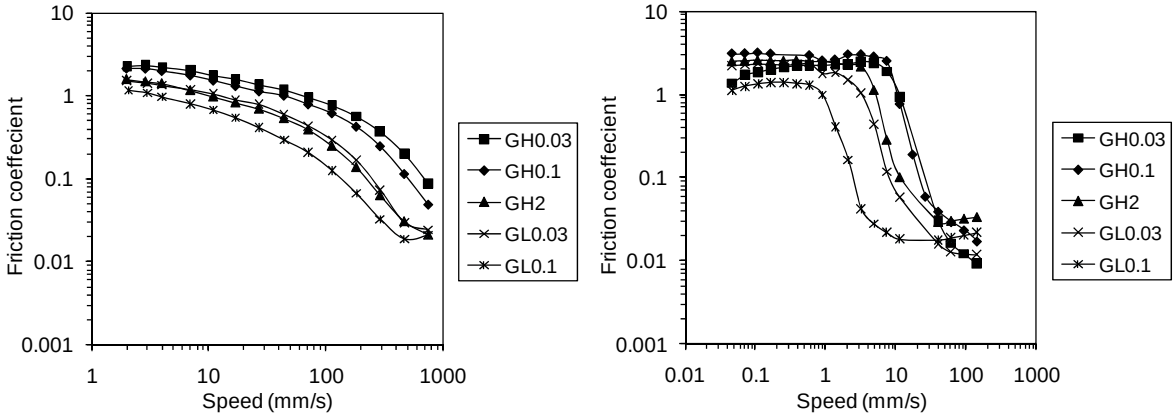

Figure 5.14. Guar comparison of MTM and MCR, Stribeck curves for a range of guar samples are presented, high molecular weight (G_H) and low molecular weight (G_L) samples at different concentrations were tested. Left, data from the MTM at the standard speed range, right, data from the MCR (data provided by Dr Anne-Laure Koliandris, University of Nottingham) across a reduced speed range encompassing the equivalent lubrication regimes. Each curve represents an average of 6 runs alternating between ascending and descending speed sequences at a 1N normal force.

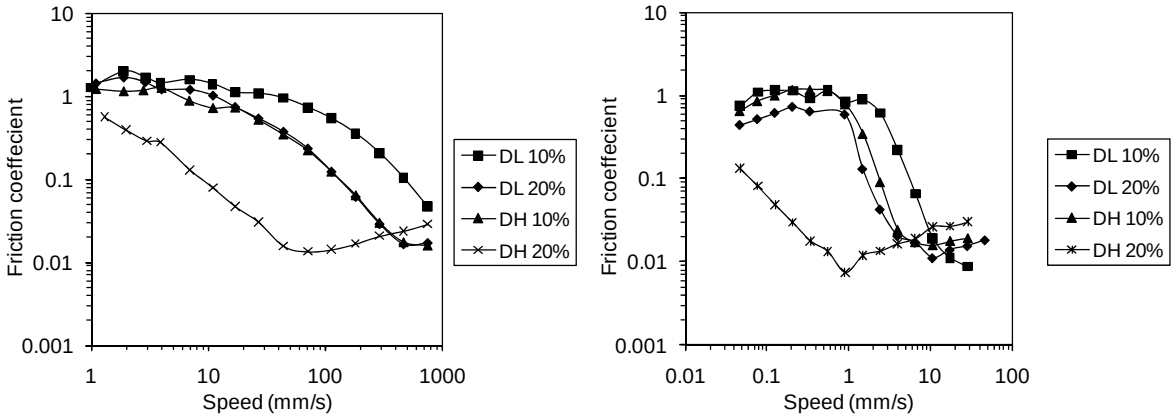

Figure 5.15. Dextran Comparison of MTM and MCR, Stribeck curves for a range of dextran samples are presented, high molecular weight (D_H) and low molecular weight (D_L) samples at different concentrations were tested. Left, data from the MTM at the standard speed range, right, data from the MCR (data provided by Dr Anne-Laure Koliandris, University of Nottingham) across a reduced speed range encompassing the equivalent lubrication regimes. Each curve represents an average of 6 runs alternating between ascending and descending speed sequences at a 1N normal force.

In conjunction with the tribology work carried out on the biopolymer samples, sensory testing was also used: a score for "lubrication" was given by a panel for each of the samples. This lubrication score was then correlated with the traction coefficient recorded for each sample at

each individual speed. For the MCR data, traction coefficients at a speed of 8mm/s gave the best correlation which falls, for most samples, within the mixed regime. Similar results were obtained by Malone *et al.* (2003), where the mixed regime is suggested to be the region of interest for mouthfeel. Applying the same methodology the best correlation for the MTM is at a speed of 26mm/s giving a correlation coefficient of 0.86 as shown in Figure 5.17. This speed falls firmly in the mixed regime for all samples, and gives a good correlation coefficient. Correlation coefficients across the different speeds are relatively high: above 0.6 for all speeds, but a definite peak around 26mm/s, is present. In comparison with the MCR correlations, the MTM gives higher correlation coefficients. This is a result of the smoother transition in friction values with increasing speed of the MTM. In the MCR sharp changes in the type of lubrication experienced are evident by the changes in gradient of the traction data, whereas for the MTM a smooth transition with increasing speed is present.

One exception is excluded from the correlations made, which is the 0.7% high molecular weight guar. It is suggested in the literature to behave differently because it has a much higher apparent viscosity from 1-1000 s^{-1} than the other samples giving a thicker coating of the mouth (Koliandris *et al.*, 2009). It is possible that for the sensory testing other effects caused an increase in rating. With increasing concentration the extent of shear thinning behaviour and also thixotropy increases (Bourriot *et al.*, 1999, Bradley *et al.*, 1989). Thixotropy for the guar samples changes the sample viscosity as a function of time. For the lower two concentrations very little thixotropic behaviour is expected, however approaching 1% w/w (depending on molecular weight) a measurable difference in viscosity with time is present meaning that this may be true for the 0.7% sample. In this case, depending on sample

preparation and age for sensory trials, the sample tested orally may be very different from the sample recorded for tribology.

The main problem with the MCR data collected is that the mixed regime is only observable over a very short speed range making it difficult to identify lubrication behaviour at one speed, across different samples, while remaining in the same lubrication regime for all. It also makes it difficult to study behaviour at the onset, middle and end of the mixed regime since it is such a small range.

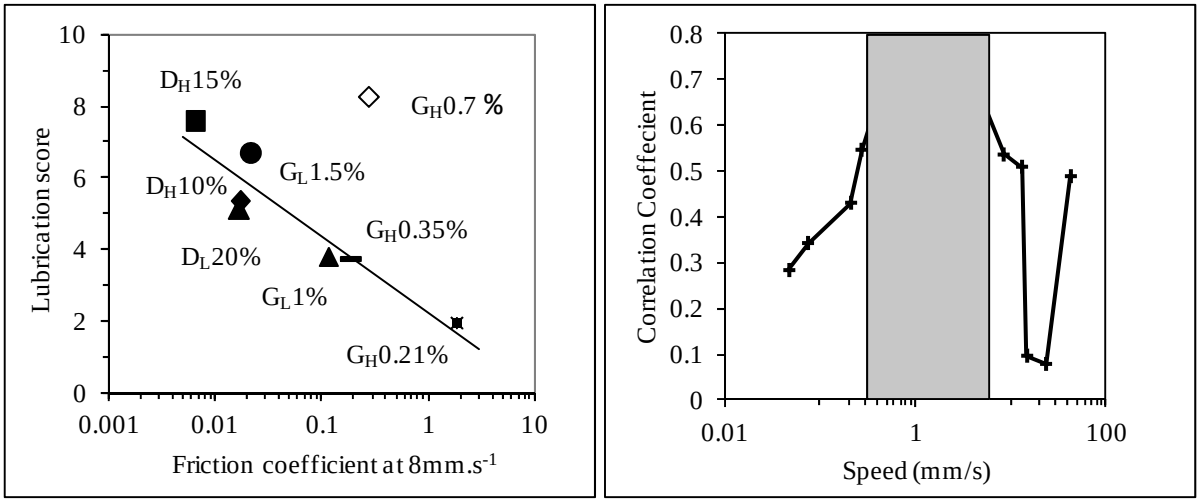

Figure 5.16. Sensory correlation with MCR (data provided by Dr Anne-Laure Koliandris, University of Nottingham), left: Correlation between sensory "lubrication" score and the traction coefficient at 8mm/s the speed which gave the strongest correlation when Gh0.7% is omitted. Right: strength of correlation across the speed ranges with the mixed regime by shading. Original data was not available to provide error bars.

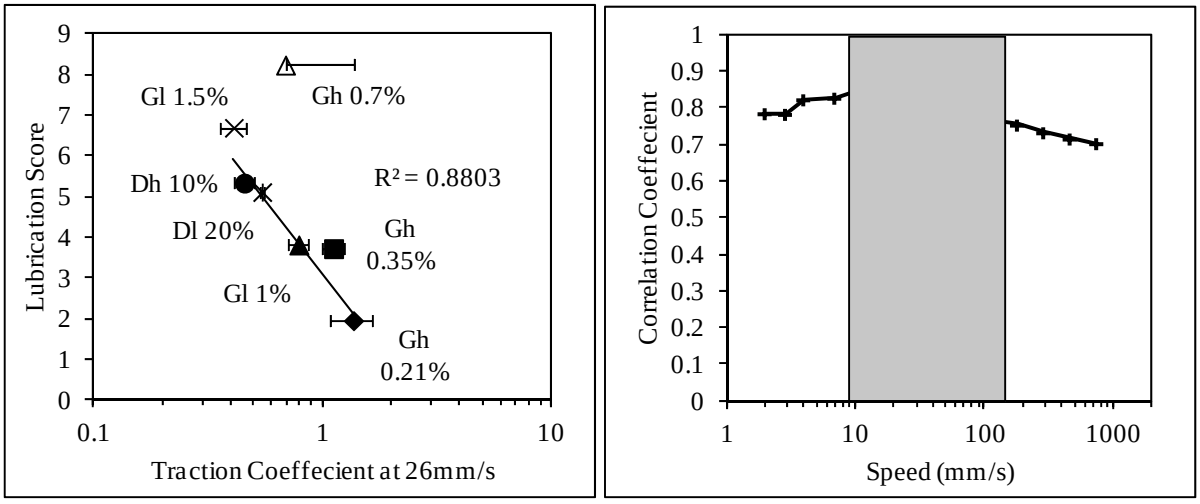

Figure 5.17. Sensory correlation with MTM, Left: Correlation between sensory "lubrication" score and the traction coefficient at 26mm/s the speed which gave the strongest correlation when Gh0.7% is omitted. Right: strength of correlation across the speed ranges with the mixed regime marked by shading.

5.3. CONCLUSIONS

In conclusion, tribology equipment modified here can allow replication of current works, as well as future studies on material behaviour under conditions which are relevant to in mouth processes and sensory perception. A range of surfaces are available for use, with lab made PDMS surfaces providing a good repeatable analogue for oral surfaces, with appropriate force and speed settings. The limitations of this are that the surfaces still do not truly replicate the pattern of papillae on the tongue or the saliva coating on the surfaces since these features are too variable and complex to replicate while maintaining a sensible production and testing timescale for experiments. However this limitation should not affect the main flow patterns and phenomena occurring under these conditions.

It has been shown for emulsions that tribology can distinguish differences in composition, which can be correlated with sensory attributes, as previous work has found (Malone *et al.*,

2003). It has also been shown that for a stable emulsion with small droplets, droplet size does not change whilst in the tribometer. Whereas for larger droplet sizes, changes are experienced during processing, indicating that time dependant tribology studies should provide further information on material behaviour during oral processes. This is explored in the following chapter.

The use of the full scale MTM offers the best options for use in the development of in-vitro systems. The tribology attachment for the rheometer, while a significantly more economical option, does not offer the range of operating conditions such as varying contact surface types and rolling friction measurements. The MCR system also lacks the smooth transitions between lubrication regimes that are observed on the MTM equipment. For simple systems it does allow some relative distinctions between different samples, but can be very sensitive to disturbances, such as the transition between lubrication regimes where the ball is lifted away from the contacts by the lubricating fluid. This affects its reproducibility as shown by frequent peaks and troughs in friction data for emulsions.

CHAPTER 6. TRIBOLOGY MIXING

6.1. INTRODUCTION

In this chapter the tribometer was further modified to allow a wider range of time dependant studies to be carried out. Previous studies in tribology have focused on the use of Stribeck curves to study lubrication behaviour of structures (detailed previously in section 2.5) (de Vicente *et al.*, 2006, Malone *et al.*, 2003). However more recent studies have indicated that for some structures such as emulsions and hydrocolloid thickened solutions, sensory attributes are affected by changes occurring in the mouth. Dresselhuis *et al.* (2008b) show that some emulsion structures coalesce in the mouth leading to increased lubrication as the sample is processed and so increased sensory scores for creaminess. Similarly Ferry *et al.* (2006) shows for starch and hydrocolloid samples that the efficiency of mixing with saliva affects the sensory properties recorded. These findings are detailed in section 2.2.2.

In this work, the testing chamber lid was replaced and a programmable water bath was added to the cell cooling jacket. A peristaltic pump was attached to allow test material to be added and removed from the cell at controlled flow rates from an external tank. A schematic of the setup can be seen in Figure 3.4. Traction coefficient of material added over time into the cell at a fixed speed was recorded to look at the mixing behaviour and lubrication. These curves were compared to expected values obtained from Stribeck curves run on a set of fixed sample concentrations along the same range expected in the timed runs. A preliminary visual investigation of mixing patterns was also carried out to obtain a better understanding of the processes occurring in the tribometer cell.

6.2. RESULTS

Time dependant behaviour of a range of food materials was studied. The effect of adding samples over time to the tribometer cell on lubrication was recorded by measuring traction at a constant surface rotation speed. This study develops the range of experiments that can be carried out using tribology, and investigates the effect of mixing and sample homogeneity on lubrication. The selection of materials for this section of work provides a variety of different behaviours. Previous tribology work has used similar samples which allows for later comparisons (de Vicente *et al.*, 2006). Samples chosen consisted of: (i) a Newtonian material (corn syrup) (de Vicente *et al.*, 2006), (ii) a shear thinning material (xanthan gum) (de Vicente *et al.*, 2005) and (iii) a mucoadhesive material (pectin) (Sriamornsak *et al.*, 2008). Each sample used has different rheological behaviour over a range of shear rates. To take into consideration the effect of viscosity on friction, viscosity of the samples were matched at a high shear rate, as this should be the environment experienced in the measurement contact of the tribometer. Figure 6.1 shows viscosity curves for the final samples concentrations used in the study, with approximate overlaps in viscosity at a shear of 1000 s^{-1}.

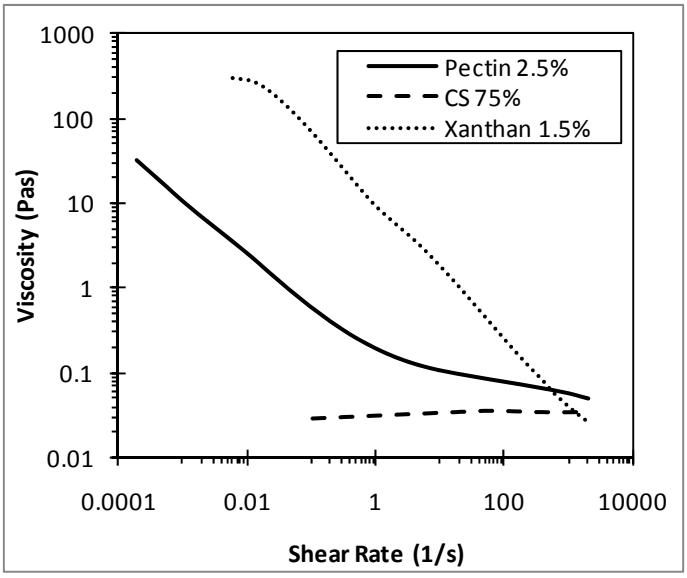

Figure 6.1. Viscosity matching of samples selected for the trial. Sample concentrations presented approximately match viscosities at "high" 1000 s-1 shear rate.

6.2.2. Timed tribology experiments

This section presents the comparison of lubrication behaviour of the samples between continuous addition of material and Stribeck curves of discrete concentrations. Stribeck curves were carried out for the three samples for a number of fixed concentrations to provide data for comparison across the range of concentrations expected during the continuous addition experiments. For the continuous experiments the tribometer cell is initially filled with water and concentrated sample is added from an external tank. The expected concentrations for the tribometer cell with time were calculated from the following mass balance equations:

$$\frac{\partial m_1}{\partial t} = q \times \left(\frac{m_2}{V_2}\right) - \left(\frac{m_1}{V_1}\right) \ldots Eqn\ 6.1$$

$$\frac{\partial m_2}{\partial t} = q \times \left(\frac{m_1}{V_1}\right) - \left(\frac{m_2}{V_2}\right) \ldots Eqn\ 6.2$$

where, subscripts 1 and 2 represent values for the tribometer cell and external tank respectively, $\frac{\partial m}{\partial t}$ is the change in sample concentration with time, q is mass flow rate through the system, m is the mass (concentration) of sample added to water and V is the vessel volume. The equations assume perfect mixing and so small differences are expected in the actual data. Equations 6.1 and 6.2 were solved using the solver for ordinary differential equations in MATLAB. Figure 6.2 shows a sample output for the 1.5% solution of Xanthan, equilibrium between the two sample containers is reached after approximately 1500 seconds.

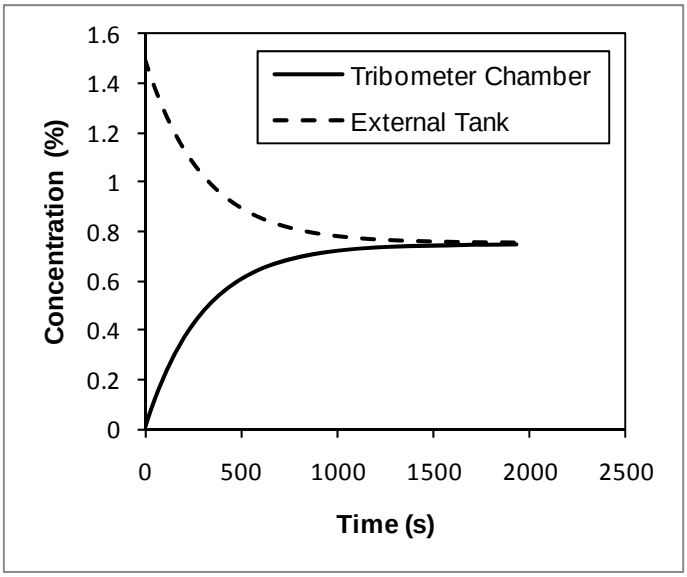

Figure 6.2. Predicted concentrations for xanthan in the tribometer cell and external tank. A mass balance determines the concentration change, volumes of each environment are fixed at 40ml each with a flow rate of 5ml/min between chambers. Initial concentration in the cell is 0%, initial tank concentration is 1.5% by weight.

The values obtained from the mass balance determine the timescale used for the experiments to ensure that equilibrium is reached, and determine the expected concentrations experienced by the tribometer cell for discrete experiments to be planned. This information can also then be used to create a plot of traction coefficient against concentration for the timed experiments carried out herein. Selecting the traction coefficient at each concentration from the Stribeck

curve experiments at 100 mm/s (the same speed as the timed experiments) allows a plot of traction against concentration to be obtained. Traction against time data for the continuous experiments can then be used with predicted concentration over time data to add a curve of traction against concentration for the continuous experiments. 100mm/s was chosen as a value firmly in the mixed regime for the samples tested (e.g. Figure 6.3) which had good repeatability offering the best distinction between concentrations.

For pectin, Stribeck curves carried out for each concentration showed clear differences in traction with concentration. Figure 6.3 presents Stribeck curves for six concentrations of pectin from 0% to 1.25% by weight. A classic Stribeck pattern is observed for all samples with decreasing friction with increasing speed highlighting the mixed nature of lubrication occurring; very little boundary and hydrodynamic behaviour is shown for the speeds studied. Traction coefficient at 100mm/s is plotted in Figure 6.4. Discrete concentration points show that traction has a smooth relation to concentration although not a linear one. Instead quite a steep decrease in friction is observed at low levels, which start to level off as concentration increases. Pectin results for continuous experiments follow quite close patterns of lubrication with concentration increase. Initially, there is some difference between the averages of each of the methods where viscosity differences are at their highest point. However, they still fall within a margin of error. The agreement of the two methods indicates that pectin requires little to mix with bulk water and to be entrained.

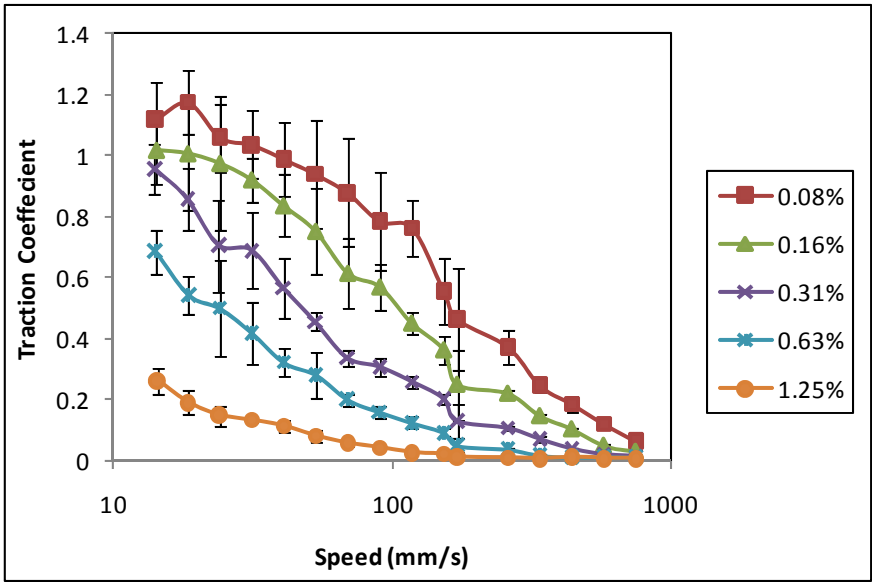

Figure 6.3. Stribeck curves for different pectin concentrations. Each curve represents an average of 6 runs alternating between ascending and descending speed sequences at a 1N normal force. A PDMS ball and disc tribopair was used for all cases.

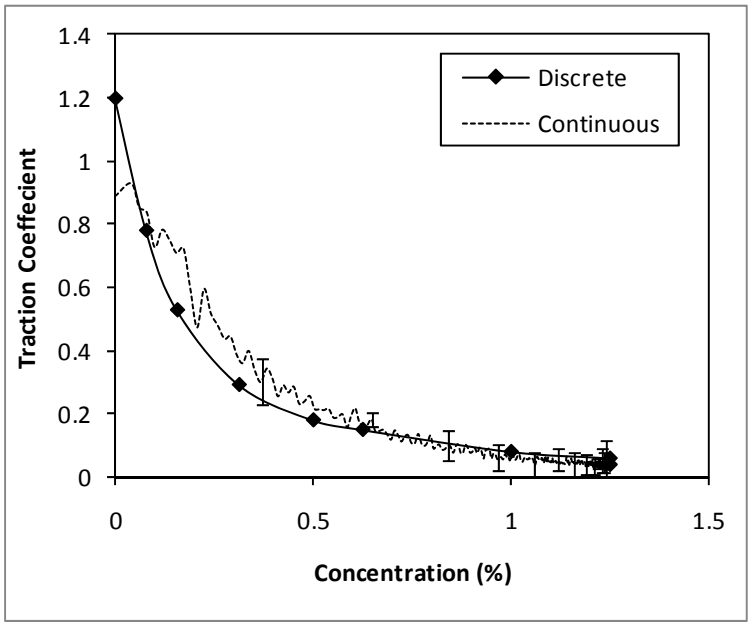

Figure 6.4. Comparison of concentration effect for pectin, discrete points represent the value of traction coefficient at 100mm/s for each concentration taken from average Stribeck curves run independently. The continuous curve represents the traction coefficient recorded at 100mm/s over a timed experiment with constant increasing pectin concentration. Time is converted to an equivalent concentration by using a mass balance. Error bars represent the average of three repeats.

Corn syrup shows more complex lubrication behaviour with concentration increase. Figure 6.5 presents Stribeck curves for five concentrations of corn syrup. For the low concentrations of 2, 10 and 20% lubrication behaviour is overlapping for speeds up to 200mm/s, while 30 and 40% show distinctly different behaviour. Beyond this, the 20% sample shows more differentiation from the lower two concentrations, while 30 and 40% continue to be discretely different levels of lubrication across the concentration range. This pattern of lubrication is also found in work by Goh *et al.* (2010) where sample concentrations of 10 and 20% corn syrup produce the same lubrication behaviour until approximately 200mm/s, when their behaviour starts to separate forming distinctly different traction coefficients. No specific explanation for this is given, however it is suggested that at lower speeds surface contact friction dominates the lubrication behaviour, and only when certain level of mixed lubrication is reached does the sample concentration show differentiation in behaviour between the samples.

At the speed of interest (100mm/s) this grouping of traction coefficient values for the lower concentrations is present, and as such the derived plot of traction coefficient against concentration, shown in Figure 6.6, does not follow a regular pattern with increasing concentration. Initially, the addition of a small amount of corn syrup increases lubrication over distilled water, however with increasing concentration relatively little effect is seen until after a concentration of 20%, where a sharp increase in lubrication is observed continuing to the maximum concentration. When compared with the continuous data a similar pattern is observed, with little change in lubrication until approximately 25% concentration is reached, where a change in gradient is observed. For this study, the traction coefficients recorded are higher than in the discrete experiments, until a concentration of 30% is reached. The

reasoning for this discrepancy is hypothesised to be a result of a delay in mixing. At low concentrations the corn syrup does not completely mix with the bulk water in the tribometer cell, so the lubrication behaviour is determined by water alone. Only when a sufficient concentration of corn syrup is present in the tribometer cell is a reduction in the traction coefficient observed. During sample preparation, when corn syrup added to water to form the required concentrations a significant mixing time was observed. Only after some agitation did the two phases mix properly. This observation suggests that this could be the reason for the differences observed in Figure 6.6.

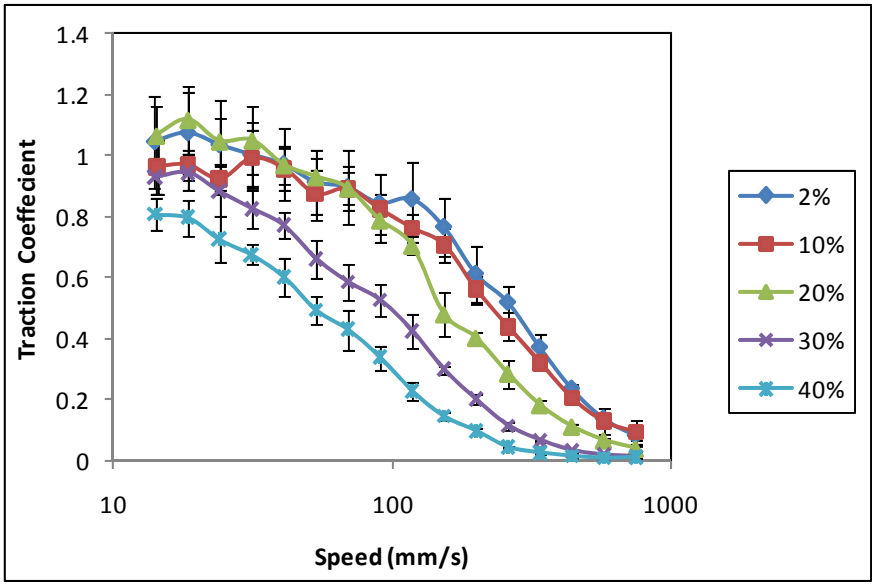

Figure 6.5. Stribeck curves for different corn syrup concentrations. Each curve represents an average of 6 runs alternating between ascending and descending speed sequences at a 1N normal force. A PDMS ball and disc tribopair was used for all cases.

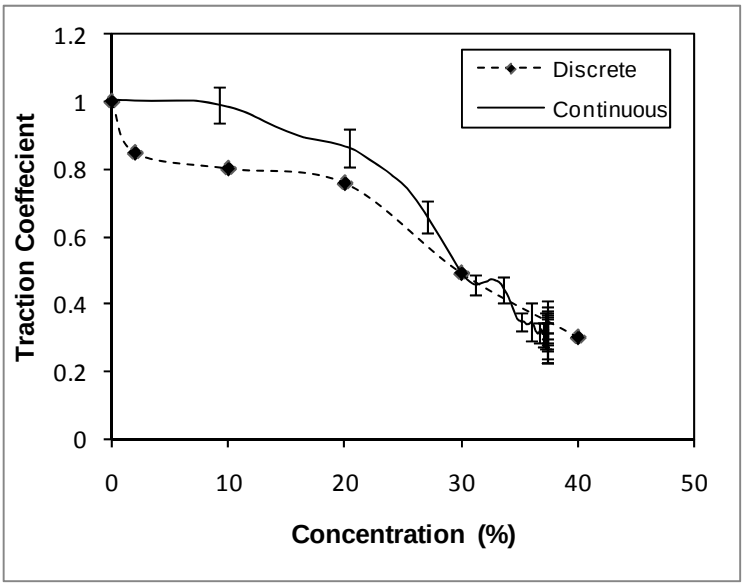

Figure 6.6. Comparison of concentration effect for corn syrup, discrete points represent the value of traction coefficient at 100mm/s for each concentration taken from average Stribeck curves run independently. The continuous curve represents the traction coefficient recorded at 100mm/s over a timed experiment with constant increasing corn syrup concentration. Time is converted to an equivalent concentration by using a mass balance. Error bars represent the average of three repeats.

The final sample tested under these conditions was xanthan. Figure 6.7 presents Stribeck curves carried out on concentrations up to 0.75%, by weight. Curves produced follow the expected Stribeck curve pattern observed in previous samples. Initially, a high traction coefficient is recorded, which reduces with increasing speed through the mixed regime. A comparably large amount of variation was observed between individual runs, creating larger error bars than for pectin and corn syrup. This makes differentiation between each concentration more difficult. However, a pattern was observed which followed roughly even increases in lubrication across the range of speeds, with increasing concentration. One proposed explanation for this increased variance is that the xanthan sample had some visible impurities when prepared, which could have influenced measurements. Another possibility is that because of the relatively high zero shear viscosity, and shear thinning behaviour of the samples, the flow patterns in the tribometer cell may have affected measurements. It is possible that regions of low shear in the recording cell formed dead zones of increased viscosity material, affecting flow patterns which could lead to large blocks of thickened material breaking off and bumping into the rotating ball, changing the steady entrainment of material. It is expected then for continuous methods differences in traction due to poor mixing will be present due to the delay in material mixed to the point where it will be entrained by the recording surfaces.

At 100mm/s xanthan shows a more linear decrease in traction vs. concentration over the range of concentrations studied when compared to the other samples. A slight drop was initially seen as in corn syrup measurements, again indicating only a small amount of material is needed to start reducing friction. However, on comparison to continuous studies, a different trend is present, with far greater variation between the two methods than in previous

materials. For the majority of the concentration range studied the continuous method shows much higher traction coefficients, except for the final concentrations. This is due to mixing of the Xanthan in the tribometer chamber, and is confirmed by the extra time required to reach a steady state, even though the mass balance shows equilibrium should have been reached in a perfectly mixed system. The main cause of the erratic and slow mixing is likely to be mainly due to the very high low shear viscosity of the Xanthan concentrations used, which is far greater than either of the other samples. Xanthan also has a much higher average molecular weight than pectin, 4200kDa and 170kDa, respectively (de Jong and van de Velde, 2007).

Overall it can be seen that mixing has an effect on traction recorded in continuous experiments. From the materials studied here this effect cannot be purely attributed to viscosity differences, as this is matched at high shears (found in the recording contact) and does not follow the trend of viscosities at low shear (found in the bulk). Therefore, the material's structure will contribute to its behaviour.

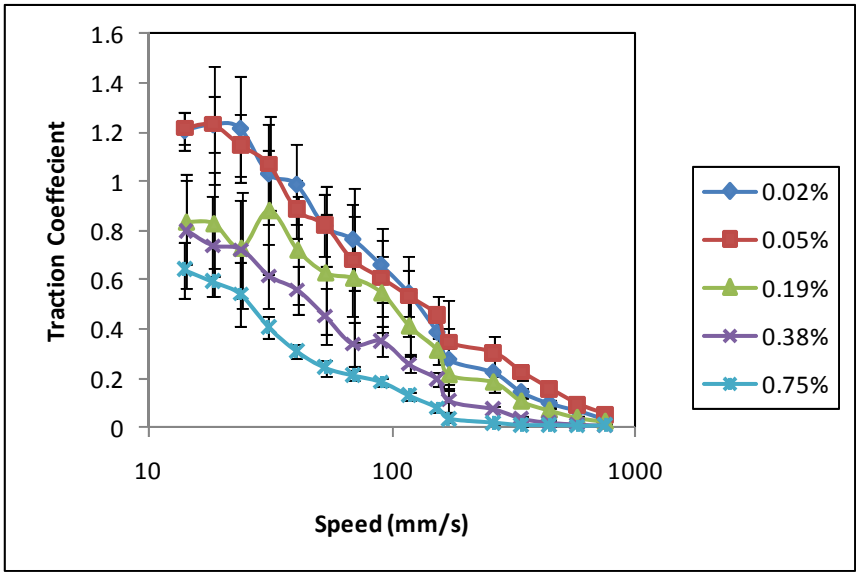

Figure 6.7. Stribeck curves for different xanthan concentrations. Each curve represents an average of 6 runs alternating between ascending and descending speed sequences at a 1N normal force. A PDMS ball and disc tribopair was used for all cases.

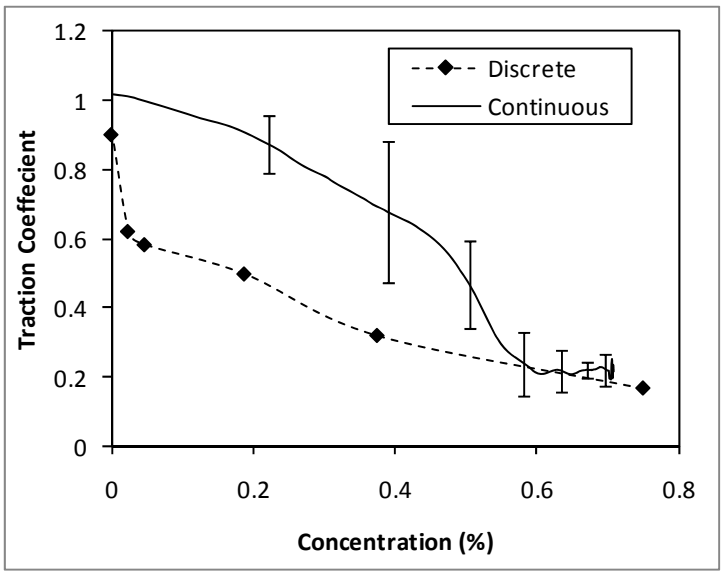

Figure 6.8. Comparison of concentration effect for Xanthan, discrete points represent the value of traction coefficient at 100mm/s for each concentration taken from average Stribeck curves run independently. The continuous curve represents the traction coefficient recorded at 100mm/s over a timed experiment with constant increasing xanthan concentration. Time is converted to an equivalent concentration by using a mass balance. Error bars represent the average of three repeats.

6.2.1. Droplet Mixing

A second study was carried out in conjunction with the continuous tribology experiments. As clear differences between the behaviour of each sample within the tribometer cell were observed, a visual investigation of droplet path of added material would highlight possible reasons for this difference. Initial investigations looked at added droplets mixing into a bulk of material with a different viscosity. Dyed corn syrup samples were added to water while recording traction at a constant 100mm/s. Figure 6.9 shows the path of a droplet at four main stages, when the droplet is added it is drawn out towards the contact point in the direction of the disc rotation although the bulk of the drop does not move a significant distance. It is also important to note that the drop stays close to the surface of the water. When material reaches the ball, the path moves around the back of the contact point where the stream starts to be broken up and begins to mix into the bulk.

Table 6.1 and Table 6.2 show mixing properties and times for corn syrup, “mixing times in the bulk” represents adding a sample near the edge of the tribometer cell while “mixing time over disc” represents samples added on the same line as the contact track on the disc. For situations where large viscosity and density differences exist, as in the conducted experiments mixing is delayed. When translated to a significant addition this can start to affect the traction recorded. However, this is not present for the small volumes added here. This delay in added material reaching the contact point is compounded by different regions of mixing created by the rotating surfaces. The results show that when adding material to different areas of the cell a difference in mixing time is observed. Faster mixing occurs around the disc area than is present in the bulk at the edges of the tribometer chamber. Observations showed that the added droplets get broken by shear, mostly around the point where the ball is located, but tend

to be diverted around the actual contact. This indicates that lubrication changes should only be seen when fluids are fully mixed. In this case, no changes in recorded traction were observed during experiments due to the very low quantities added. However, for the previous studies where traction was changed, it is assumed that mixing of the two initial samples had taken place.

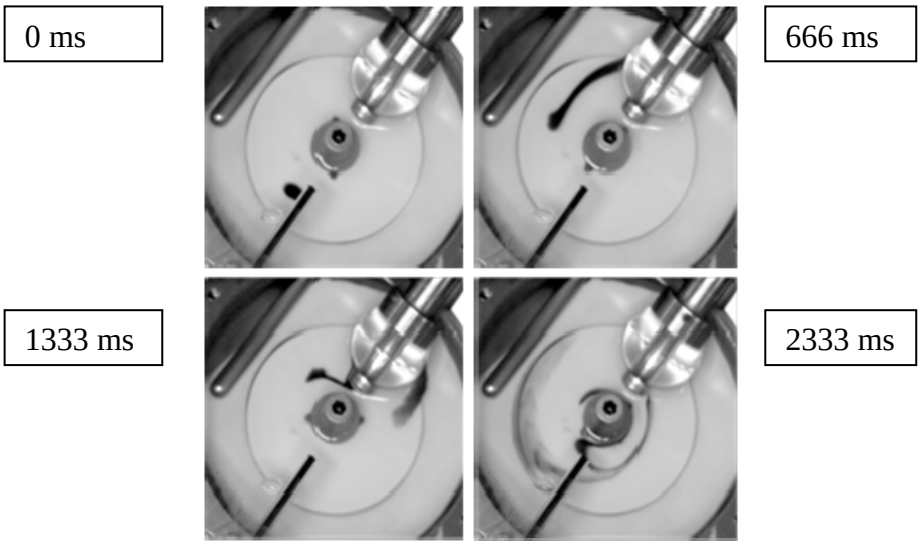

Figure 6.9. Corn syrup droplet path, images taken at four points along a single droplet path of corn syrup into water, from top left clockwise, initial drop, extension, contact with ball, and movement into the bulk. Average speed was set at 100mm/s with a slide roll ratio of 50%.

Table 6.1. Mixing times in the bulk

Addition to Bulk			
Concentration	Average time (s) (±2)	Viscosity ratio	Density Difference (kg/m3)
40%	16	3.08	133
55%	22	7.18	177
75%	25	41.3	227

Table 6.2. Mixing times over disc

Addition to disc			
Concentration	Average time (s) (±2)	Viscosity ratio	Density Difference (kg/m3)
40%	4	3.08	133
55%	7	7.18	177
75%	10	41.3	227

With the information from both studies it is clear that when dealing with inhomogeneous samples in the tribometer cell a certain degree of mixing can affect the lubrication behaviour recorded. Ideally, when using tribology to study food material behaviour in the mouth the use of saliva as an initial volume which then has a food material added to it would best represent in-vivo consumption. However, in order to carry out Stribeck curves on this mix of material as in most previous tribology studies the sample would have to be pre mixed. The reason for this is that the Stribeck curve gives discrete traction coefficients for a number of speeds; if a poorly mixed sample is tested the early data points would represent a different sample than the later data points as mixing occurs. However, pre-mixing the sample does not provide an accurate representation of oral processing. In the mouth the degree of mixing will be different depending on the material properties and residence times. In addition in many cases saliva causes structural changes in food materials due to the enzyme content which may have an enhanced affect if allowed to fully mix and have time to act.

In order to further the use of tribology as an in-vitro mouth method this mixing element is important. The use of Stribeck curves on pure materials can provide good information on the lubrication behaviour of products. However, even in the limited range of studies carried out to date, some anomalous samples do not compare well with sensory data. An example of this can be seen in work previously detailed in section 5.2.4 by Koliandris *et al.* (2009), where a series of guar gum solutions were tested both by tribology and sensory analysis. Samples at increasing concentration and differing molecular weights correlated linearly between "lubrication score" given and traction coefficient at 8mm/s. However, one sample at 0.7% high molecular weight guar did not follow the trend and had significantly higher lubrication score when compared with recorded traction coefficient. The lubrication score is significantly

higher than expected for the recorded traction coefficient and is suggested by the author of the sensory trials to be an effect of the sample's high low shear viscosity. However, a mechanism to explain the behaviour is not given. In section 5.2.4 a possible explanation for this difference is that at this concentration guar may display thixotropic behaviour leading to a difference in behaviour over time as the sample is sheared (Bradley *et al.*, 1989). Both the sensory scores and the recorded traction coefficient could be affected by this, resulting in an artificially high lubrication score or low traction coefficient. It is also possible that the thickness of the sample means that it performs differently in the mouth, making the evaluation based on an inhomogeneous sample. Previously, this mixing time has been shown to affect the sensory scoring of samples where thicker samples, were perceived as less salty because of the limited movement of the sample to contact the taste buds, despite containing the same level of salt (Koliandris *et al.* 2010). A time dependent study with an element of mixing with water or saliva may provide different traction coefficients for this sample and future studies. Currently, the work carried out here in tribometer cell does not accurately provide predicative data to correct the difference seen for the guar sample. However, with further modification of the cell geometry to mimic mouth dimensions, and more accurate saliva analogues and volumes, testing over the timescales in the mouth could provide more accurate correlations with sensory data over simply using Stribeck curves. Data produced from Stribeck curves of pure sample material and of saliva/sample mixes at different stages of mixing, in addition to time dependant tribology experiments would help to better correlate with in-vivo experiences.

6.3. CONCLUSIONS

Tribology equipment has been modified to allow dynamic lubrication to be recorded, in this study material is introduced and mixed into the recording cell. A selection of materials found

in food products were tested for mixing and lubrication behaviour, and clear differences between samples were seen as a result of structure and mixing behaviour with water. Preliminary mixing studies in the tribometer cell have been conducted. This shows that having an inhomogeneous sample can have a large effect on lubrication behaviour, and this effect could have implications for oral processing as residence times in the mouth do not allow much time for mixing. Future tribology experiments, and correlations with in mouth behaviour, should consider this.

Whilst previously researchers have only relied upon Stribeck measurements, findings from this work suggest that a fixed speed timed experiment would be more appropriate for comparison with sensory perception scores in some cases. This method should compare more with mixing occurring in the mouth when consuming products. In order to validate the findings of this work it would be important to use saliva, or a synthetic alternative, instead of water, in order to draw comparisons with sensory scores. Furthermore, an in-vitro study should be carried out encompassing materials with available sensory trial data and over timescales more relevant to the mouth.

CHAPTER 7. DYNAMIC TRIBOLOGY

7.1. INTRODUCTION

Having developed a better understanding of the tribology equipment in Chapter 5 and extending the range of experiments that can be carried out in Chapter 6, this chapter focuses on dynamic lubrication measurements which follow a material change. In this study the ordering and gelation of three biopolymers was investigated under shear: κ-carrageenan, gellan and agarose at varying polymer and KCl concentrations. Under these conditions a concentrated dispersion of small gel particles is produced. This unique fluid material in published works is explored further in section 2.3.2 and discussed in more detail later in this chapter.

The impact of a physical change in material structure on lubrication properties would have implications for an individual's perception of food products in the mouth. Processes such as melting and agglomeration in the mouth could be studied and correlated with lubrication behaviour in future work, extending the range of work carried out using tribology. Work carried out by Benjamins *et al.* (2009) at a similar time to this work has also highlighted for emulsion products that coalescence in the mouth alters their perception with time.

The approach taken was to control the temperature profile within the tribometer cell to induce conformational ordering of the structures and to investigate these events input on lubrication. The change was also followed using a standard rheometer at a constant shear rate, in order to compare the two techniques and the materials produced. The structural properties of the final gel, were compared with findings described in the literature. The effect of polymer

concentration was explored for the three samples. For carrageenan and gellan as salt promotes gelation, additionally the effect of KCl concentration was explored.

7.2. RESULTS

Three biopolymer samples, κ-carrageenan, gellan and agarose were studied by rheology and tribology. Temperature induced gelation of the samples in the rheometer was studied at a constant shear of $200s^{-1}$. This shear rate is taken from Gabriele *et al.* (2009) as a shear where homogeneous fluid gel particles are created. Molten samples were loaded at 60°C, between the rheometer plates, and viscosity was recorded as the sample was cooled. The effects of biopolymer and KCl content for κ-carrageenan and gellan were measured. All the materials tested produced curves that can be generalised and split into three main sections over the temperature range. A typical curve generated during preliminary experiments is shown in Figure 7.1. The figure presents three repeat experiments of a 0.25% κ-carrageenan sample cooled at 1.5°C/min. Viscosity measurements at a constant shear of $200s^{-1}$ from 40 to 20°C were taken between a 60mm parallel plate geometry (detailed in section 3.2.13). At higher temperatures no ordering occurs. Here a slight viscosity increase can be observed of the order of 0.5 mPas, as expected where cohesive forces between molecules increase with reducing temperature (part 1). This continues until a sharp increase is seen at the onset of conformational ordering; this temperature varies dependant on polymer and KCl concentration for this example. The following part of the curve shows the ordering process of the polymer until it is complete (part 2), this then gives way to third regime where viscosity is purely temperature dependant once again (part 3). In this final section a slight reduction in viscosity is sometimes present. This is a result of the breaking up and smoothing of any aggregates to an equilibrium point that have formed during the ordering process. This effect

is often more pronounced in systems which have a very fast ordering process. This same pattern is evident in tribology measurements. Initial values tend to be stable with slight increases from the change in viscosity observed, although a larger increase in comparison with viscosity measurements was seen over this section. Traction is then seen to increase at the point of ordering, before stabilising once complete at a new level.

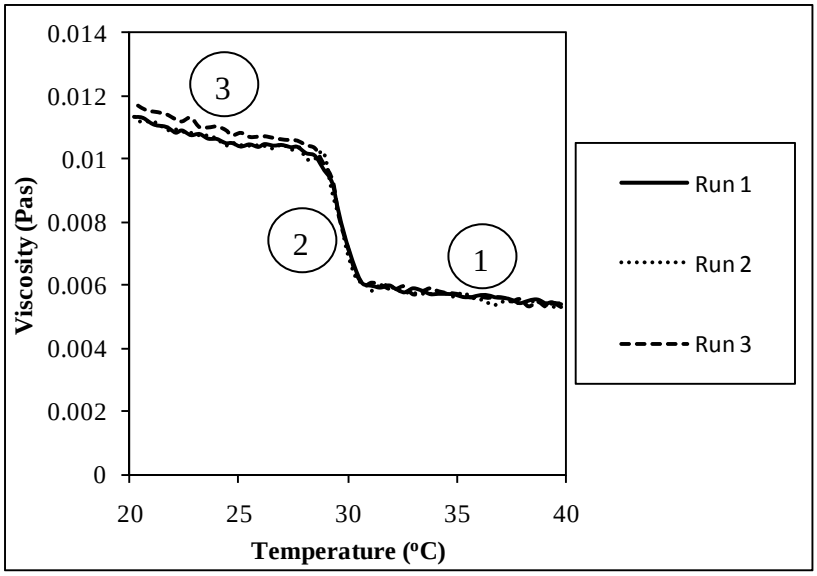

Figure 7.1. Characteristic viscosity curve for temperature induced ordering, viscosity curves for three repeats of a 0.25% carrageenan sample are shown. Samples were sheared at 200s^{-1} and cooled at 1.5°C/min from 40 to 20°C using a 60mm parallel plate geometry.

Figure 7.2 presents rheology and tribology results for temperature induced ordering of κ-carrageenan at three concentrations, 0.25, 0.5 and 1%. The same material was tested by both tribology and rheology. Initially at high temperatures an unordered solution is present while at low temperatures a fluid gel is present (Gabriele *et al.* 2009). The patterns observed for rheology followed those described previously: with increasing concentration of biopolymer an increase in the gelation temperature and the size of the change in viscosity during the ordering process was present. The increase in gelation temperature with increasing carrageenan concentration is a result of ions which exist as part of the carrageenan powder which enhance

ordering (as with increasing KCl concentration detailed below). During and after ordering it is expected that bulk viscosity is dependent on the flow of particles in the material moving past one another. As such, an increase in polymer concentration should decrease the deformability of gel particles which hinders movement, leading to an increased viscosity, which is observed. In the tribology results the initial pattern is not the same as in rheology. The lowest concentration results in the highest value of traction. It is expected that here because of the low concentration of carrageenan, insufficient material is present to properly lubricate, making the lubrication behaviour similar to that of water. When sufficient concentration is reached the carrageenan is able to lubricate efficiently to where the two higher concentration samples sit.

It is possible that the viscosity change with concentration, including the contribution of the increased change in viscosity brought about by the c* (detailed later in the chapter), produces the pattern of differences seen in the initial traction measurements. However, shear rate at the contact is unknown, as it cannot be measured with the current equipment and is difficult to calculate because the gap size can change. The shear rate experienced is not uniform since the flow patterns of material being entrained into the gap is not well defined. The viscosity of the material in the gap is therefore unknown so its contribution is difficult to confirm. Previous work has also suggested that it is not just viscosity which affects the extent of lubrication but also the structure of the material. In work by de Vicente *et al.*, (2006) suspensions of Carbopol microgels are shown to lubricate very differently to aqueous polymer solutions because of their difference in microstructure even when the data was corrected for viscosity effects.

Increasing biopolymer concentration increases onset temperature and the overall traction coefficient change in tribology studies. Because of the initial pattern of tractions recorded for the different concentrations, the final traction values of each of the samples once again do not follow the same pattern as in the rheology studies. After ordering, competing characteristics mean that a pattern across materials is not apparent. For carrageenan the final traction for 0.25 and 1% samples show the same value, despite having a different increase in traction upon ordering and final viscosities, while the 0.5% sample shows a reduced friction compared with the others. The higher concentration samples have more material to lubricate and so are expected to produce lower traction coefficients. However they are also expected to have harder particles. This could mean that while there is more material to lubricate and separate the contacts, there could also be an increased difficulty in deforming particles allowing them into the contact thus creating less lubrication.

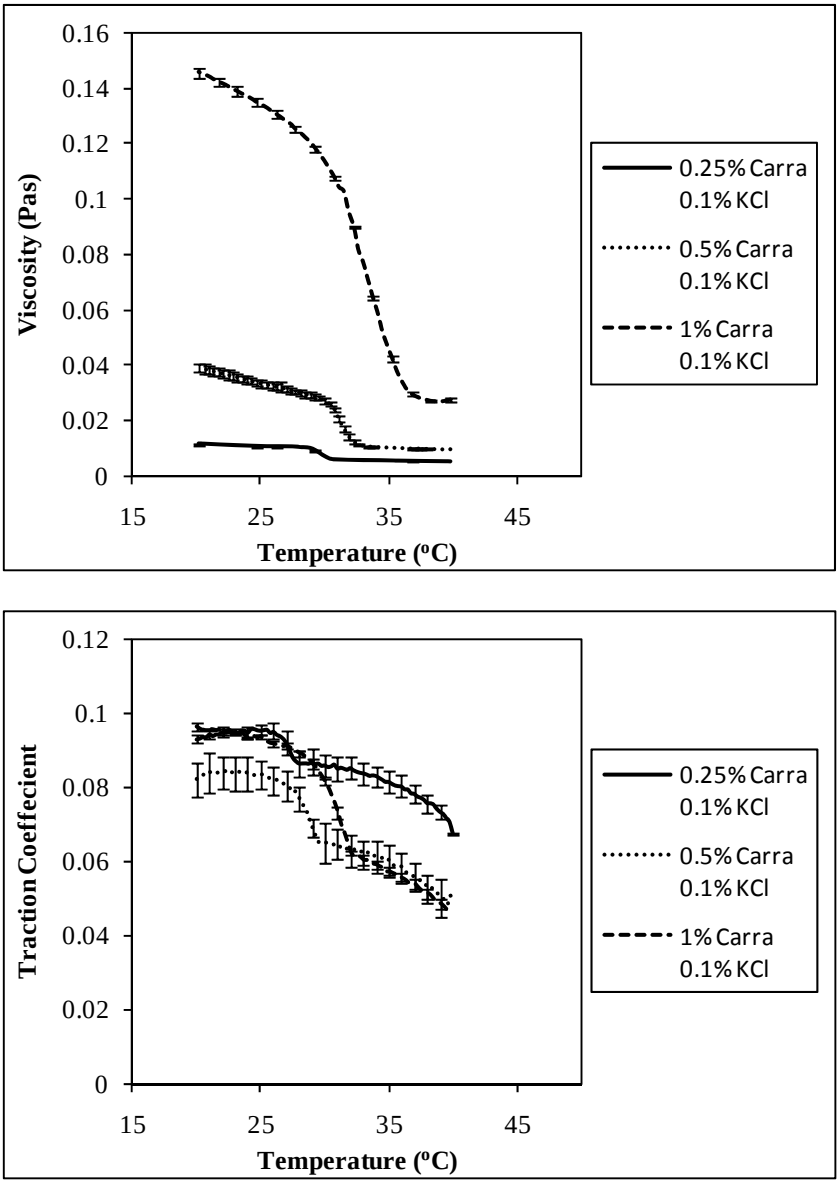

Figure 7.2. Carrageenan concentration effects, top, Viscosity curves of κ-Carrageenan gels during temperature induced ordering. Samples were cooled at 1.5 C/min at a constant shear of $200s^{-1}$, using 60mm parallel plate geometry. Curves represent an average of three experiments and error bars show one standard deviation from the mean. Bottom, Traction curves of κ-Carrageenan gels during temperature induced ordering. Samples were cooled at a rate of 1.5 C/min at a constant speed of 500mm/s and normal force of 2N. A steel ball and elastomer disc tribopair was used. Curves represent an average of three experiments and error bars show one standard deviation from the mean.

Further testing was carried out on carrageenan samples by repeating experiments using different KCl concentrations of 0.1, 0.2 and 0.3%. Once again onset of gelation temperature increased with increasing content, as did the extent of change in viscosity, although over a shorter range of temperatures and viscosities than for sample concentration (Figure 7.3). Charge screening with increasing salt concentration will reduce the electrostatic repulsion between chains and enhance conformational ordering (Rochas and Rinaudo, 1984). For carrageenan the increase in gelation temperature with KCl is much greater than for sample concentration. For 0.3% KCl gelation begins at approximately 47.5˚C and completes in less than 1˚C because of this the viscosity at the end of ordering reaches a peak which then reduces unlike the other samples. This is suggested to be due to the particles forming large linked chains over a very short timescale, which are then subsequently broken up into an equilibrium particle size (Gabriele *et al.*, 2009).

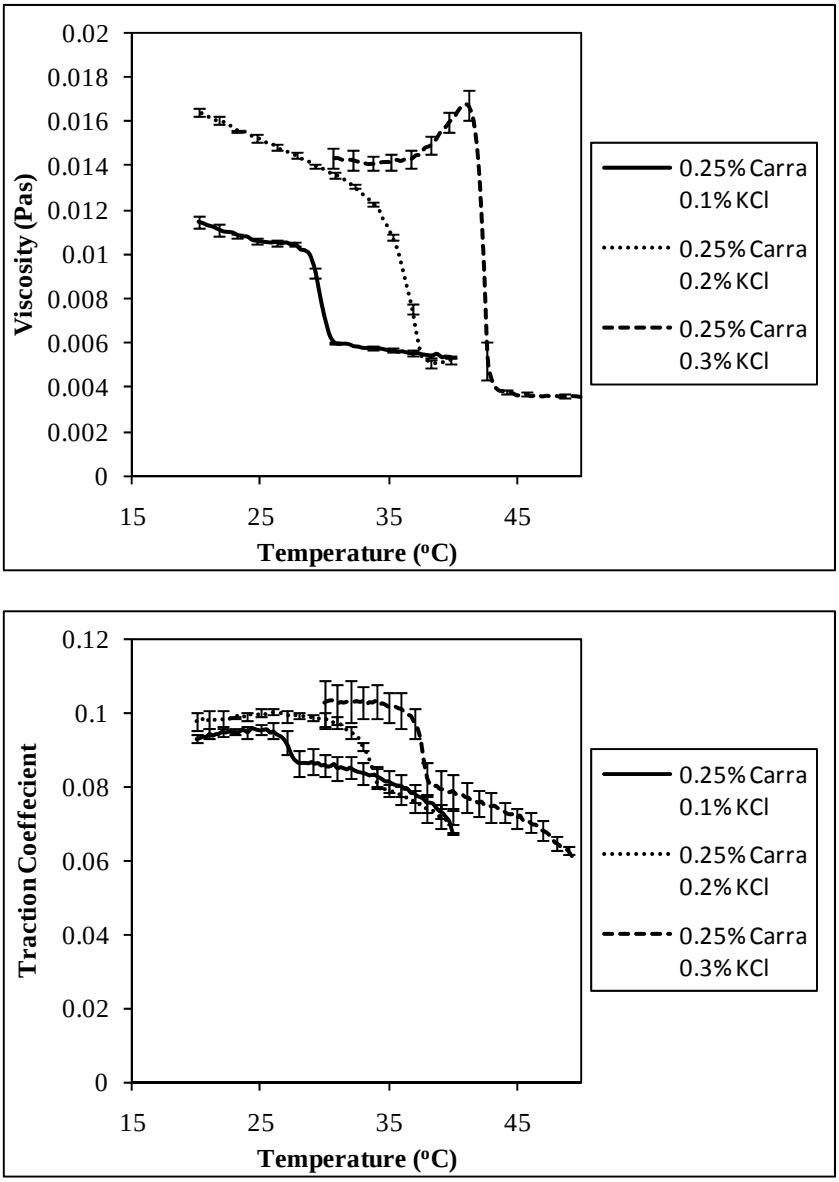

Figure 7.3. KCl effects on carrageenan, top, Viscosity curves of κ-Carrageenan gels during temperature induced ordering. Samples were cooled at 1.5 C/min at a constant shear of 200s-1, using a 60mm parallel plate geometry. Curves represent an average of three experiments and error bars show one standard deviation from the mean. Bottom, Traction curves of κ-Carrageenan gels during temperature induced ordering at. Samples were cooled at a rate of 1.5 C/min at a constant speed of 500mm/s and normal force of 2N. A steel ball and elastomer disc tribopair was used. Curves represent an average of three experiments and error bars show one standard deviation from the mean.

Figure 7.4 shows a comparison curve between ordering of 1% κ-carrageenan, 0.1% KCl in the rheometer and tribometer. Data was normalised to show the ordering process recorded by each technique and the tribology curve has been shifted 3.5°C to compensate for the recorded temperature lag. The curves follow the same pattern, but some key features are present across experiments. The initial temperature region before ordering in tribology experiments shows a much steeper increase in traction compared with rheology. Some increase in this region is expected since with decreasing temperature an increase in viscosity will be observed. It is also possible at this point that the solution present has some interaction and deposition on the recording surface influencing the initial traction data.

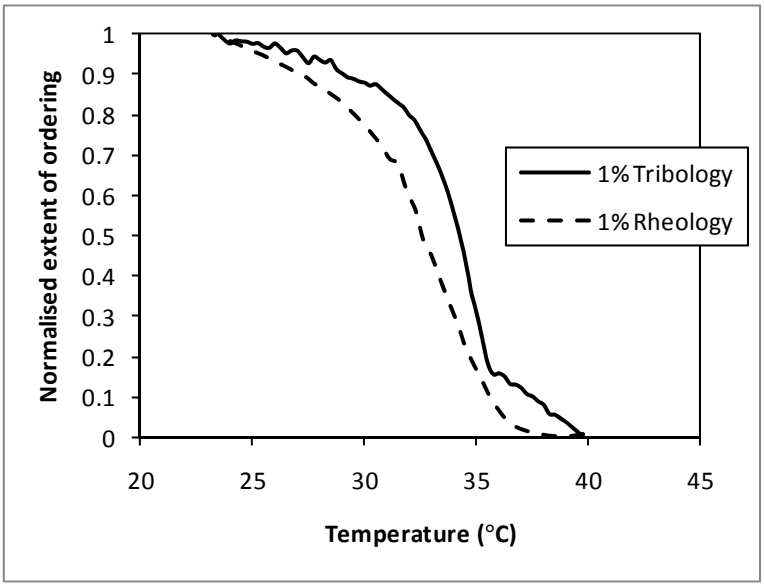

Figure 7.4. Normalised κ-carrageenan ordering curve, data for 1% κ-carrageenan 0.1% KCl following the ordering process by tribology and rheology.

Samples of gellan were also prepared in the same manner, considering gellan concentration and KCl concentration. Rheology and tribology data for most samples followed the same trends as for carrageenan. With increasing concentration an increase in onset of ordering temperature and extent of viscosity or traction change was observed. Appendix 1 shows data

for ordering with varying gellan concentration. One exception is present at 0.5% gellan with 0.2% KCl (Figure 7.5), where less of an increase in viscosity during ordering is seen compared to 0.1% KCl. However, no such pattern is seen in tribology measurements. It is unclear why, especially given that independent repeats were carried out. However, it could be as a result of the small differences between the final values for these samples (0.03-0.05 Pas) compared with the differences seen with increasing gellan concentration (0.015-0.15 Pas). Another explanation is the nature of the measurements carried out: for rheology bulk properties are measured whereas for tribology the thin film behaviour is assessed. For this sample a difference in bulk structure may have been present, which did not affect tribology measurements. A single curve for 1% gellan is once again normalised and compared for both the techniques in Figure 7.6. The ordering rate matches between the two techniques, however for the tribology data a steeper increase with reducing temperature for the initial stages before ordering is observed, as with the previous carrageenan data.

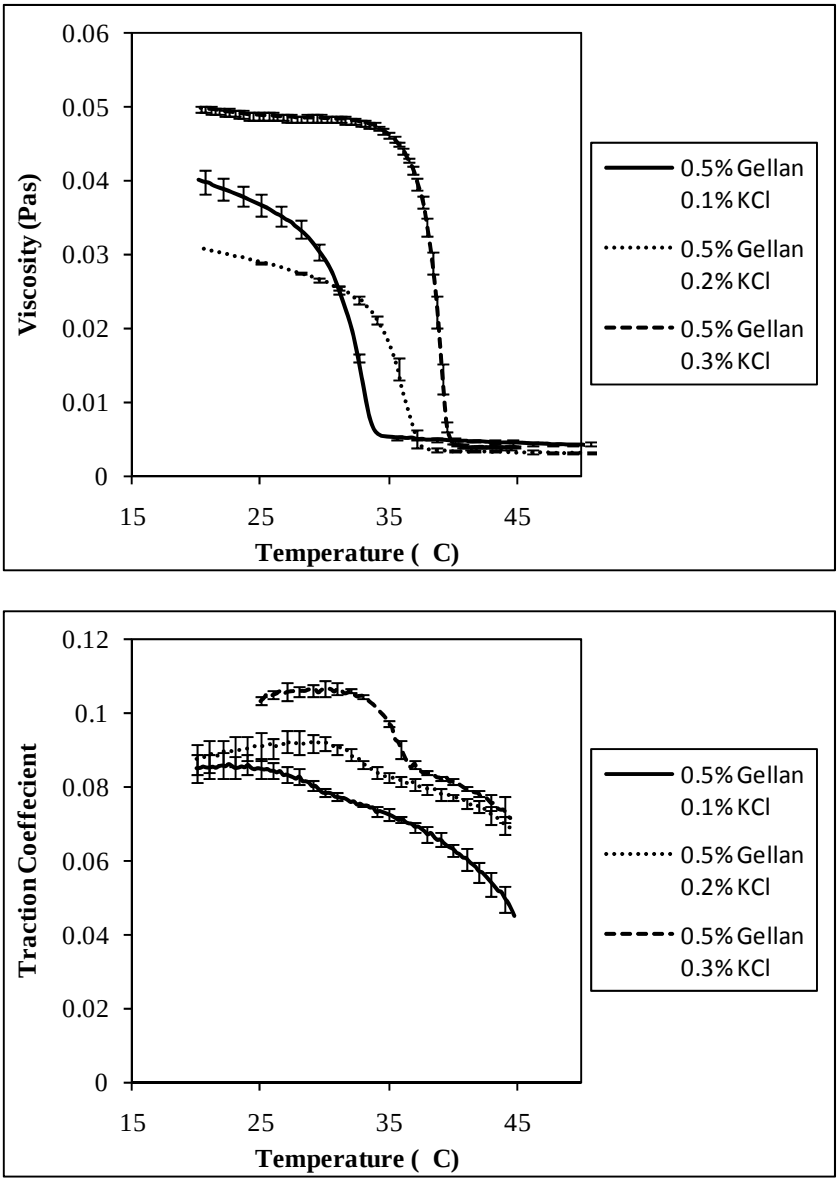

Figure 7.5. KCl effects on gellan ordering, top, Viscosity curves of Gellan gels during temperature induced ordering. Samples were cooled at 1.5 C/min at a constant shear of 200s-1, using a 60mm parallel plate geometry. Curves represent an average of three experiments and error bars show one standard deviation from the mean. Bottom, Traction curves of Gellan gels during temperature induced ordering. Samples were cooled at a rate of 1.5 C/min at a constant speed of 500mm/s and normal force of 2N. A steel ball and elastomer disc tribopair was used. Curves represent an average of three experiments and error bars show one standard deviation from the mean.

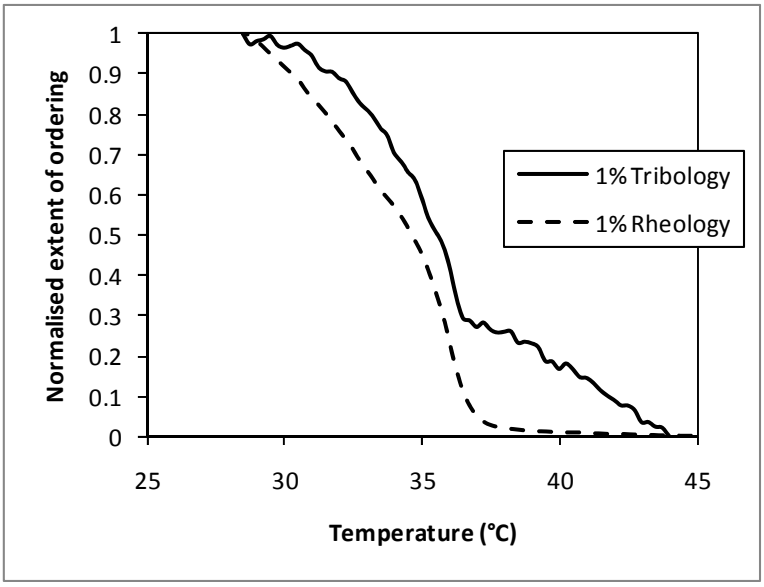

Figure 7.6. Normalised gellan ordering curves, data for 1% gellan 0.1% KCl following the ordering process by tribology and rheology.

Finally, agarose samples were prepared using both methods. Only polymer concentration effects were studied as even a small addition of salts created very quick forming and hard gels, which prevented accurate measurement and created large visible gel chunks, rather than a fluid gel sample. Patterns observed showed once again the same key features with increasing concentration (data presented in Appendix 1). However, at the lower concentrations an extended ordering temperature range when compared with gellan and carrageenan is present. When comparing normalised data in Figure 7.7 for agarose as with previous samples, the rate of change in traction during ordering, and the onset of ordering temperature, determined by a sharp gradient change in the curves, are similar between methods.

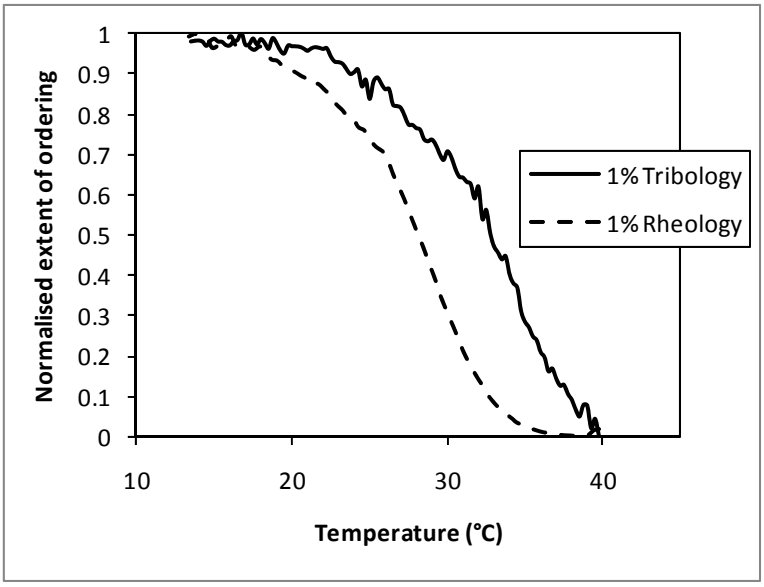

Figure 7.7. Normalised agarose ordering curves, data for 1% gellan 0.1% KCl following the ordering process by tribology and rheology.

During the viscosity studies each material shows that as biopolymer concentration increases, an increase in initial viscosity is observed. This relationship for each material should be linear on a double log plot to the c* concentration, above which the gradient of the relationship increases (Morris *et al.*, 1981). Below the concentration the chains within the sample exist without fully interacting with each other, and viscosity is determined by the number of chains present. When their concentration increases to a point where they start to interact, their movement is restricted by tangling with other chains. This concentration is dependent on material (Clegg, 1995). For the range of concentrations in this work, the relationship between initial viscosity and sample concentration is not linear. This suggests the c* concentration could be present within the range studied for a shear rate of $200s^{-1}$. Figure 7.8 shows a double log plot of the correlation, with the viscosity of ordering taken from the point just before ordering changes the viscosity gradient on viscosity/temperature curves for each material. However, since only three concentration points are available for each

biopolymer the relationship is not conclusive. Previous work by Cook *et al.* (2011) has isolated this c* concentration for guar gum, λ-carrageenan and HPMC to be between 0.2 and 0.6% w/w at zero shear, depending on material used. Similarly values were obtained for guar gum, λ-carrageenan, locust bean gum and scleroglucan which are in agreement with the range of values used here (Garrec and Norton, 2011).

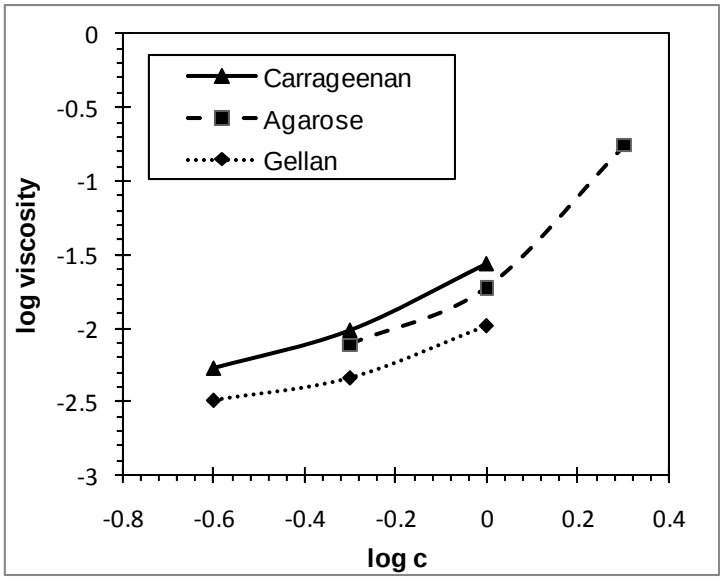

Figure 7.8. Viscosity dependence on polymer concentration, double log plot of initial viscosity against concentration (w/w %) for each biopolymer. Values are taken from the initial section of viscosity measurements previously.

Work in Gabriele *et al.* (2009) characterises particle sizes created in shear rates greater than $1s^{-1}$ in the rheometer. Under a uniform shear particles are around 5 microns reducing with increasing shear rate. Above this value for any given sample, shear thinning behaviour over a range of shear rates is similar. Below this value, large irregular particles were found, leading to a slightly higher viscosity over the range as well as an increased error between measurements. Below the $1s^{-1}$ shear rate the material is able to form large links between chains which are not broken by the applied shear. The formation of these large particles creates an irregular distribution of particles which affects bulk rheology measurements

resulting in more variation. Comparisons of material produced in the rheometer and tribometer were made by measuring viscosity from 0.1 to a maximum of $200s^{-1}$. Ideally this would be complemented with particle size and density measurements but this was not possible in the timeframe available. The maximum shear rate matches the production shear rate, ensuring that further structure breakdown does not occur, affecting results and producing hysteresis in the viscosity curves. It is expected that under these conditions uniform mixing occurs in the tribometer cell, and that sufficiently high shear is created through the sample to prevent large particles forming. Preliminary experiments at lower speeds produced inhomogeneous samples containing large gel particles, and findings from Chapter 6 suggest that these conditions would be required to produce a homogeneous sample.

In the case of carrageenan samples, at 0.5% seen in Figure 7.9(b) repeatability was good and no difference is seen between samples, indicating that reasonably uniform particles of comparable size order are being produced. From previous literature the particle sizes expected are around 5 microns (Gabriele *et al.* 2009). The same is true for 1% samples, however differences are seen for the 0.25% carrageenan sample (Figure 7.9(a)): viscosity over most of the range tested is lower for the material from tribology than from rheology. This is unexpected since tribology would be likely to produce less uniform samples, given that the sample size is larger and the shear across the sample is not uniform. However, is it also expected that the shear experienced would be higher as material entrained would be exposed to large forces in the recording gap, so any material forming while being entrained would be exposed to this. It is also unexpected as with increasing KCl concentration the difference between samples is no longer present past the 0.1% KCl sample. However, results produced were repeatable and so it is possible that as this is the weakest gel tested the high shears

present in the tribometer created much smaller particles than in other cases. This is reinforced by data from gellan, where small differences are seen between samples of 0.25% and 0.5% created in the different equipment. The differences between samples are much smaller than seen previously, however the same reasoning could be applied (Figure 7.10). For agarose samples in each concentration no differences are seen, again suggesting that similar particles are produced in both environments. However, higher variability between repeats was seen possibly indicating the presence of some larger, more irregular particles (Appendix 1). Both these occurrences can be explained given the much higher viscosities created across the concentrations used compared with carrageenan and gellan giving rise to a greater number of less flexible particles.

Further examination of the viscosity curves show in some cases for carrageenan and agarose samples a small change in the shape of the curve was observed at approximately $20s^{-1}$. A levelling out of the viscosity occurs until around $90s^{-1}$ where a sharp decrease then takes place. This behaviour could be explained as a change in the material structure during shearing: at the low shears very little movement occurs in the sample meaning some inter-particle connections may still be present, which hinder movement. When the plateau is reached a sufficiently high shear is applied to stretch these connections which then break and allow the particles to move more freely and align giving a sharper decrease in viscosity. This bridging between particles is shown in previous work such as Gabriele *et al.* (2009) and is shown to depend on the sample and processing environment. This bridging behaviour could also offer an explanation for some differences seen between tribology and rheology samples. For tribology samples a spoonful of material is needed to be transferred from the tribometer cell to the rheometer for viscosity testing whereas the rheology sample is already in place.

This could allow the rheology sample to form more structure which would be broken in the tribology sample when moving. However, a difference is not always present despite the repeated method and so this cannot be solely responsible for differences observed. The remainder of the viscosity graphs are presented in Appendix 1.

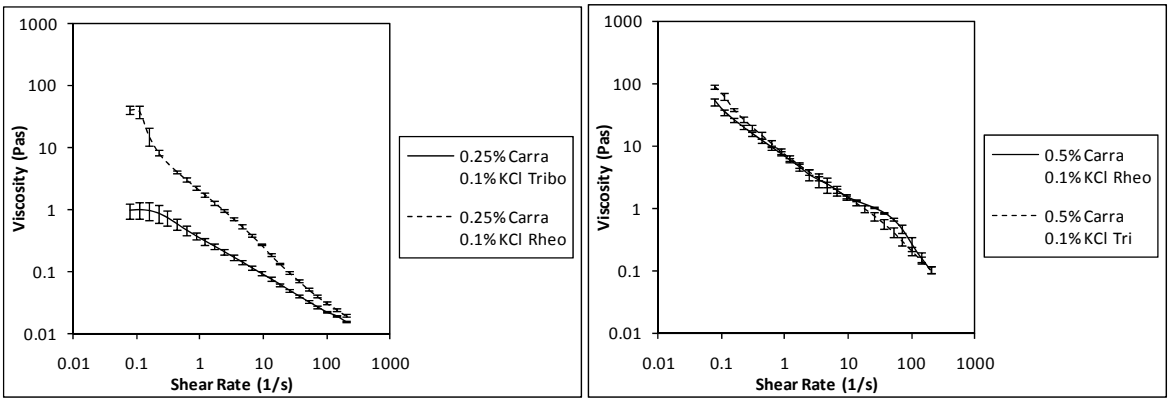

Figure 7.9. Viscometry post production of κ-carrageenan samples, comparison of material formed in the tribometer and rheometer for samples of two concentrations. Viscosity curves between 0.1 and 200 s-1 were carried out at 10°C, data is an average of three separate runs with error bars of one standard deviation from the mean.

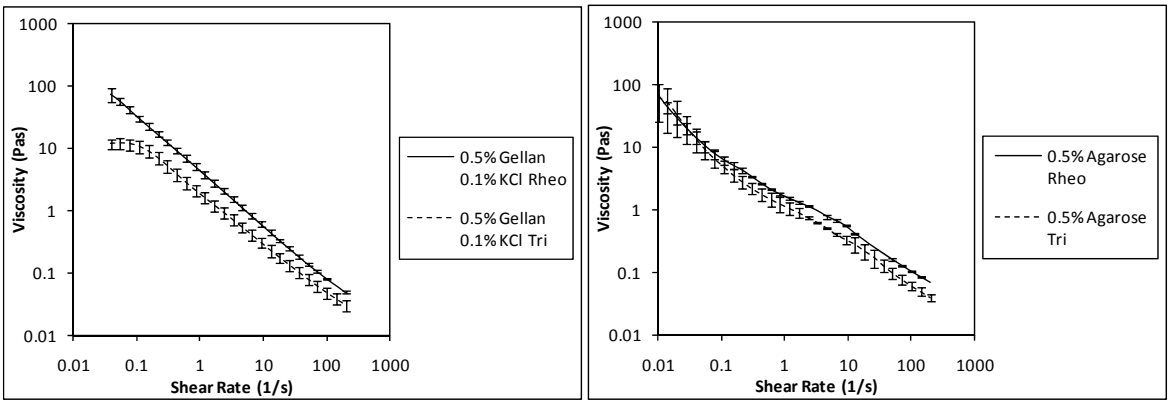

Figure 7.10. Viscometry post production of gellan and agarose, comparison of material formed in the tribometer and rheometer. Viscosity curves between 0.1 and 200 s-1 were carried out at 10°C, data is an average of three separate runs with error bars of one standard deviation from the mean.

Analysis of the patterns recorded during ordering of the samples was carried out to try to ascertain how each technique shows the ordering process taking place and what similarities are present between them. Initially, a comparison of the onset of ordering temperature is made for all samples. Values for temperature were taken at the point where a gradient change is present. Temperature values for tribology data have been increased by 3.5°C to account for the lag caused by the location of the temperature probe, as detailed in materials and methods section 3.2.12. Data for κ-Carrageenan is presented in Figure 7.11; a linear dependence on both polymer and KCl concentration is apparent, although more concentrations would be needed to confirm the dependency. Some difference between the two techniques is seen at the higher concentrations but values are still within experimental errors. It is possible that at the higher concentrations, the increased viscosity of the sample hinders mixing and therefore heat transfer within the tribometer cell creating a larger temperature profile across the sample, increasing the lag experienced. A similar correlation is seen in Figure 7.12 for gellan samples and in Figure 7.13 for agarose. Linear relationships for both experimental conditions hold. For rheology this change in viscosity has previously been identified to be a result of the ordering process as discussed earlier by Gabriele *et al.* (2009). This indicates the traction changes recorded during tribology are a result of the ordering process taking place.

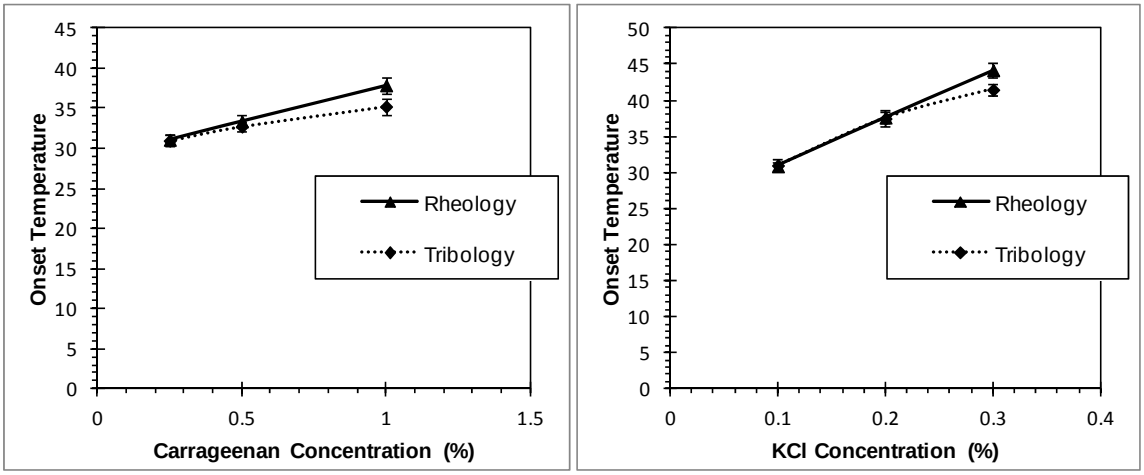

Figure 7.11. Onset of ordering temperatures for κ-carrageenan, temperature at the point of ordering is taken where a gradient change on viscosity or traction curves is present. KCl effects are studied at 0.25% κ-Carrageenan concentration.

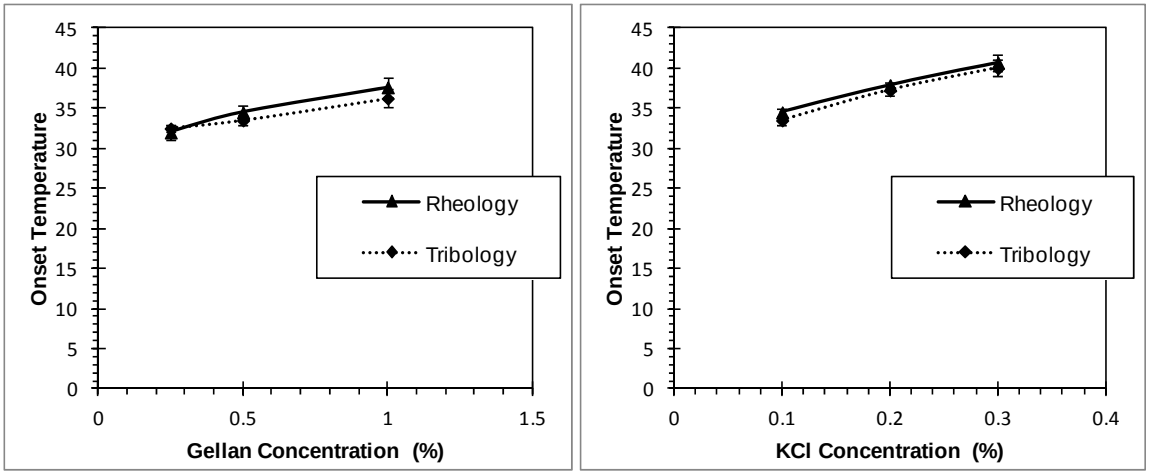

Figure 7.12. Onset of ordering temperatures for gellan samples, temperature at the point of ordering is taken where a gradient change on viscosity or traction curves is present. KCl effects are studied at 0.5% Gellan concentration.

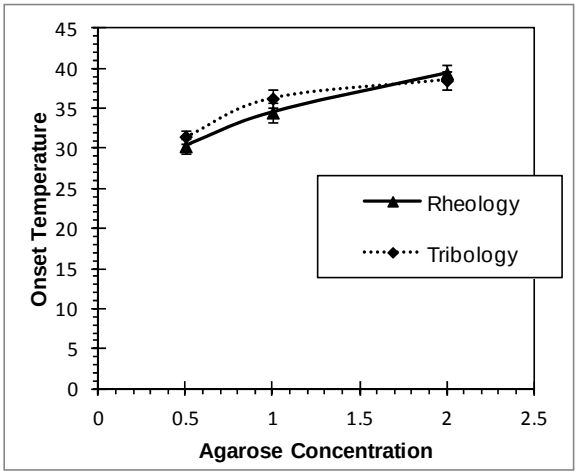

Figure 7.13. Onset of ordering temperature for agarose samples, temperature at the point of ordering is taken where a gradient change on viscosity or traction curves is present.

Differences are present between the two measurement techniques, an example of this is seen with 0.5% agarose, where the change in traction during ordering is not apparent from the graph however a change of approximately 0.05 Pas is observed in viscosity. Some effect could be attributed to shear experienced in the tribometer. Previous rheology work has shown a dependency on shear rate on the extent of ordering. The shear used in this study is taken from the range in Gabriele *et al.* (2009), $200s^{-1}$ is at a point where shear is high enough to give uniform particles, but at higher shears particles become so small that their effect on the viscosity is reduced, making it difficult to distinguish between samples. For carrageenan a difference of 0.005 Pas between the onset and end of ordering is observed at $700s^{-1}$, compared with 0.03 Pas at $200s^{-1}$. Shear in the tribometer is difficult to quantify because of the recording cell volume and the free changing nature of the shearing gap, so it is possible that it is higher than in the rheometer, resulting in samples with less distinguishable ordering changes. A final explanation for the difference is that while the rheometer generates data from the whole of the sample, tribology data is gathered from a small section between the contacts of the two surfaces. As this gap is often very small the material that passes through

may not be an accurate representative of the bulk of the fluid. This could be an effect of bulk mixing which prevents all of the material being entrained. Work in Chapter 6 highlighted that when working with materials that have a high low shear viscosity there is little mixing within the measurement cell and so the material in the contact is not regularly replaced. This effect could also be a result of particles being excluded from the gap between surfaces. Previous work in emulsion tribology by Malone *et al.* (2003) has suggested that in the boundary and mixed regime the gap size is often smaller than that of the oil droplets and so the gap is mostly filled with the continuous water phase. A similar situation may exist in the fluid gel system with most particles being excluded except the smallest or weakest which can be broken down and entrained. A recent study by Gabriele *et al.* (2010) has looked at lubrication of agarose fluid gels to identify their mechanism of lubrication. Here, traction data for a pre-made fluid gel is presented over a range of different speeds to a maximum of 100mm/s. Three distinct regions over the speed range were identified, at low speeds up to about 20mm/s speed is not high enough to entrain the particles, so only the fluid medium can enter and lubricate. This causes a reduction in traction coefficient. When speed reaches a point which is fast enough to entrain particles an increase in traction coefficient occurs where the gap is of a similar size to the particles and so a single layer provides lubrication. Traction is then determined by the rolling and sliding of those particles through the gap which begins to increases the traction coefficient. In addition to this as the surfaces become more separated an increasing number of particles are able to fill the gap creating a film which is comparably larger than the entrained particles, allowing less restrictive motion between the contacts and lowering traction coefficient. The speed ranges at which each of these situations are present is dependent on a number of factors. The material used and particle size and hardness associated, the surface properties, normal force and SRR will all affect the type of lubrication

at each speed. In this study a value of 500mm/s is much higher than the literature value and so it is expected that full multilayer particle lubrication should be present. However, previous work by de Vicente *et al.* (2006) looked at lubrication by carbopol microgel suspensions and a similar shape lubrication curve is present in neutralised carbopol samples. In this case, the multilayer lubrication stage occurs around 100-200mm/s compared with 35mm/s. This indicates that it is not clear the type of lubrication present in this study at 500mm/s, and so further investigation should clarify this.

7.3. CONCLUSIONS

In conclusion, the study of a dynamic process in tribology can be carried out. The equipment can be set up to run at a variety of temperatures and can produce data over temperature profiles. Gel samples can be structured under shear to created fluid gels containing gel particles. These temperature profiles are comparable to the ranges available during viscosity measurements. It is useful to look at temperature effects on foods such as melting, viscosity changes or structure breakdown, which would occur during an acclimatisation period in the mouth. In this case, temperature induced ordering of different biopolymers was studied showing that this process can be followed using tribology. The data presented proves to be of good quality and repeatability and has implications for future work, which looks as structuring or destructuring processes in the mouth. Tribology can provide different patterns of behaviour than rheology on structuring of a material, however this can be extended to melting behaviour as well as a host of other dynamic processes such as enzyme denaturing or phase inversion. This information can be used to further mimic and understand processes which occur in an oral environment which so far rheology alone cannot fully explain.

An overall pattern in most cases of increasing polymer or KCl concentration increases onset temperature and extent of viscosity or lubrication change has been presented. However lubrication properties of the material cannot be completely predicted by comparison to rheology data in these cases. Investigating viscosity across a range of samples after production in both pieces of equipment, where no differences were found it is assumed similar particles were produced, in the case of small differences for low concentration samples the high shears associated with the narrow gap sizes in tribology are suggested to have created very small particles leading to a viscosity reduction.

CHAPTER 8. CONCLUSIONS AND FUTURE WORK

Detailed conclusions were presented at the end of each chapter. The current chapter details the overall outcomes of this work and proposes ideas to build on what has been carried out.

8.1. CONCLUSIONS

The aim of the work presented in this thesis was to develop in-vitro methods that relate to the phenomena occurring during oral processing. Different rigs have been developed to consider model food systems under conditions similar to those experienced in the mouth: a low shear environment similar to the initial intake of food material into the mouth; the effect of compression relating to chewing; a high shear environment associated with lubrication and tongue/palate interactions. The following sections detail specific conclusions made for each of the in-vitro methods developed.

8.1.1. Stirred tank environment

For the gels investigated in the stirred tank experiments (as detailed in Chapter 4), it was shown that the structure of the sample does not affect diffusion of salt under quiescent conditions. The developed system can be used to quantify salt release from a range of structures under oral conditions, which relates to the period during which food is initially in contact with the mouth, and the diffusion from any material deposited on the tongue after swallowing. The complementary mathematical model developed during this work can predict the release of salt from these gel structures, and from alternative geometries which are closer to actual food structures.

8.1.2. Compression tank environment

The compression rig developed (as discussed in Chapter 4) relates to conditions in the mouth, such as chewing and tongue/palate interactions, where breakdown of material occurs. For the samples used here salt release is unaffected by compression forces, until they are sufficiently high to break the gel structure where salt release increases. Similar behaviour for other tastants and flavours would be expected under these conditions.

8.1.3. Tribology

The work from Chapter 5 shows that the developed configuration (for example, utilising two soft surfaces, low normal forces, temperature control, an external circulation tank and constant speed experiments) provides the best range of conditions for carrying out in-vitro testing, which can be related to tongue/palate interactions. The use of the MTM system shows more reliable results and allows a wider range of processing conditions to be used (such as different ball materials) than alternative tribology equipment that was investigated, such as rheometer attachments.

Timed experiments, presented in Chapter 6, using this tribology equipment to study inhomogeneous polysaccharide solutions (i.e. samples similar to those experienced during real consumption) show that the ability of the polysaccharide to mix with a bulk material affects the pattern of lubrication experienced. This phenomenon has been shown to occur in the mouth for liquid samples. Thus, the tribology method developed in this work (which considers lubrication at different points during mixing), could be used to predict the patterns in the mouth for this type of sample. For example the unexpectedly high sensory scores

experienced by high concentration guar samples seen in section 5.2.4 were thought to be a result of the sample thickness and lack of mixing in the mouth.

The developed tribology equipment can also be used to explore responses to dynamic processes occurring in the mouth during eating (as discussed in Chapter 7). In this case structuring of hydrocolloids was studied however processes such as melting, emulsion breakdown and enzyme interactions more relevant to the mouth could use the same method.

8.2. FUTURE WORK

The developed stirred tank rig shows good repeatability for salt release, so potential for comparison of material release for non-volatile components. The use of a wider variety of common food products or model materials which structure foods would provide a more detailed insight into salt release patterns. The equipment can be extended depending on the material studied to include the use of ion specific probes for following release, for example the individual species release pattern of a product containing both sodium and potassium ions could be studied. Similarly, for the developed compression environment the range of samples studied can be increased. Of particular interest would be the use of mixed biopolymer gels, which other research (Sala *et al.*, 2010) has highlighted could produce different fracture properties and serum release. Both systems could also be used for volatile release studies with appropriate headspace capture and analysis equipment, as in other works (see section 2.4). Extension of the work to focus on timescales more applicable to oral conditions would also provide interesting information, for example salt containing microspheres of gel

could be tested as an attempt to validate predictions made by the developed mathematical model.

The use of tribology to better understand processes occurring in the mouth is still in its early stages, so further development of equipment used here to closer represent oral surfaces and forces needs to be continued. Measurements of lubrication in the tribometer cell of an inhomogeneous mixture are dependent on structure and so a mixing study using PEPT or similar techniques would be of value to better understand the physics of mixing and entrainment. With the preliminary work carried out, shorter timescale experiments looking at mimicking the tasting and swallowing cycles of eating could be undertaken. For gelation work, physical properties of the created gels are a function of their environment, especially shear, as such a more extensive range of rheometer conditions could be used and compared with material produced in the tribometer. Some visualisation of fluid gels created by both techniques to indicate shears experienced by the material during tribological testing could be undertaken. An extension of gelation behaviour of gels could look at the melting processes of materials to relate to in mouth melting of products, or other structure breakdown phenomena. For all systems used, sensory data from panels would allow direct comparisons of results, for emulsion samples and some gel samples used this could be achieved, and would be beneficial especially for the future proposed work.

References

Adams, S., Singleton, S., Juskaitis, R. and Wilson, T. (2007) In-Vivo Visualisation of Mouth-Material Interactions by Video Rate Endoscopy. **Food Hydrocolloids**, 21: (5-6): 986-995.

Altmann, N., Cooper-White, J.J., Dunstan, D.E. and Stokes, J.R. (2004) Strong through to Weak `Sheared' Gels. **Journal of Non-Newtonian Fluid Mechanics**, 124: (1-3): 129-136.

Anton_Parr (2011) **Tribology — Measurement of Friction, Lubrication and Wear** [online]. http://www.anton-paar.com/Tribology-%E2%80%94-Measurement-of-Friction-Lubrication-and-Wear/Tribology/60_Corporate_en?product_id=385 [Accessed 2011]

Arai, E. and Yamada, Y. (1993) Effect of the Texture of Food on the Masticatory Process. **Japan Journal of Oral Biology**, 35: 10.

Archbutt, L. and Deeley, R.M. (1900) **Lubrication and Lubricants, a Treatise and Practice of Lubrication**. London: C Griffin & Co. Ltd ISBN-10: 1142047970

Armenteros, M., Aristoy, M.-C., Barat, J.M. and Toldrá, F. (2011) Biochemical and Sensory Changes in Dry-Cured Ham Salted with Partial Replacements of Nacl by Other Chloride Salts. **Meat Science**, In Press, Corrected Proof.

Ball, P., Woodward, D., Beard, T., Shoobridge, A. and Ferrier, M. (2002) Calcium Diglutamate Improves Taste Characteristics of Lower-Salt Soup. **European Journal of Clinical Nutrition**, 56: (6): 519-523.

Barkhausen, J., Goyen, M., von Winterfeld, F., Lauenstein, T., Arweiler-Harbeck, D. and Debatin, J. (2002) Visualization of Swallowing Using Real-Time Truefisp Mr Fluoroscopy. **European Radiology**, 12: (1): 129-133.

Bartz, W.J. (1978) Tribology, Lubricants and Lubrication Engineering -- a Review. **Wear**, 49: (1): 1-18.

Barwell, F.T. (1974) The Tribology of Wheel on Rail. **Tribology**, 7: (4): 146-150.

Beauchamp, G.K. and Stein, L.J. (2008) "Salt Taste". In Allan, I.B.;Akimichi, K.;Gordon, M.S.;Gerald, W.;Thomas, D.A.;Richard, H.M.;Peter, D.;Donata, O.;Stuart, F.;Gary, K.B.;Bushnell, M.C.;Jon, H.K. & Esther, G. (Eds.) **The Senses: A Comprehensive Reference**. New York, Academic Press 401-408.

Benjamins, J., Vingerhoeds, M.H., Zoet, F.D., de Hoog, E.H.A. and van Aken, G.A. (2009) Partial Coalescence as a Tool to Control Sensory Perception of Emulsions. **Food Hydrocolloids**, 23: (1): 102-115.

Bertino, M., Beauchamp, G. and Engelman, K. (1982) Long-Term Reduction in Dietary Sodium Alters the Taste of Salt. **The American Journal of Clinical Nutrition**, 36: (6): 1134-1144.

BNF (1981) Salt in the Diet. **Nutrition Bulletin**, 6: (3): 171-188.

Boland, A.B., Buhr, K., Giannouli, P. and van Ruth, S.M. (2004) Influence of Gelatin, Starch, Pectin and Artificial Saliva on the Release of 11 Flavour Compounds from Model Gel Systems. **Food Chemistry**, 86: (3): 401-411.

Boland, A.B., Delahunty, C.M. and van Ruth, S.M. (2006) Influence of the Texture of Gelatin Gels and Pectin Gels on Strawberry Flavour Release and Perception. **Food Chemistry**, 96: (3): 452-460.

Bongaerts, J.H.H., Fourtouni, K. and Stokes, J.R. (2007) Soft-Tribology: Lubrication in a Compliant Pdms-Pdms Contact. **Tribology International**, 40: (10-12): 1531-1542.

Bot, A., van Amerongen, I.A., Groot, R.D., Hoekstra, N.L. and Agterof, W.G.M. (1996) Large Deformation Rheology of Gelatin Gels. **Polymer Gels and Networks**, 4: (3): 189-227.

Bourriot, S., Garnier, C. and Doublier, J.-L. (1999) Phase Separation, Rheology and Structure of Micellar Casein-Galactomannan Mixtures. **International Dairy Journal**, 9: (3-6): 353-357.

Bradley, T.D., Ball, A., Harding, S.E. and Mitchell, J.R. (1989) Thermal Degradation of Guar Gum. **Carbohydrate Polymers**, 10: (3): 205-214.

Bull, N.L. and Buss, D.H. (1980) Contributions of Foods to Sodium Intakes. **The Proceedings of the Nutrition Society**, 39: (30A).

Burseg, K.M.M., Brattinga, C., de Kok, P.M.T. and Bult, J.H.F. (2010) Sweet Taste Enhancement through Pulsatile Stimulation Depends on Pulsation Period Not on Conscious Pulse Perception. **Physiology & Behavior**, 100: (4): 327-331.

Busch, J.L.H.C., Tournier, C., Knoop, J.E., Kooyman, G. and Smit, G. (2009) Temporal Contrast of Salt Delivery in Mouth Increases Salt Perception. **Chemical Senses**, 34: (4): 341-348.

Carpenter, R.P., Lyon, D.H. and Hasdell, T.A. (2000) **Guidelines for Sensory Analysis in Food Product Development and Quality Control**. Gaithersburg, Md.: Aspen Publishers. ISBN-10: 0834216426

Cassin, G., Heinrich, E. and Spikes, H.A. (2001) The Influence of Surface Roughness on the Lubrication Properties of Adsorbing and Non-Adsorbing Biopolymers. **Tribology Letters**, 11: (2): 95-102.

Chanamai, R. and McClements, D.J. (2002) Comparison of Gum Arabic, Modified Starch, and Whey Protein Isolate as Emulsifiers: Influence of pH, $CaCl_2$ and Temperature. **Journal of Food Science**, 67: (1): 120-125.

Chen, J. (2009) Food Oral Processing--a Review. **Food Hydrocolloids**, 23: (1): 1-25.

Chojnicka-Paszun, A., Macakova, L., Stokes, J.R., de Kruif, C.G. and Jongh, H.H.J.d. (Submitted) Lubrication, Rheology and Adsorption of Polysaccharide Solutions.

Chojnicka, A. (2009) Sensory Perception and Friction Coefficient of Milk with Increasing Fat Content (Submitted).

Chojnicka, A., Sala, G., de Kruif, C.G. and van de Velde, F. (2009) The Interactions between Oil Droplets and Gel Matrix Affect the Lubrication Properties of Sheared Emulsion-Filled Gels. **Food Hydrocolloids**, 23: (3): 1038-1046.

Clarke, C. (2004) **The Science of Ice Cream**. Royal Society of Chemistry. ISBN-10: 0854046291

Clegg, S.M. (1995) **Physico-Chemical Aspects of Food Processing**. Glasgow: Blackie Academic & Professional. ISBN-10: 0751402400

Collings, W.D. and Spangenberg, M.D. (1980) "Sodium Background". In Moses, C. (Ed.) **Sodium in Medicine and Health**. Baltimore, MD, US, Reese Press. ISBN: 0960521410

Cook, D.J., Hollowood, T.A., Linforth, R.S.T. and Taylor, A.J. (2011) Perception of Taste Intensity in Solutions of Random-Coil Polysaccharides above and Below C*. **Food Quality and Preference**, 13: (7-8): 473-480.

Cook, N.R., Cutler, J.A., Obarzanek, E., Buring, J.E., Rexrode, K.M., Kumanyika, S.K., Appel, L.J. and Whelton, P.K. (2007) Long Term Effects of Dietary Sodium Reduction on Cardiovascular Disease Outcomes: Observational Follow-up of the Trials of Hypertension Prevention (Tohp). **BMJ**, 334: (7599): 885-.

Coren, S., Ward, L.M. and Enns, J.T. (2004) **Sensation and Perception**. J. Wiley & Sons. ISBN-10: 0471451479

Crank, J. (1975) **The Mathematics of Diffusion**. 2.Oxford Science Publications. ISBN-10: 0198534116

Czichos, H. (1978) **Tribology: A Systems Approach to the Science and Technology of Friction, Lubrication, and Wear**. Amsterdam, The Netherlands: Elsevier. ISBN-10: 0444553037

Davidson, J.M., Linforth, R.S.T. and Taylor, A.J. (1998) In-Mouth Measurement of Ph and Conductivity During Eating. **Journal of Agricultural and Food Chemistry**, 46: (12): 5210-5214.

de Jong, S. and van de Velde, F. (2007) Charge Density of Polysaccharide Controls Microstructure and Large Deformation Properties of Mixed Gels. **Food Hydrocolloids**, 21: (7): 1172-1187.

de Vicente, J., Stokes, J.R. and Spikes, H.A. (2005) Lubrication Properties of Non-Adsorbing Polymer Solutions in Soft Elastohydrodynamic (Ehd) Contacts. **Tribology International**, 38: (5): 515-526.

de Vicente, J., Stokes, J.R. and Spikes, H.A. (2006) Soft Lubrication of Model Hydrocolloids. **Food Hydrocolloids**, 20: (4): 483-491.

de Wijk, R.A. and Prinz, J.F. (2005) The Role of Friction in Perceived Oral Texture. **Food Quality and Preference**, 16: (2): 121-129.

de Wijk, R.A. and Prinz, J.F. (2007) Fatty Versus Creamy Sensations for Custard Desserts, White Sauces, and Mayonnaises. **Food Quality and Preference**, 18: (4): 641-650.

de Wijk, R.A., Wulfert, F. and Prinz, J.F. (2006) Oral Processing Assessed by M-Mode Ultrasound Imaging Varies with Food Attribute. **Physiology & Behavior**, 89: (1): 15-21.

Desmond, E. (2006) Reducing Salt: A Challenge for the Meat Industry. **Meat Science**, 74: (1): 188-196.

Dickinson, E. (2003) Hydrocolloids at Interfaces and the Influence on the Properties of Dispersed Systems. **Food Hydrocolloids**, 17: (1): 25-39.

Dickinson, E. (2007) Food Colloids... How Do Interactions of Ingredients Control Structure, Stability and Rheology? **Current Opinion in Colloid & Interface Science**, 12: (4-5): 155-157.

Dickinson, E. (2009) Hydrocolloids as Emulsifiers and Emulsion Stabilizers. **Food Hydrocolloids**, 23: (6): 1473-1482.

Dranca, I. and Vyazovkin, S. (2009) Thermal Stability of Gelatin Gels: Effect of Preparation Conditions on the Activation Energy Barrier to Melting. **Polymer**, 50: (20): 4859-4867.

Dresselhuis, D.M., de Hoog, E.H.A., Cohen Stuart, M.A. and van Aken, G.A. (2008a) Application of Oral Tissue in Tribological Measurements in an Emulsion Perception Context. **Food Hydrocolloids**, 22: (2): 323-335.

Dresselhuis, D.M., de Hoog, E.H.A., Cohen Stuart, M.A., Vingerhoeds, M.H. and van Aken, G.A. (2008b) The Occurrence of in-Mouth Coalescence of Emulsion Droplets in Relation to Perception of Fat. **Food Hydrocolloids**, 22: (6): 1170-1183.

Dubow, J.S. and Childs, N.M. (1998) New Coke, Mixture Perception, and the Flavor Balance Hypothesis. **Journal of Business Research**, 43: (3): 147-155.

Durack, E., Alonso-Gomez, M. and Wilkinson, M.G. (2008) Salt: A Review of Its Role in Food Science and Public Health. **Current Nutrition & Food Science**, 4: 290-297.

Einstein, A. (1905) Über Die Von Der Molekularkinetischen Theorie Der Wärme Geforderte Bewegung Von in Ruhenden Flüssigkeiten Suspendierten Teilchen. **Annalen der Physik**, 322: (8): 549-560.

Elmore, J.S. and Langley, K.R. (1996) Novel Vessel for the Measurement of Dynamic Flavor Release in Real Time from Liquid Foods. **Journal of Agricultural and Food Chemistry**, 44: (11): 3560-3563.

Ertekin, C. and Aydogdu, I. (2003) Neurophysiology of Swallowing. **Clinical Neurophysiology**, 114: (12): 2226-2244.

Etiévant, P.V., Andrée (2006) **Flavour in Food**. Woodhead Publishing. ISBN-10: 0849334373

Ferry, A.L., Hort, J., Mitchell, J.R., Cook, D.J., Lagarrigue, S. and Valles Pamies, B. (2006) Viscosity and Flavour Perception: Why Is Starch Different from Hydrocolloids? **Food Hydrocolloids**, 20: (6): 855-862.

Finney, M. and Meullenet, J.F. (2005) Measurement of Biting Velocities at Predetermined and Indivdual Crosshead Speed Instrumental Imitative Tests for Predicting Sensory Hardness of Gelatin Gels. **Journal of Sensory Studies**, 20: (2): 114-129.

Fischer-Cripps, A.C. (2000) **Introduction to Contact Mechanics**. Springer. ISBN-10: 0387989145

Floury, J., Rouaud, O., Le Poullennec, M. and Famelart, M.-H. (2009) Reducing Salt Level in Food: Part 2. Modelling Salt Diffusion in Model Cheese Systems with Regards to Their Composition. **LWT - Food Science and Technology**, 42: (10): 1621-1628.

Gabriele, A., Spyropoulos, F. and Norton, I.T. (2009) Kinetic Study of Fluid Gel Formation and Viscoelastic Response with Kappa-Carrageenan. **Food Hydrocolloids**, 23: (8): 2054-2061.

Gabriele, A., Spyropoulos, F. and Norton, I.T. (2010) A Conceptual Model for Fluid Gel Lubrication. **Soft Matter**, 6: (17): 4205-4213.

Garrec, D.A. and Norton, I.T. (2011) The Influence of Hydrocolloid Hydrodynamics on Lubrication. **Food Hydrocolloids**, In Press, Corrected Proof.

Gilsenan, P.M. and Ross-Murphy, S.B. (2000) Rheological Characterisation of Gelatins from Mammalian and Marine Sources. **Food Hydrocolloids**, 14: (3): 191-195.

Girgis, S., Neal, B., Prescott, J., Prendergast, J., Dumbrell, S., Turner, C. and Woodward, M. (2003) A One-Quarter Reduction in the Salt Content of Bread Can Be Made without Detection. **European Journal of Clinical Nutrition**, 57: (4): 616-620.

Goh, S.M., Versluis, P., Appelqvist, I.A.M. and Bialek, L. (2010) Tribological Measurements of Foods Using a Rheometer. **Food Research International**, 43: (1): 183-186.

Harris, J.J., Smith, A.M., Campbell-Lynch, S. and Shelton, R.M. (2008) Dramatic Changes in Bulk Deformation Behaviour of Gellan Gum on Cross-Linking with Mixed Cations. **Gums and Stabilisers for the Food Industry**, 14: 79.

Hasenhuettl, G.L. and Hartel, R.W. (2008) **Food Emulsifiers and Their Applications**. Springer. ISBN-10: 0387752838

Heath, M.R., Prinz, J. F. (1991) **Processing of Foods and the Sensory Evaluation of Texture**. Oxford: Chapman and Hall. ISBN-10: 0834212382

Hiiemae, K., Heath, M.R., Heath, G., Kazazoglu, E., Murray, J., Sapper, D. and Hamblett, K. (1996) Natural Bites, Food Consistency and Feeding Behaviour in Man. **Archives of Oral Biology**, 41: (2): 175-189.

Hiiemae, K.M. and Palmer, J.B. (1999) Food Transport and Bolus Formation During Complete Feeding Sequences on Foods of Different Initial Consistency. **Dysphagia**, 14: (1): 31-42.

Holm, K., Wendin, K. and Hermansson, A.-M. (2009) Sweetness and Texture Perceptions in Structured Gelatin Gels with Embedded Sugar Rich Domains. **Food Hydrocolloids**, 23: (8): 2388-2393.

Hori, K., Ono, T., Tamine, K.-i., Kondo, J., Hamanaka, S., Maeda, Y., Dong, J. and Hatsuda, M. (2009) Newly Developed Sensor Sheet for Measuring Tongue Pressure During Swallowing. **Journal of Prosthodontic Research**, 53: (1): 28-32.

Humphrey, S.P. and Williamson, R.T. (2001) A Review of Saliva: Normal Composition, Flow, and Function. **The Journal of Prosthetic Dentistry**, 85: (2): 162-169.

Imeson, A. (1997) **Thickening and Gelling Agents for Food**. 2.Springer. ISBN-10: 0751400939

Imeson, A. (2009) **Food Stabilisers, Thickeners and Gelling Agents**. John Wiley and Sons. ISBN-10: 1405132671

Jack, F.R., Piggott, J.R. and Paterson, A. (1995) Cheddar Cheese Texture Related to Salt Release During Chewing, Measured by Conductivity—Preliminary Study. **Journal of Food Science**, 60: (2): 213-217.

Jalabert-Malbos, M.-L., Mishellany-Dutour, A., Woda, A. and Peyron, M.-A. (2007) Particle Size Distribution in the Food Bolus after Mastication of Natural Foods. **Food Quality and Preference**, 18: (5): 803-812.

Juteau, A., Cayot, N., Chabanet, C., Doublier, J.L. and Guichard, E. (2004) Flavour Release from Polysaccharide Gels: Different Approaches for the Determination of Kinetic Parameters. **Trends in Food Science & Technology**, 15: (7-8): 394-402.

Katsiari, M.C., Voutsinas, L.P., Alichanidis, E. and Roussis, I.G. (1997) Reduction of Sodium Content in Feta Cheese by Partial Substitution of Nacl by Kcl. **International Dairy Journal**, 7: (6-7): 465-472.

Klemm, D. and Heinze, T. (2006) **Polysaccharides Ii**. Springer. ISBN-10: 3540371028

Klink, I. M., Phillips, R. J., & Dungan, S. R. (2011). Effect of emulsion drop-size distribution upon coalescence in simple shear flow: A population balance study. **Journal of Colloid and Interface Science**, 353(2): 467-475.

Koli, J.M., Basu, S., Nayak, B.B., Kannuchamy, N. and Gudipati, V. (2011) Improvement of Gel Strength and Melting Point of Fish Gelatin by Addition of Coenhancers Using Response Surface Methodology. **Journal of Food Science**.

Koliandris, A.-L., Morris, C., Hewson, L., Hort, J., Taylor, A.J. and Wolf, B. (2010) Correlation between Saltiness Perception and Shear Flow Behaviour for Viscous Solutions. **Food Hydrocolloids**, 24: (8): 792-799.

Koliandris, A.-L., Tengah, N., Mills, T., Bakalis, S. and Wolf, B. (2009) "Investigation into the Friction Behaviour of Polysaccharide Solutions". Poster presented at Food and Behaviour Research Conference , Cardiff

Koliandris, A., Lee, A., Ferry, A.-L., Hill, S. and Mitchell, J. (2008) Relationship between Structure of Hydrocolloid Gels and Solutions and Flavour Release. **Food Hydrocolloids**, 22: (4): 623-630.

Law, M.R., Frost, C.D. and Wald, N.J. (1991) By How Much Does Dietary Salt Reduction Lower Blood Pressure? I--Analysis of Observational Data among Populations. **BMJ**, 302: (6780): 811-815.

Lide, D.R. (2004) **Crc Handbook of Chemistry and Physics**. 85.CRC Press. ISBN-10: 0849304865

Lindemann, B. (2001) Receptors and Transduction in Taste. **Nature**, 413: (6852): 219-225.

Liu, H., Xu, X.M. and Guo, S.D. (2007) Rheological, Texture and Sensory Properties of Low-Fat Mayonnaise with Different Fat Mimetics. **LWT - Food Science and Technology**, 40: (6): 946-954.

Malone, M.E. and Appelqvist, I.A.M. (2003) Gelled Emulsion Particles for the Controlled Release of Lipophilic Volatiles During Eating. **Journal of Controlled Release**, 90: (2): 227-241.

Malone, M.E., Appelqvist, I.A.M. and Norton, I.T. (2003) Oral Behaviour of Food Hydrocolloids and Emulsions. Part 1. Lubrication and Deposition Considerations. **Food Hydrocolloids**, 17: (6): 763-773.

Mangione, M.R., Giacomazza, D., Cavallaro, G., Bulone, D., Martorana, V. and San Biagio, P.L. (2007) Relation between Structural and Release Properties in a Polysaccharide Gel System. **Biophysical Chemistry**, 129: (1): 18-22.

McCurdy, R.D., Goff, H.D., Stanley, D.W. and Stone, A.P. (1994) Rheological Properties of Dextran Related to Food Applications. **Food Hydrocolloids**, 8: (6): 609-623.

Mielle, P., Tarrega, A., Sémon, E., Maratray, J., Gorria, P., Liodenot, J.J., Liaboeuf, J., Andrejewski, J.-L. and Salles, C. (2010) From Human to Artificial Mouth, from Basics to Results. **Sensors and Actuators B: Chemical**, 146: (2): 440-445.

Mioche, L., Hiiemae, K.M. and Palmer, J.B. (2002) A Postero-Anterior Videofluorographic Study of the Intra-Oral Management of Food in Man. **Archives of Oral Biology**, 47: (4): 267-280.

Miyoshi, E. (2009) Our Recent Findings on the Functional Properties of Gellan Gum. **Graduate School of Human Sciences, Osaka University**, 35: 23.

Morris, C., Labarre, C., Koliandris, A.-L., Hewson, L., Wolf, B., Taylor, A.J. and Hort, J. (2010) Effect of Pulsed Delivery and Bouillon Base on Saltiness and Bitterness Perceptions of Salt Delivery Profiles Partially Substituted with Kcl. **Food Quality and Preference**, 21: (5): 489-494.

Morris, E.R., Cutler, A.N., Ross-Murphy, S.B., Rees, D.A. and Price, J. (1981) Concentration and Shear Rate Dependence of Viscosity in Random Coil Polysaccharide Solutions. **Carbohydrate Polymers**, 1: (1): 5-21.

Mossaz, S., Jay, P., Magnin, A., Panouillé, M., Saint-Eve, A., Déléris, I., Juteau, A. and Souchon, I. (2010) Measuring and Predicting the Spreading of Dairy Products in the Mouth: Sensory, Instrumental and Modelling Approaches. **Food Hydrocolloids**, 24: (8): 681-688.

Murata, Y., Miyashita, M., Kofuji, K., Miyamoto, E. and Kawashima, S. (2004) Drug Release Properties of a Gel Bead Prepared with Pectin and Hydrolysate. **Journal of Controlled Release**, 95: (1): 61-66.

Myant, C., Spikes, H.A. and Stokes, J.R. (2010) Influence of Load and Elastic Properties on the Rolling and Sliding Friction of Lubricated Compliant Contacts. **Tribology International**, 43: (1-2): 55-63.

Nakada, M. (1994) Trends in Engine Technology and Tribology. **Tribology International**, 27: (1): 3-8.

Neyraud, E., Prinz, J. and Dransfield, E. (2003) Nacl and Sugar Release, Salivation and Taste During Mastication of Salted Chewing Gum. **Physiology & Behavior**, 79: (4-5): 731-737.

Noort, M.W.J., Bult, J.H.F., Stieger, M. and Hamer, R.J. (2010) Saltiness Enhancement in Bread by Inhomogeneous Spatial Distribution of Sodium Chloride. **Journal of Cereal Science**, 52: (3): 378-386.

Norton, I.T., Jarvis, D.A. and Foster, T.J. (1999) A Molecular Model for the Formation and Properties of Fluid Gels. **International Journal of Biological Macromolecules**, 26: (4): 255-261.

NRC (1999) **Recommended Dietary Allowances**. 10.Washington D.C.: Nation Academies Press.

Nussinovitch, A. (1997) **Hydrocolloid Applications: Gum Technology in the Food and Other Industries**. Blackie Academic & Professional.

Panouillé, M., Saint-Eve, A., de Loubens, C., Déléris, I. and Souchon, I. (2011) Understanding of the Influence of Composition, Structure and Texture on Salty Perception in Model Dairy Products. **Food Hydrocolloids**, 25: (4): 716-723.

Paphangkorakit, J. and Osborn, J.W. (1998) Effects on Human Maximum Bite Force of Biting on a Softer or Harder Object. **Archives of Oral Biology**, 43: (11): 833-839.

Phillips, G.O. and Williams, P.A. (2000) **Handbook of Hydrocolloids**. CRC Press. ISBN-10: 084930850X

Pivk, U., Godinot, N., Keller, C., Antille, N., Juillerat, M.-A. and Raspor, P. (2008) Lipid Deposition on the Tongue after Oral Processing of Medium-Chain Triglycerides and Impact on the Perception of Mouthfeel. **Journal of Agricultural and Food Chemistry**, 56: (3): 1058-1064.

Prinz, J.F., Huntjens, L. and de Wijk, R.A. (2006) Instrumental and Sensory Quantification of Oral Coatings Retained after Swallowing Semi-Solid Foods. **Archives of Oral Biology**, 51: (12): 1071-1079.

Prinz, J.F., Janssen, A.M. and de Wijk, R.A. (2007) In Vitro Simulation of the Oral Processing of Semi-Solid Foods. **Food Hydrocolloids**, 21: (3): 397-401.

Rabe, S., Krings, U., Banavara, D.S. and Berger, R.G. (2002) Computerized Apparatus for Measuring Dynamic Flavor Release from Liquid Food Matrices. **Journal of Agricultural and Food Chemistry**, 50: (22): 6440-6447.

Ramanathan, E. (2006) **Aieee Chemistry**. Sura Books. ISBN-10: 8172542933

Rehm, B.H.A. (2009) **Alginates: Biology and Applications**. Springer. ISBN-10: 3642100813

Roberts, W.H. (1986) Some Current Trends in Tribology in the Uk and Europe. **Tribology International**, 19: (6): 295-311.

Rochas, C. and Rinaudo, M. (1984) Mechanism of Gel Formation in K-Carrageenan. **Biopolymers**, 23: (4): 735-745.

Rossetti, D., Bongaerts, J.H.H., Wantling, E., Stokes, J.R. and Williamson, A.M. (2009) Astringency of Tea Catechins: More Than an Oral Lubrication Tactile Percept. **Food Hydrocolloids**, 23: (7): 1984-1992.

Rousselot (2011) **Rousselot Gelatin** [online].
http://www.rousselot.com/en/applications/edible-applications/dairy/ [Accessed 2011]

Sala, G., Stieger, M. and van de Velde, F. (2010) Serum Release Boosts Sweetness Intensity in Gels. **Food Hydrocolloids**, 24: (5): 494-501.

Salles, C., Tarrega, A., Mielle, P., Maratray, J., Gorria, P., Liaboeuf, J. and Liodenot, J.J. (2007) Development of a Chewing Simulator for Food Breakdown and the Analysis of in Vitro Flavor Compound Release in a Mouth Environment. **Journal of Food Engineering**, 82: (2): 189-198.

Sandford P, A., Baird, J. and Cottrell I, W. (1981) "Xanthan Gum with Improved Dispersibility". **Solution Properties of Polysaccharides**. Washington DC, American Chemical Society 31-41.

Schipper, R.G., Silletti, E. and Vingerhoeds, M.H. (2007) Saliva as Research Material: Biochemical, Physicochemical and Practical Aspects. **Archives of Oral Biology**, 52: (12): 1114-1135.

Shaker, R., Cook, I.J., Dodds, W.J. and Hogan, W.J. (1988) Pressure-Flow Dynamics of the Oral Phase of Swallowing. **Dysphagia**, 3: 79-84.

Shannon, R.D. (1976) Revised Effective Ionic Radii and Systematic Studies of Interatomic Distances in Halides and Chalcogenides. **Acta Crystallographica Section A**, 32:(5): 751-767

Silva, A., Fabio, S. and Dantas, R. (2008) A Scintigraphic Study of Oral, Pharyngeal, and Esophageal Transit in Patients with Stroke. **Dysphagia**, 23: (2): 165-171.

Sleator, R.D. and Hill, C. (2007) Food Reformulations for Improved Health: A Potential Risk for Microbial Food Safety? **Medical Hypotheses**, 69: (6): 1323-1324.

Spikes, H. (2001) Tribology Research in the Twenty-First Century. **Tribology International**, 34: (12): 789-799.

Sriamornsak, P., Wattanakorn, N., Nunthanid, J. and Puttipipatkhachorn, S. (2008) Mucoadhesion of Pectin as Evidence by Wettability and Chain Interpenetration. **Carbohydrate Polymers**, 74: (3): 458-467.

Stiles, W. (1920) The Penetration of Electrolytes into Gels: I: The Penetration of Sodium Chloride into Gels of Agar-Agar Containing Silver Nitrate. **Biochem. J.**, 14: (1): 58-50.

Stiles, W. (1923) The Indicator Method for the Determination of Coefficients of Diffusion in Gels, with Special Reference to the Diffusion of Chlorides. **Proceedings of the Royal Society of London. Series A, Containing Papers of a Mathematical and Physical Character**, 103: (721): 260-275.

Stribeck, R. (1902) Die Wesentlichen Eigenschaften Der Gleit- Und Rollenlager. **Zeitschrift des Vereins Deutscher Ingenieure**, 36: 1341–1348 1432–1438, and 1463–1470.

Sworn, G., Sanderson, G.R. and Gibson, W. (1995) Gellan Gum Fluid Gels. **Food Hydrocolloids**, 9: (4): 265-271.

Talke, F.E.D. (2000) "An Overview of Current Tribology Problems in Magnetic Disk Recording Rechnology". **Tribology and Interface Engineering Series**. Elsevier 15-24.

Tang, J., Tung, M.A. and Zeng, Y. (1996) Compression Strength and Deformation of Gellan Gels Formed with Mono- and Divalent Cations. **Carbohydrate Polymers**, 29: (1): 11-16.

van Vliet, T. (2002) On the Relation between Texture Perception and Fundamental Mechanical Parameters for Liquids and Time Dependent Solids. **Food Quality and Preference**, 13: (4): 227-236.

Varela, P. and Fiszman, S.M. (2011) Hydrocolloids in Fried Foods. A Review. **Food Hydrocolloids**, 25: (8): 1801-1812.

Verhagen, J.V. and Engelen, L. (2006) The Neurocognitive Bases of Human Multimodal Food Perception: Sensory Integration. **Neuroscience & Biobehavioral Reviews**, 30: (5): 613-650.

Williams, P.A., Phillips, G.O. and Chemistry, R.S.o. (2000) **Gums and Stabilisers for the Food Industry 10**. Royal Society of Chemistry.

Xu, W.L., Bronlund, J. and Kieser, J. (2005) Choosing New Ways to Chew: A Robotic Model of the Human Masticatory System for Reproducing Chewing Behaviors. **Robotics & Automation Magazine, IEEE**, 12: (2): 90-100.

Yabuki, K. (1927) On the Diffusion of the Silver Ion in a Gel: (Studies in the Physico-Chemical Properties of Gel. I.). **J Biochem**, 8: (1): 137-156.

Yanes, M., Durán, L. and Costell, E. (2002) Effect of Hydrocolloid Type and Concentration on Flow Behaviour and Sensory Properties of Milk Beverages Model Systems. **Food Hydrocolloids**, 16: (6): 605-611.

Zaretsky, E.V. (1990) Liquid Lubrication in Space. **Tribology International**, 23: (2): 75-93.

APPENDIX 1

Gellan concentration effects (top, rheology, bottom, tribology)

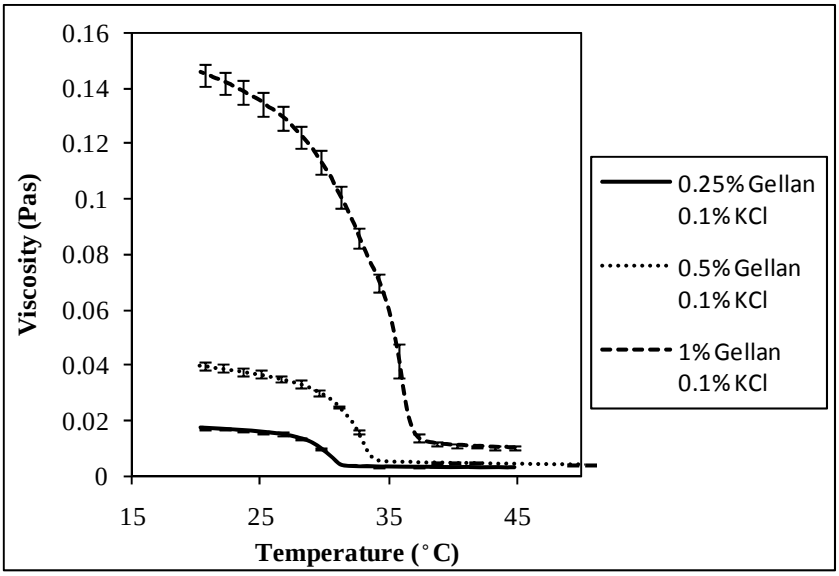

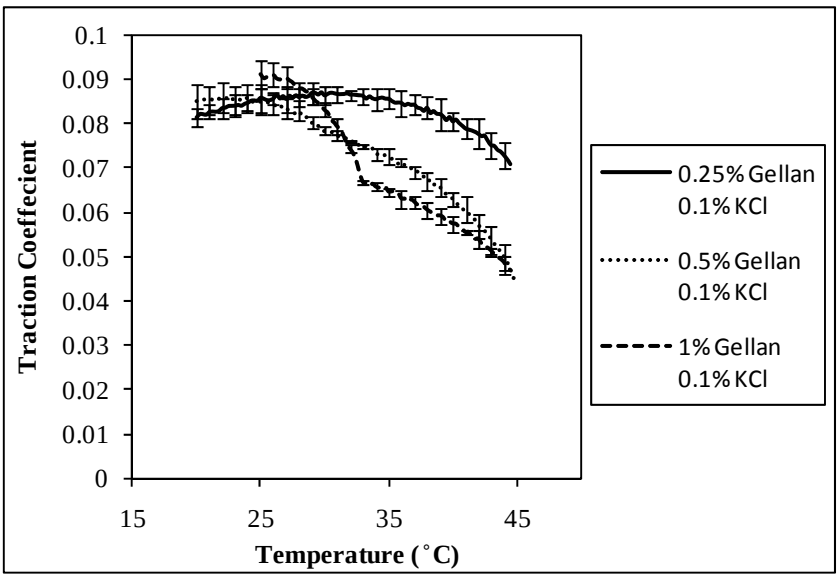

Top, Viscosity curves of gellan gels during temperature induced ordering at different gellan concentrations. Samples were cooled at 1.5˚C/min at a constant shear of $200s^{-1}$, using a 60mm parallel plate geometry. Curves represent an average of three experiments and error bars show one standard deviation from the mean.

Bottom, Traction curves of gellan gels during temperature induced ordering at different gellan concentrations. Samples were cooled at a rate of 1.5˚C/min at a constant speed of 500mm/s and normal force of 2N. A steel ball and elastomer disc tribopair was used. Curves represent an average of three experiments and error bars show one standard deviation from the mean.

Agarose concentration effects (top, rheology, bottom, tribology)

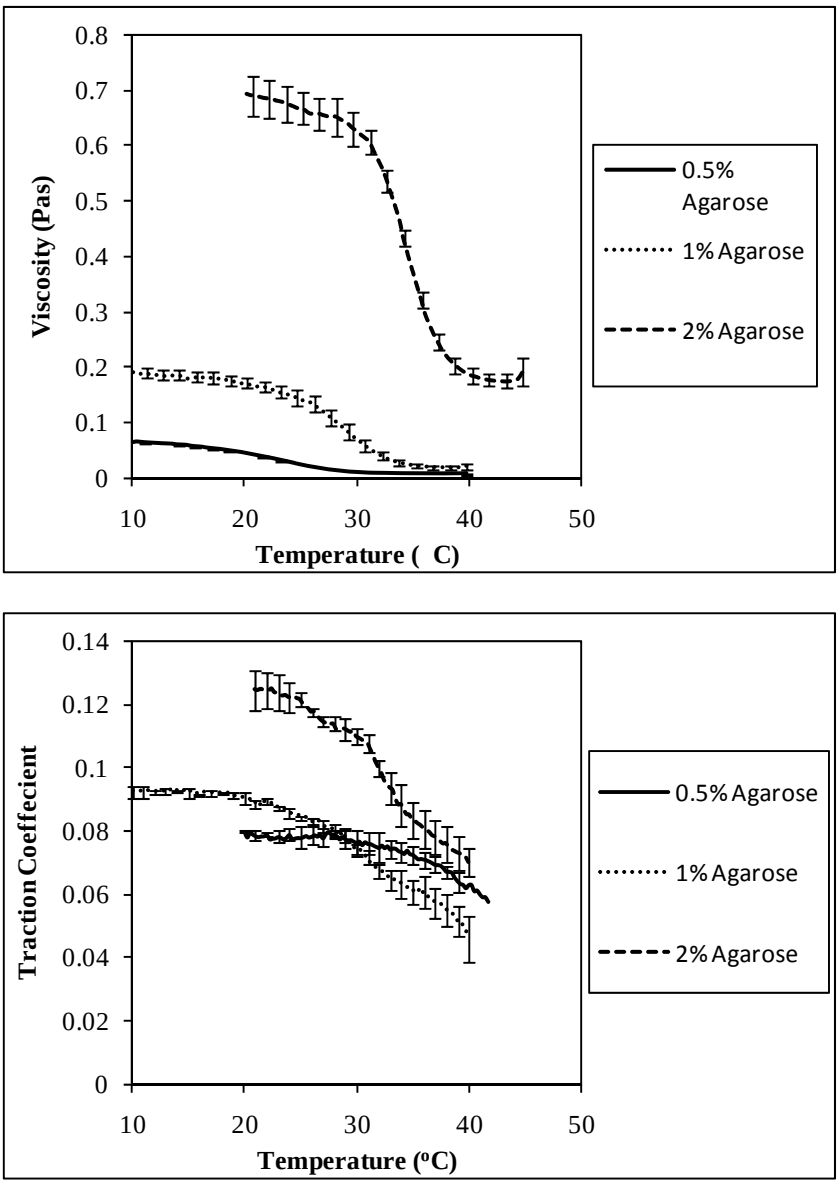

Top, Viscosity curves of agarose gels during temperature induced ordering at different agarose concentrations. Samples were cooled at 1.5 C/min at a constant shear of $200s^{-1}$, using a 60mm parallel plate geometry. Curves represent an average of three experiments and error bars show one standard deviation from the mean.

Bottom, Traction curves of agarose gels during temperature induced ordering at different agarose concentrations. Samples were cooled at a rate of 1.5 C/min at a constant speed of 500mm/s and normal force of 2N. A steel ball and elastomer disc tribopair was used. Curves represent an average of three experiments and error bars show one standard deviation from the mean.

Rheology post production with varying carrageenan concentration

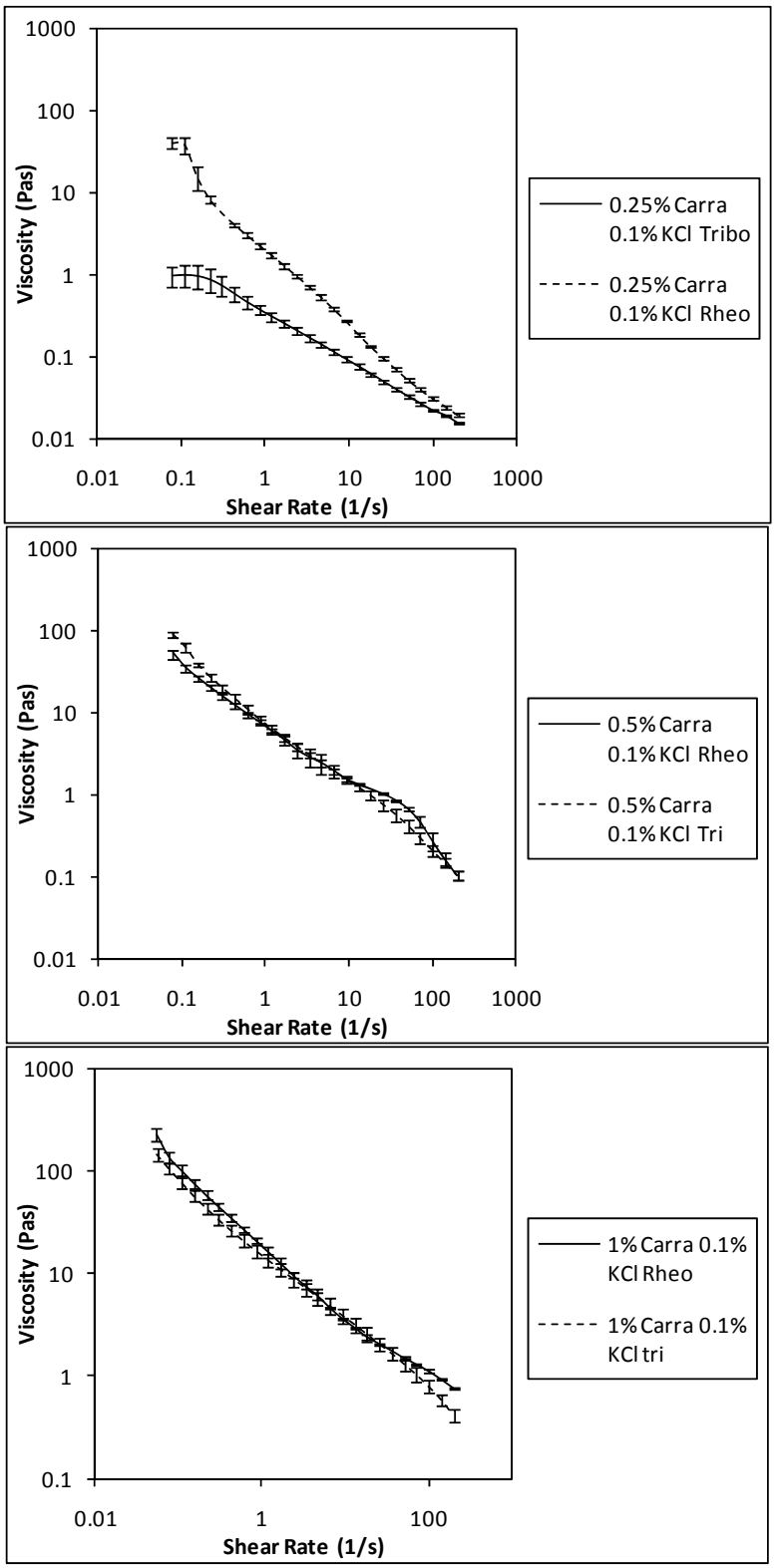

Viscosity comparison of material formed in the tribometer and rheometer for κ-Carrageenan samples of each concentration. Viscosity curves between 0.1 and 200 s^{-1} were carried out at 10°C, data is an average of three separate runs with error bars of one standard deviation from the mean.

Rheology post production with varying salt content (carrageenan)

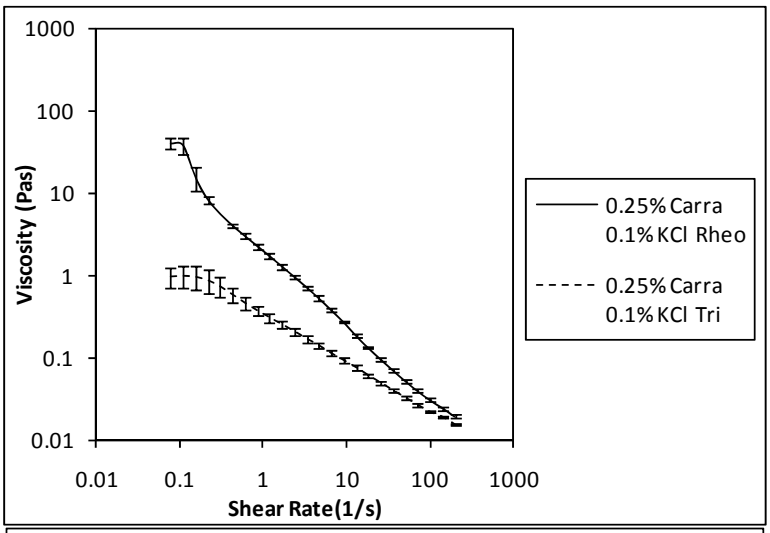

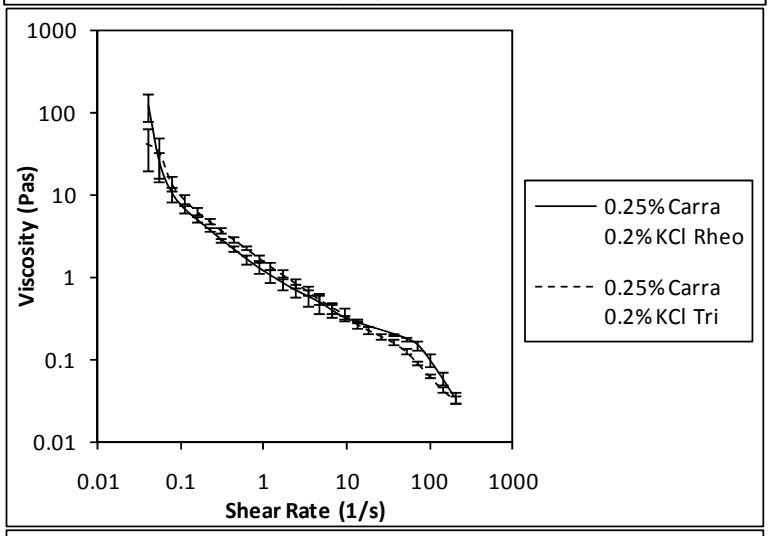

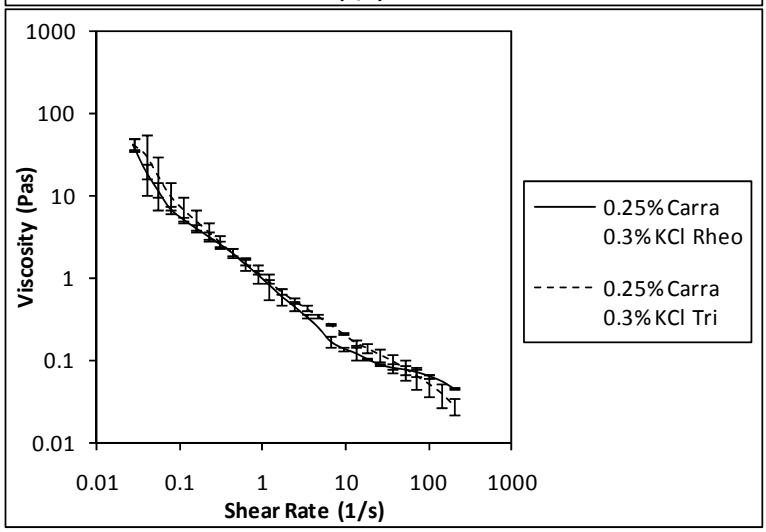

Viscosity comparison of material formed in the tribometer and rheometer for κ-Carrageenan samples of each KCl concentration. Viscosity curves between 0.1 and 200 s^{-1} were carried out at 10°C, data is an average of three separate runs with error bars of one standard deviation from the mean.

Rheology post production with varying gellan content

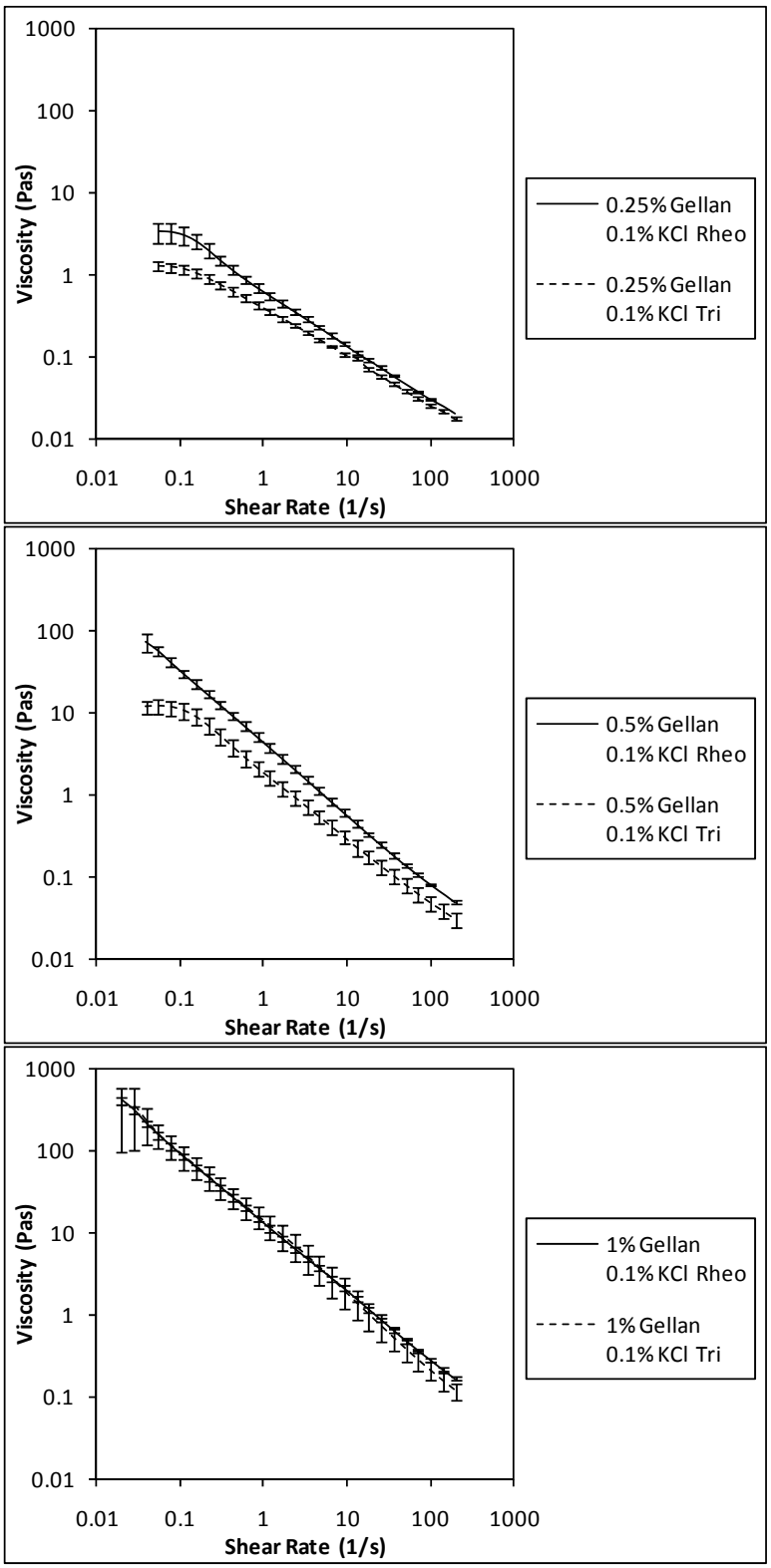

Viscosity comparison of material formed in the tribometer and rheometer for Gellan samples of each concentration. Viscosity curves between 0.1 and 200 s^{-1} were carried out at 10°C, data is an average of three separate runs with error bars of one standard deviation from the mean.

Rheology post production with varying salt content (gellan)

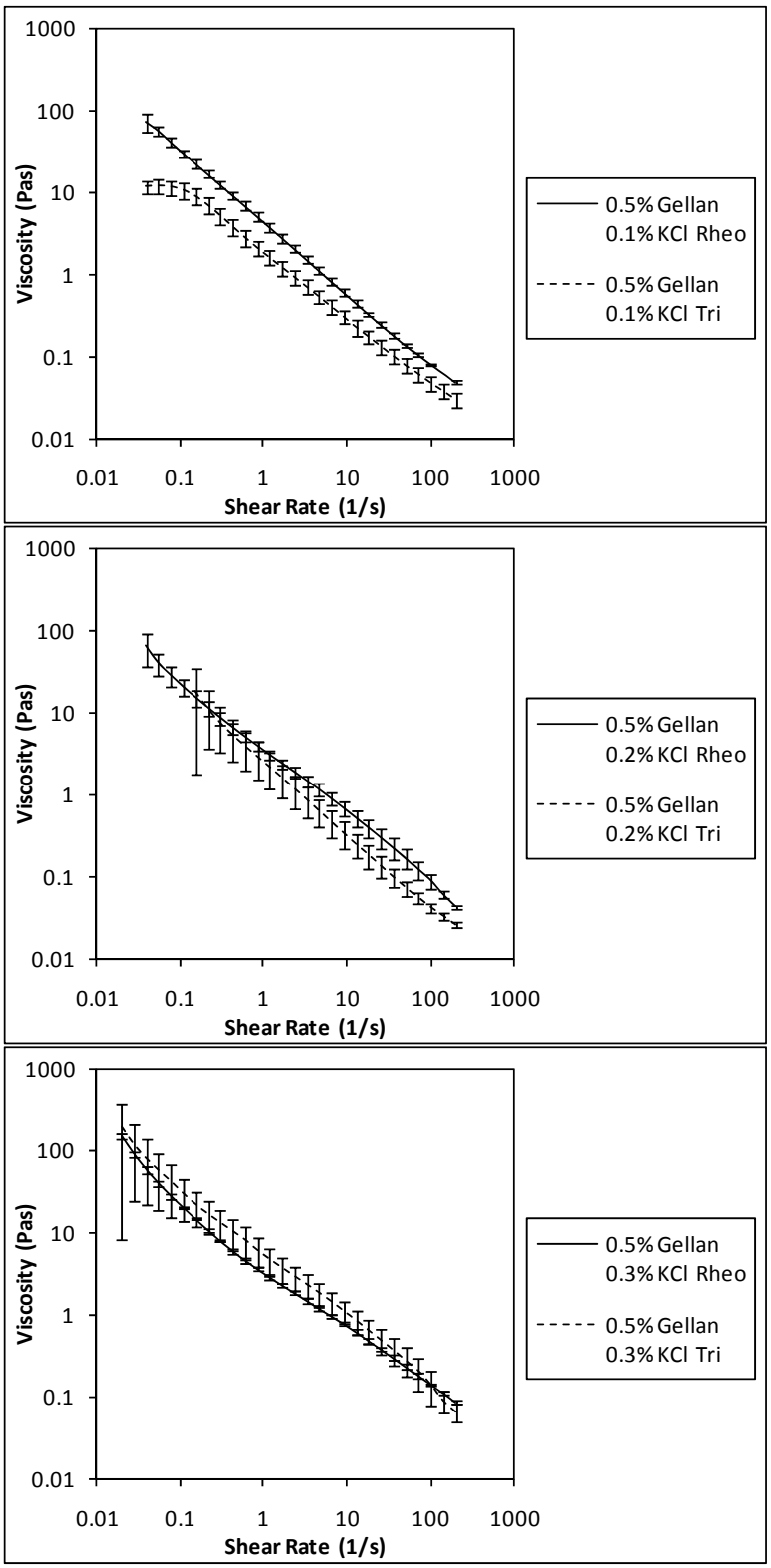

Viscosity comparison of material formed in the tribometer and rheometer for Gellan samples of each KCl concentration. Viscosity curves between 0.1 and 200 s^{-1} were carried out at 10°C, data is an average of three separate runs with error bars of one standard deviation from the mean.

Rheology post production with varying Agarose concentration

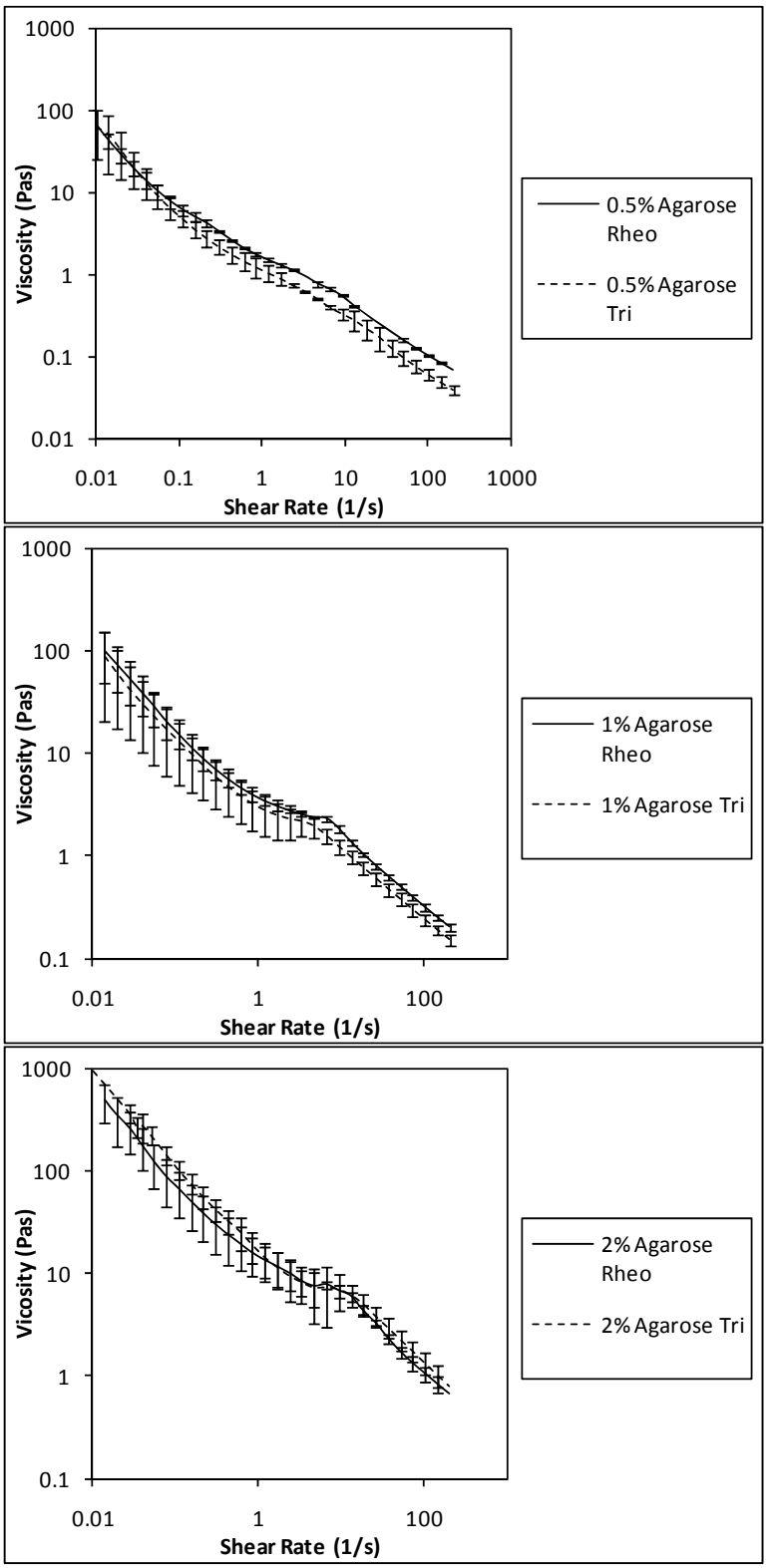

Viscosity comparison of material formed in the tribometer and rheometer for Agarose samples of each concentration. Viscosity curves between 0.1 and 200 s^{-1} were carried out at 10°C, data is an average of three separate runs with error bars of one standard deviation from the mean.

APPENDIX 2

Matlab code to determine effective diffusivity of cylindrical samples

```
% COMSOL Multiphysics Model M-file
% Generated by COMSOL 3.4 (COMSOL 3.4.0.248, $Date: 2007/10/10 16:07:51 $)
function [suma,c]=cylindermodifiedactual(Deff)
load 05gellan25C.txt
time=X05gellan25C(:,1); %#ok<COLND>


con=620;
LRT=length(Deff);
for a=1:LRT
    deff=Deff(a,:);
flclear fem

% COMSOL version
clear vrsn
vrsn.name = 'COMSOL 3.4';
vrsn.ext = '';
vrsn.major = 0;
vrsn.build = 248;
vrsn.rcs = '$Name:  $';
vrsn.date = '$Date: 2007/10/10 16:07:51 $';
fem.version = vrsn;

% Geometry
g1=cylinder3('0.0375','0.045','pos',{'0','0','0'},'axis',{'0','0','1'},'rot
','0');
g4=cylinder3('0.006','0.0075','pos',{'0','0','0.02'},'axis',{'0','0','1'},'
rot','0');

% Analyzed geometry
clear s
s.objs={g1,g4};
s.name={'CYL1','CYL2'};
s.tags={'g1','g4'};

fem.draw=struct('s',s);
fem.geom=geomcsg(fem);
% COMSOL Multiphysics Model M-file
% Generated by COMSOL 3.4 (COMSOL 3.4.0.248, $Date: 2007/10/10 16:07:51 $)

% Geometry
g2=cylinder3('0.011','0.007891','pos',{'0','0','0.02'},'axis',{'0','0','1'}
,'rot','0');

% Analyzed geometry
clear s
s.objs={g1,g2};
s.name={'CYL1','CYL2'};
s.tags={'g1','g2'};
```

```
fem.draw=struct('s',s);
fem.geom=geomcsg(fem);
% COMSOL Multiphysics Model M-file
% Generated by COMSOL 3.4 (COMSOL 3.4.0.248, $Date: 2007/10/10 16:07:51 $)

% Geometry
[g5]=geomcopy({g2});
[g6]=geomcopy({g5});
g6=move(g6,[0,0,0]);
g7=geomcomp({g1,g6},'ns',{'CYL1','CYL3'},'sf','CYL1-
CYL3','face','none','edge','all');
g8=geomcomp({g7},'ns',{'CO1'},'sf','CO1','face','none','edge','all');

% Analyzed geometry
clear s
s.objs={g2,g8};
s.name={'CYL2','CO2'};
s.tags={'g2','g8'};

fem.draw=struct('s',s);
fem.geom=geomcsg(fem);

% COMSOL Multiphysics Model M-file
% Generated by COMSOL 3.4 (COMSOL 3.4.0.248, $Date: 2007/10/10 16:07:51 $)

% Initialize mesh
fem.mesh=meshinit(fem, ...
                  'hauto',5);

% (Default values are not included)

% Application mode 1
clear appl
appl.mode.class = 'FlDiffusion';
appl.assignsuffix = '_di';
clear bnd
bnd.type = {'N0','cont'};
bnd.ind = [1,1,1,1,2,2,2,2,1,2,2,1];
appl.bnd = bnd;
clear equ
equ.D = {10,deff};
equ.init = {0,con};
equ.ind = [1,2];
appl.equ = equ;
fem.appl{1} = appl;
fem.frame = {'ref'};
fem.border = 1;
fem.outform = 'general';
clear units;
units.basesystem = 'SI';
fem.units = units;

% ODE Settings
clear ode
clear units;
units.basesystem = 'SI';
ode.units = units;
```

```
fem.ode=ode;
% Multiphysics
fem=multiphysics(fem);

% Extend mesh
fem.xmesh=meshextend(fem);

% Solve problem
fem.sol=femtime(fem, ...
                'solcomp',{'c'}, ...
                'outcomp',{'c'}, ...
                'tlist',[0:100:12226], ...
                'tout','tlist', ...
                'linsolver','cg', ...
                'prefun','amg'); %#ok<NBRAK>

% Save current fem structure for restart purposes
fem0=fem;

c(:,a)=postinterp(fem0,'c',[0;0;0.001],'T',time); %#ok<AGROW>

suma(a,:)=sum((c(:,a)-X05gellan25C(:,2)).^2);

end
```

Matlab code to vary particle size

```
function [c,ctest,timetest]=sphere(radius)
load 1gellan25C.txt
time=X1gellan25C(:,1);
diff=1.12*10^-9;

LRT=length(radius);
for a=1:LRT
    rad=radius(a,:);

basis=0.008912;
factor=radius(a,:)/basis;
con=513;
newcon=con;
water=0.0358856*factor;

flclear fem

% COMSOL version
clear vrsn
vrsn.name = 'COMSOL 3.4';
vrsn.ext = '';
vrsn.major = 0;
vrsn.build = 248;
vrsn.rcs = '$Name:  $';
vrsn.date = '$Date: 2007/10/10 16:07:51 $';
fem.version = vrsn;
```

```
% Geometry
g1=sphere3(rad,'pos',{'0','0','0'},'axis',{'0','0','1'},'rot','0');
g2=sphere3(water,'pos',{'0','0','0'},'axis',{'0','0','1'},'rot','0');

% Analyzed geometry
clear s
s.objs={g1,g2};
s.name={'SPH1','SPH2'};
s.tags={'g1','g2'};

fem.draw=struct('s',s);
fem.geom=geomcsg(fem);
parr={point3(0,0.02,0)};
g3=geomcoerce('point',parr);

% Analyzed geometry
clear s
s.objs={g1,g2};
s.name={'SPH1','SPH2'};
s.tags={'g1','g2'};

fem.draw=struct('s',s);
fem.geom=geomcsg(fem);

% COMSOL Multiphysics Model M-file
% Generated by COMSOL 3.4 (COMSOL 3.4.0.248, $Date: 2007/10/10 16:07:51 $)

% Initialize mesh
fem.mesh=meshinit(fem, ...
                  'hauto',5);

% (Default values are not included)

% Application mode 1
clear appl
appl.mode.class = 'FlDiffusion';
appl.assignsuffix = '_di';
clear bnd
bnd.type = {'N0','cont'};
bnd.ind = [1,1,1,1,2,2,2,2,1,1,2,2,1,2,2,1];
appl.bnd = bnd;
clear equ
equ.D = {10,diff}; %#ok<LTARG>
equ.init = {0,newcon};
equ.ind = [1,2];
appl.equ = equ;
fem.appl{1} = appl;
fem.frame = {'ref'};
fem.border = 1;
fem.outform = 'general';
clear units;
units.basesystem = 'SI';
fem.units = units;

% ODE Settings
clear ode
clear units;
```

```
units.basesystem = 'SI';
ode.units = units;
fem.ode=ode;
% Multiphysics
fem=multiphysics(fem);

% Extend mesh
fem.xmesh=meshextend(fem);

% Solve problem
fem.sol=femtime(fem, ...
                'solcomp',{'c'}, ...
                'outcomp',{'c'}, ...
                'tlist',[0:0.001:20], ...
                'tout','tlist', ...
                'linsolver','cg', ...
                'prefun','amg');

% Save current fem structure for restart purposes
fem0=fem;

timetest=[0:0.001:20];

c(:,a)=postinterp(fem0,'c',[0;0.02*factor;0],'T',time);
ctest(:,a)=postinterp(fem0,'c',[0;0.02*factor;0],'T',timetest);
end
```